HUMAN TIME AWARENESS AND FEEDBACK-DRIVEN IMPROVEMENTS OF TIME REPRODUCTION

by

Farah Nikhath Bader

A Dissertation
Submitted to the
Graduate Faculty
of
George Mason University
in Partial Fulfillment of
The Requirements for the Degree
of
Doctor of Philosophy
Neuroscience

Committee:

Dr. Martin Wiener, Dissertation Director

Dr. Craig McDonald, Committee Member

Dr. William G. Kennedy, Committee Member

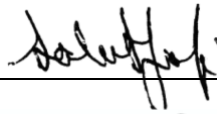

Dr. Saleet Jafri, Director of Interdisciplinary Program in Neuroscience

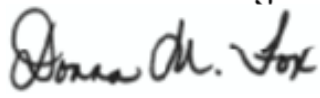

Dr. Donna M. Fox,
Associate Dean Office of Student Affairs
& Special Programs, College of Science

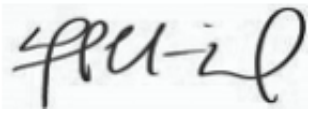

Dr. Fernando R. Miralles-Wilhelm
Dean, College of Science

Date: 7/29/22

Summer Semester 2022
George Mason University
Fairfax, VA

Human Time Awareness And Feedback-Driven Improvements Of Time Reproduction

A Dissertation submitted in partial fulfillment of the requirements for the degree of Doctor of Philosophy at George Mason University

by

Farah Nikhath Bader
Master's of Public Health
Johns Hopkins Bloomberg School of Public Health, 2008
Bachelor of Science
Emory University, 2004

Director: Martin Wiener, Assistant Professor
Department of Psychology

Summer Term 2022
George Mason University
Fairfax, VA

DEDICATION

This is dedicated to my mother, Naseem Bader, who has remained ever-present with a sympathetic ear and incredible support; to my sister, Shakeela Bader, for motivating me and giving me the inspiration in times of struggle, to my father Ali Asad Bader for his constant praise; and most of all, to my husband Tonu Nauage for his unflinching love, words of wisdom, patience, and encouragement throughout the years.

ACKNOWLEDGEMENTS

I want to thank Mohammad Al-Quraishi, Chloe Mondok, Ayana Cameron, Keri Gladhill, Colleen Gerrity and Candice Stanfield-Wiswell for assistance with data collection in the fMRI-EEG experiments and providing encouragement during my time at GMU. I want to also express my deepest gratitude to Martin Wiener for challenging me to excel, for always having faith in my potential as a researcher, and for his endless encouragement and patience.

TABLE OF CONTENTS

LIST OF TABLES

LIST OF FIGURES

LIST OF ABBREVIATIONS

Anterior Cingulate Cortex ..... ACC
Attention Deficit Hyperactivity Disorder ..... ADHD
Autism Spectrum Disorder ..... ASD
Basal ganglia ..... BG
Blood Oxygen Level Dependent ..... BOLD
Catechol-O-methyltransferase ..... COMT
Contingent Negative Variation ..... CNV
Dopamine ..... DA
Electroencephalogram ..... EEG
Event Related Potential ..... ERP
Neurofibromatosis NF1
Oxford Liverpool Inventory of Feelings and Experiences ..... O-LIFE
Error Positivity ..... P_e
Posterior Parietal Cortex ..... PPC
Pre-supplementary motor area ..... preSMA
Prefrontal cortex ..... pfC
Reinforcement Learning ..... RL
Reward Prediction Error ..... RPE
Scalar Expectancy Theory ..... SET
Supplementary motor area ..... SMA
Temporal Order Judgement ..... TOA
Time-Adaptive Opponent Process Drift Diffusion ..... ToPDDM
Transcranial Magnetic Stimulation ..... TMS
Ventral Striatum ..... VS

ABSTRACT

HUMAN TIME AWARENESS AND FEEDBACK-DRIVEN IMPROVEMENTS OF TIME REPRODUCTION

Farah Nikhath Bader, Ph.D.

George Mason University, 2022

Dissertation Director: Dr. Martin Wiener

Time perception is critical for cognitive and behavioral functions ranging from speech to motor control. Learning to time durations can cause errors; therefore, recognizing and correcting the temporal errors is essential for individual timing self-awareness, which humans innately possess. Conflicting reports over whether humans can discern the direction of the timing error (earliness/lateness) can be addressed by introducing feedback in behavioral tasks. To better comprehend the extent of human timing self-awareness and how feedback modulates the process of learning to time, three experiments were conducted utilizing the computerized visual temporal reproduction task. Participants viewed a blue square for a set amount of time selected from a mixed set of durations ranging from 1.5-6 seconds and then re-created the square's on-screen time using a keypress and received adaptive non-directional feedback for their performance. Each trial could be repeated following feedback, allowing a "re-do" to learn from the successes or errors in the first trial. In the first experiment, I tested two

groups of participants on versions where non-directional feedback was provided after every response, or not provided at all. Temporal estimates were more accurate and precise with post-trial non-directional feedback, revealing a metacognitive ability and tendency to adjust temporal responses.

To examine the neural underpinnings of these previous behavioral findings, a fMRI-EEG study was performed with the same paradigm. Blood oxygen level dependent (BOLD) activation in the supplementary motor area (SMA), an area highly implicated in time perception and sharpening of temporal estimates, was observed as the durations was encoded and reproduced. Notably, significant EEG-informed fMRI activity in the SMA showed that the contingent negative variation signal covaried with the BOLD signal during the encoding phase. Additional BOLD activations were witnessed in areas associated with the brain's performance monitoring system and the default mode network along with more timing-related areas parietally, frontally, and subcortically.

The third experiment profiled an environment of temporal uncertainty in which every trial was not always followed by a redo opportunity. Two groups of participants were tested in settings where the frequencies of single (initial only) and double (initial and redo) trials varied. Group members receiving a low frequency of redo trials (80% single, 20% double) exhibited lower absolute temporal error and were more precise in their temporal estimates than participants allotted to the high frequency group. This demonstrated that both groups learned the underlying trial structure of the settings, adapted, and adjusted their temporal responses accordingly.

Holistically, these studies offered deeper insights into timing self-awareness, the mechanism for improving time estimates through a redo opportunity and varied feedback, the region-specific neural responses to temporal judgements, and how we learn to time in uncertain environments.

INTRODUCTION

Imagine that it is your turn to bat on a lovely Spring day. The pitcher throws the baseball, and it speeds towards you. Bat poised in hand, you fixate on the ball and swing with ferocity, but barely miss the ball. You groan at your hapless timing, but you know that you have one last chance to learn from your past folly. Muscles taut, you concentrate and prepare for the pitch again. Miraculously, in this instance, your timing and movement are synchronized with the ball, and you hear the thwack of the bat, signaling success. Briefly, you smile, elated by the unexpected reward of not striking out and run to first base as fast as your legs can carry you.

Critical to the success of the batter in this example is her finely tuned sense of time perception. Her ability to evaluate her own timing behavior and update her motor movements to hit the ball in the second try involves perceiving and estimating time accurately. The ability is needed for communication (language), motor action and control, survival, and even consciousness itself (Meck, 2005; Grondin, 2010). Subjective time perception is impacted in degrees by emotion, developmental stages, age, gender, clinical disorders/conditions and body temperature (Matthews & Meck, 2016). Attention is a key determinant that highly influences the perception of time; targeting the attentional resources towards processing the interval duration can dilate the temporal judgements and essentially lengthen subjective time (Matthews & Meck, 2016). Furthermore, the past must be integrated with the present in this scenario as the batter's previous

experience with timing the event and when to swing draws forth the past memories of misses and hits, culminating in the final, successful play (Matthews & Meck, 2016).

Research Questions

Past behavioral and electrophysiological evidence show that humans are cognitively aware of timing errors; however, questions remain concerning the extent of this time awareness (Akdogan & Balci, 2017; Kononowicz, 2019; Riemer et al., 2019). Are humans aware of the direction of their timing errors (earliness or lateness) or is this cognizance limited to only error magnitude? Furthermore, how does the process of learning to time impact this awareness? This dissertation addresses these questions by incorporating feedback into a classical task of time measurement, the visual time reproduction. A set of three studies examine these points of research inquiry: the first compares non-directional feedback with absence of feedback; the second is a simultaneous fMRI-EEG study which investigates the neural regions involved in time awareness and learning time, and the third study probes the impact of temporal uncertainty on our level of time awareness.

Models of Time Perception

How does this very carefully executed process of timing operate in the brain? Any exploration of the theories of time perception includes the widely supported model: scalar expectancy theory (SET) (Gibbon et al., 1984; Treisman, 2013; Wearden, 2004). This theory posits an internal clock in the brain that measures interval durations, consisting of

a pacemaker that emits pulses at a specified rate, and an accumulator that sums and integrates the pulses from the pacemaker (Gibbon et al., 1984; Treisman, 2013; Wearden, 2004). The closing of a switch indicates the start of the interval duration and is highly influenced by attention, which modulates the entry of pulses and the switch operation. The clock readout of the duration involves comparing the present reading to previously encoded counts from memory and then making a decision about the duration. When the switch opens again, the duration measurement is complete (Gibbon et al., 1984; Treisman, 2013; Wearden, 2004).

How might SET be implemented in the brain? A leading neurobiological theory is the Striatal Beat Frequency model (Matell & Meck, 2000, 2004). Here, the "clock" is comprised of a cortico-striatal-thalamic network in which cortical neurons oscillating at specific frequencies are detected by the striatum, during a timed event (Matell & Meck, 2000;2004). When the oscillatory patterns are coincident between the cortico-striatal network, medium striatal neurons become active and the synaptic inputs from the cortex and thalamus are integrated and evaluated to code a particular duration (Matell & Meck, 2000;2004). Any subsequent oscillatory phase change is reset by dopaminergic input from the substantia nigra pars compacta, marking a new timing event (Matell & Meck, 2000; 2004).

Another theory that supplements SET and is more applicable to how we *learn* to time is the Behavioral Theory of Timing (BeT). According to this model, the pulses are transitions between different behaviors (Killeen & Fetterman, 1988) and are modeled as Poisson processes with a rate constant that is proportional to the rate of reinforcement,

which in turn controls the pacemaker and the rate of learning (Killeen & Fetterman, 1988; Bizo & White, 1994).

Another perspective on how the brain's internal timekeeping mechanisms may function relies on Bayesian principles to explain it (Freestone & Church, 2016). Here, the Bayesian prior is derived from information about a duration from experience with past intervals. The current readout of the duration is the likelihood estimate. The posterior estimate, which is the probability that the estimated time will match the actual elapsed time, is determined by multiplying the prior and likelihood together. This is how the brain learns to time using Bayesian updating and eventually the posterior estimate becomes the prior for the next trial. The maximum of the posterior aligns with traditional learning curves and is inversely proportional to the measurement error of the temporal estimate and the coefficient of variation (CV). Lower CVs signal higher rates of learning (Freestone & Church, 2016).

An alternate viewpoint is that timing is an intrinsic feature of neuronal networks and that time perception does not require centralized components (Mauk & Buonomano, 2004). In essence, there are multiple "population clocks" that modify their firing patterns and fire in sync either in a sequential or complex pattern to "time" an event (Buonomano & Laje, 2010). These state-dependent networks usually involve an active state of currently firing neurons in a recurrent network and a hidden state of neurons whose activity is either facilitated or inhibited (Goel & Buonomano, 2014).

Most relevant to the present study are time-adaptive drift diffusion models (Simen et al., 2011). Traditionally, drift diffusion models are used to determine how real-time

decisions are made and involve modeling the rate of accumulating evidence in a noisy environment until a certain threshold is reached and a response is generated (Ratcliff, 1978; Ratcliff & McKoon, 2008). When applied to interval timing, the modified drift diffusion model transforms into the Time-Adaptive Opponent Process Drift Diffusion model (ToP DDM). This model accumulates evidence related to the elapsed time using adjustable drift rates and a fixed interval to encode the duration (Simen et al., 2011). These drift diffusion parameters can be adapted fairly quickly, and the interval duration can be learned rapidly in one trial and with only one exposure to the duration (Simen et al., 2011). Furthermore, this model can handle frequent and rapid transitions of interval durations due to quick updates of the temporal representations of the experienced duration (Simen et al., 2011).

Performance on the beat-the-clock procedure - a task where a key must be pressed prior to an offset of a green square to obtain a scaled reward (higher reward closer to the target) - provides evidence of how rapidly humans learn to time interval durations (Simen & Balci, 2011). Animal work in support of this model includes studies showing the patterns of neuronal firing activity in the monkey parietal cortex (Leon & Shadlen, 2003), the pre-supplementary area (pre-SMA) (Mita et al., 2009) and thalamic neurons in the rat (Komura et al., 2001) are consistent with ToPDDM.

There are many information processing models that delineate how time perception proceeds in the brain with each model inching closer to addressing how interval durations are learned. Examining the underlying processes linked to these models, whether it be SET, striatal beat frequency, BeT, state-dependent networks, Bayesian mechanisms, or

ToP DDM leads to an understanding of normal timing behavior. Therefore, when timing errors occur, one can infer what part of the process went awry. Comparably to the role of timing theories in describing how and where timing errors may arise, my paradigm is also specifically designed to capture the timing errors and to shed light into the level of awareness of timing ability.

Time Reproduction Task

Although time perception can be studied in numerous ways, I selected to focus on one: the visual temporal reproduction task. In the temporal reproduction task, participants are exposed to visual stimuli that is presented on a computer screen for an interval duration selected from a random mix of durations during the estimation phase. Notably, the duration is not verbally defined beforehand at the start of a trial. Participants are subsequently asked to reproduce the elapsed time of this same stimuli with a stopwatch-like motor response during the reproduction phase (Wiener, 2014). The motor response can be performed in a myriad of ways from holding down a key for the entirety of the requested interval, pressing a key once to start the interval and another to stop it, or pressing the key to terminate the duration (Mioni, Stablum, McClintock & Grondin, 2014). My study used the last method.

I chose this task because past studies of error monitoring have focused on two-alternative forced choice (2AFC) task for decision-making, memory, and perceptual experiments which are limiting because the 2AFC paradigm only permits dichotomous or binary responses (Akdogan & Balci, 2017). Even studies investigating time awareness

have followed this pattern and have used tasks where participants are asked to choose "short" or "long" to describe experienced durations (Droit-Volet & Izaute, 2009). The time reproduction task is different in that it allows an investigation of error metrics that are continuous, parametric, and may be graded, offering insight into directionality of the error in the form of under-reproduction (earliness) or over-reproduction (lateness) (Akdogan & Balci, 2017). Essentially, the time reproduction task provides a window into whether humans are aware of timing error direction rather than focusing only on whether the temporal responses are correct or not (Akdogan & Balci, 2017).

Departing from describing my behavioral paradigm, I will now delve deeper into the brain regions that are involved in time perception.

Neuroanatomy of Time Perception

Traditionally, the core areas that have been associated with timing networks include the supplementary motor area (SMA), frontal and parietal cortices, and the basal ganglia, and the hippocampus. More recently, the insula and other regions associated with the default mode network have risen to the forefront.

Supplementary Motor Area and other Traditional Timing Regions

An early quantitative meta-analysis that evaluated the probability of activation by Wiener and colleagues (2010) noted that SMA and the inferior frontal gyrus, displayed activation in all types of timing tasks and showed concordance in four separate meta-analysis of motor, perceptual, subsecond (<1 second) and supra-second (>1 second) tasks

(Wiener et al., 2010). This led to a key finding – the brain area that is recruited depends on the task context and the timescale of interval duration. Sub-second tasks were more likely to involve higher activations in the cerebellum and basal ganglia structures whereas supra-second tasks involved the pre-frontal cortex and SMA. Relatedly, motor-heavy tasks activated the SMA proper and perceptual tasks evoked more activity in the pre-SMA (Wiener et al., 2011; Schwartze et al., 2012).

The SMA, in particular, has been a core component of dissociable timing networks and has appeared repeatedly in other more recent meta-analyses (Nani et al., 2019; Cona et al., 2021). Additionally, the basal ganglia, insula, and intraparietal sulcus are all associated with internally cued timing (Teghill et al., 2019). Aligned with these findings, yet another meta-analysis using data from 114 experiments showed time-related activation in the globus pallidus, putamen, bilateral thalamus, anterior insula, and the intraparietal sulcus, inferior frontal gyrus, pre-SMA and SMA, pre-central gyrus, right superior temporal gyrus, and middle gyrus (Cona et al., 2021).

Frontal Cortex

For longer durations and when there is involvement of memory, attention, or decision-making in storing the durations, the frontal cortex is recruited (Mioni et al., 2020). Studies have shown that time-based prospective memory, verbal estimation of time, and time production are dependent on frontal cortex function (McFarland, 2009). The prefrontal cortex (pFC) in particular has taken center stage in time discrimination tasks (Lewis & Miall, 2003; Onoe et al., 2001; Rao et al., 2001) and has been known to encode visual interval durations following saccades in primates (Genovesio et al., 2009).

Patient with right pFC lesions display time perception deficits (Koch et al., 2002;2003). Furthermore, brain stimulation studies with transcranial magnetic stimulation (TMS) revealed that stimulating the right dorsolateral prefrontal cortex in a time reproduction task led participants to under-reproduce the interval durations during the reproduction phase (Jones et al., 2004), again reiterating the importance of the frontal cortex. Animal studies provided more evidence of frontal cortex involvement in time perception; primates who measured interval durations in a ready-set-go task (Meirhaeghe et al., 2021) had frontal cortex activity that reflected the mean interval of the distribution, revealing a temporal scaling feature predictive of the encoded durations (Meirhaeghe et al., 2021).

Parietal Cortex

Also invoked in making temporal judgements is the parietal cortex, stemming from its role in multimodal and multisensory processing. The parietal cortex is associated with the common magnitude system in the brain that is responsible for perception of other magnitudes – space, time, size, number or velocity (Beudel et al., 2009; Bueti & Walsh, 2009; Walsh, 2003). In particular, the posterior parietal cortex (PPC) plays a pivotal role in the interaction between spatial and temporal dimensions (Beudel et al., 2009; Bueti & Walsh, 2009; Walsh, 2003). If TMS application inhibits the right PPC in healthy controls performing a variant of the time reproduction task that instructs subjects to indicate when half of the duration they were initially exposed to had elapsed, there is a directional bias and an under-reproduction of the midpoint of the interval (Olivera et al., 2009). In patients with PPC inactivation due to right hemisphere brain damage and

spatial neglect who did not receive TMS, this same directional bias in this task persisted (Olivera et al., 2009). Further evidence for the PPC's role in temporal processing and hemispheric bias stems from another study where healthy participants performed the time reproduction task with cathodal transcranial brain stimulation over the parietal cortex (Vicario, Martino & Koch, 2013). Participants stimulated over the right parietal cortex experienced changes in accuracy and overestimated the duration whereas left parietal cortex stimulation elicited lower variability in the time reproductions (Vicario, Martino, & Koch, 2013).

Basal Ganglia

The basal ganglia (BG) are an important network of subcortical nuclei recruited in timing studies (Allman, 2012; Fontes, et al., 2016). The basal ganglia's role in motor control, procedural memory, reinforcement learning, and cognition is well-suited to a role in learning interval durations (Allman, 2012; Fontes et al., 2016). The striatum's role as a coincident detector in the beat frequency model further illustrates the importance of the basal ganglia in timing (Mattell & Meck, 2003). Patient studies of Parkinson's Disease patients reveal that the BG is needed for time production and reproduction in the millisecond to seconds range (Jones et al., 2008). Even in healthy participants, changes in dopaminergic input to the putamen due to dopamine precursor depletion has led to time impairments (Coull et al., 2012). These various studies demonstrated that the basal ganglia encoded the duration of any motor action, essentially providing a temporal representation of the interval duration (Rammsayer, 1997; Fontes et al., 2016).

Hippocampus

Another subcortical structure critical to time perception is the hippocampus by virtue of its association with learning and memory. The hippocampus' ability to chart moments in time in a temporally organized fashion is mediated by time cells, or neurons in the human hippocampus and the entorhinal cortex that fire in order to quantitatively encode interval durations (Eichenbaum, 2017). Time cells rescaled rapidly when durations change (Eichenbaum, 2017; Petter et al., 2011), were frequently recruited during memory retrieval and encoding (Umbach et al., 2020), and are implicated in temporal ordering, organization, and sequencing of episodic memory. Location-wise, these neurons are found in proximity to neurons that are involved in mapping the spatial context (Eichenbaum, 2017).

Insular Cortex

Less widely studied but equally as important is the insular cortex in making temporal judgements. Primarily involved in assessing the physiological state to evaluate interoceptive awareness, the insula is a barometer of internal bodily state, and this region has been suggested to use metrics such as the heartrate to determine a sense of time (Vicario et al., 2010; Craig et al., 2009). Notably, the insula can communicate with the basal ganglia, supplementing information on temporal encoding (Rao et al., 2001; Craig, 2009). There is a directional gradient in insular activation with longer (supra-second) time reproduction tasks; higher neural activity is observed in the posterior area during the

encoding phase and greater anterior insula activation is seen during reproduction (Wittman et al., 2010). Additionally, there is a ramping up of activity, suggestive of an accumulator, reinforcing the insula's role in demarcating the passage of time (Wittman et al., 2010). In auditory temporal discrimination tasks, where a decision must be made whether a tone is longer or shorter than a standard, there is also insular and operculum activation (Tregellas et al., 2006; Craig et al., 2009).

Default Mode Network

Another sparsely studied network in relation to time perception is the default mode network, which steps online during the brain's resting state when there is no stimulus or task to engage the brain (Raichle et al., 2001). Interactions between time-related and default-mode related activations are more pronounced when judging suprasecond intervals over two seconds (Morillion et al., 2009) and could relate to mentalizing interval durations. Specifically, the posterior cingulate, a major node in the default mode network, has been implicated in episodic retrieval and functions as a bridge between memory and time perception (Ustin et al., 2017). Notably, the posterior cingulate also connects the lateralized frontoparietal network and subcortical structures such as the anterior insular cortex and the BG, again neural regions connected to timing (Ustin et al., 2017). Another structure, the precuneus, shows heightened connectivity to the default mode network during resting state cognition, also revealing its importance as a default mode structure and in self- awareness (Utevsky et al., 2014). Stimulation of the precuneus using TMS disrupts episodic memory retrieval (Ye et al., 2018). Lowered

BOLD precuneus activity is seen in Parkinson's Disease patients who are both ON and OFF their medications in the encoding phase and the OFF-medicated PD patients in the reproduction phase of a time reproduction task (Dusek et al., 2012). Taken together, these studies on the precuneus demonstrate a linkage to time disorientation.

The expansive range of brain areas and neural networks involved in time perception reinforces the notion that timing an interval duration is a complex process. A deeper inspection of the function of each brain structures linked with time perception reveals the multiple cognitive operations needed, from attention, memory, decision-making to self-awareness for formulating an accurate estimate of time. These cognitive operations are also critical for developing timing awareness and the learning of interval durations; therefore, familiarity with the neuroanatomy informs our knowledge.

THE BRAIN'S PERFORMANCE MONITORING SYSTEM

When learning a new task (e.g., temporal processing of interval duration) or executing a motor program, environmental conditions can change quickly, and humans must adapt. A neural evaluation system whose responsibility is to detect errors, register conflict, respond and adapt to shifting task conditions, all without external feedback is critical (Ulpsberger et al., 2014). Generally, the brain's performance monitoring system fulfills this role, and not only must this brain network assess what caused any errors but also send a cognitive control signal to represent and resolve the error (Ulpsberger et al., 2014).

Behavioral Adjustments

Adaptive Mechanisms

Compensatory mechanisms to correct the error include an increased reaction time leading to post-error slowing or an increase or decrease in post-error accuracy (Laming, 1979; Rabbit, 1979). Whether these mechanisms are beneficial (Botvinick et al., 2001; King et al., 2010; Maier et al., 2011) and engender a slower, more cautious strategy that enhances performance or maladaptive (Buzzell et al., 2017; Jentzsch & Dudschig, 2009; Notebaert et al., 2009; Ullsperger & Danielmeier; Van der Borght et al., 2016) and operate as a distraction to worsen performance is debatable (Beatty et al., 2018) and beyond the scope of the current study.

Neural Biomarkers of Performance Monitoring

Performance monitoring signals can be traced by neural biomarkers. An oft-referenced electrophysiological marker is the event-related negativity, a frontocentral, response-locked event related potential (ERP) generated by the medial frontal cortex when there is mismatch between the actual and target outcome or response conflict (Falkenstein et al., 1991; Gehring et al., 1993). In the time-frequency domain, frontal midline theta oscillations can also reflect an error response which eventually leads to cognitive control and behavioral adjustments (Ullsperger et al., 2014; Cavanagh & Frank, 2014).

Neuroanatomy of the Performance Monitoring System

The neural circuitry involved in the tracking of errors includes the medial, ventral and orbitofrontal prefrontal cortex, the anterior cingulate cortex (ACC) and the lateral pre-frontal cortex (Ridderinkhof et al., 2004; Ulspsburger et al., 2014). The posterior medial pFC determined the value of the on-going behavioral strategy and updated the value of each action. The ventral pFC compares the values between multiple different actions or strategies and the hierarchically organized lateral pFC exerts over top-down attentional control. The basal ganglia (caudate, putamen and thalamus) select an appropriate response, facilitates or inhibits actions, and engages in reinforcement learning. The orbitofrontal cortex monitors the outcomes and assigns credits (Ulspsburger et al., 2014). The ACC is involved in error monitoring and explore-exploit paradigm which entails evaluating the need for strategy switching and committing to the strategy

switch when attempting to conduct a goal-directed action (Tervo et al., 2021). As expected, the neurochemistry underlying performance monitoring relies on dopamine for its role in reward prediction error (Joacham & Ullsperger, 2009). Other transmitters (serotonin, norepinephrine, and GABA) have also been linked to performance monitoring (Jocham & Ullsperger, 2009).

Neurons with the medial frontal cortex (dorsal anterior cingulate cortex and pre-supplementary area) encode domain-specific and domain-general performance monitoring signals associated with conflict (selecting between two or more options), conflict probability, and errors. Both neuron types are mixed together in the medial frontal cortex (Fu et al., 2022). Single neuron recordings in epilepsy patients as they performed a Stroop task, and a multi-source interference task provided a means to probe the geometry of the medial frontal cortical neurons (Fu et al., 2022). At the population level, domain-general neurons could be readout with 90% accuracy in single trials, but domain specific neurons could still code for different conflict conditions (Fu et al., 2022).

In a recent study of hierarchical reasoning, neurons in the primate dorsomedial cortex (including the preSMA) and the anterior cingulate cortex were recorded to assess whether unfavorable task outcomes stemmed from either misjudgment of stimuli or due to selecting the wrong rule following a covert rule switch (Sarafyazd & Jazayeri, 2019). While both regions were implicated in evaluating the confidence associated with a lower-level decisions that informed the later, higher level decisions (Sarafyazd & Jazayeri, 2019), the ACC had a more robust and direct role in causal inference and attribution of errors to rule switches (Sarafyazd & Jazayeri, 2019). This finding was not surprising

given that the ACC is modulated by reward history (Seo &Lee, 2007; Amiez et al., 2006) and expectations (Shidara & Richmond, 2002) and is connected to reward dependent adaptive behavior including motor action selection (Shima & Tanji, 1998), foraging (Hayden et al., 2011), exploration and exploitation (Quildoran et al., 2008), and decision-making in risky conditions (Kennerly et al., 2006; Sarafyazd & Jazayeri, 2019).

Performance monitoring is associated with learning new tasks, monitoring for errors, adjusting after an error and comparing the actual and intended outcomes of actions. All of these roles are important for recognizing and correcting for timing errors. Therefore, understanding the roles, neuroanatomy, and the theories underlying performance monitoring feeds into a fuller comprehension of the self-awareness of the timing error, which is the topic of the next section.

TEMPORAL METACOGNITION

Recognizing and correcting temporal errors without any external sensory input or prior learning is a critical component of performance monitoring and is also essential for metacognition and self-awareness of one's cognitive state (Fleming & Yeung, 2012). This has led scientists to ponder the degree to which humans can self-assess miscalculations in temporal accuracy and variance. Behavioral studies have shown that humans can track the magnitude (whether near or far from target) and direction of errors (earliness or lateness) in time reproduction tasks and can self-report their errors with a high degree of confidence (Akdogan & Balci, 2017).

Electrophysiology and Behavioral Studies

Electrophysiology studies have added to the body of evidence on temporal metacognition. An M/EEG study using a temporal production task with the objective of repeatedly producing the same single interval duration, involved asking respondents to first judge their own performance (Kononowicz et al., 2018). Afterwards, they were provided with 100% directional feedback in two blocks out of the six and 15% feedback on the remaining blocks. The initial self-assessment of their performance prior to feedback matched the true interval duration and β power value, a numerical quantity corresponding to the signal strength of the beta oscillation (15-40 Hz) at a specific time and frequency. Beta power operated as an index of the actual duration and the self-evaluative ability to track timing errors, such that increases in the power reflected the

increases in duration (Kononowicz et al., 2018). In yet another single duration temporal production study, Brocas et al. (2018) tasked participants to generate interval durations of 30+ sec repeatedly for 10 trials and introduced a reward scheme to incentivize making accurate temporal estimates. In this study, participants accurately self-evaluated their performance after a block of trials and correctly identified what proportion of trials were above or below the target interval duration (Brocas et al., 2018). Although accurate in their assessments of bias or tendency to overestimate or underestimate, the participants were less successful in prediction beforehand or correction of their responses (Brocas et al., 2018). More recently, this self-awareness of timing ability and the capacity to track reward history has been observed in rodents (Kononowicz et al., 2022). Rats self-produced a single duration (always 3.2) and revealed their knowledge of whether a small or large error was made by choosing between two ports with differing quantities of pellet rewards associated with the size of the error commission (Kononowicz et al., 2022).

Metric Error Monitoring Systems

Temporal metacognition is the ability to self -assess and introspect one's timing ability without prior sensory input or learning and can involve predicting errors in timing (Kononowicz et al., 2009). Error tracking mechanisms have been reported for temporal, numerosity (Dunyan & Balci, 2018,2019), and spatial errors (Dunyan & Balci, 2020), implying that there may be a common metric error-monitoring system that underpins magnitude-based representations (Duyan and Balcı 2019, Bader & Wiener, 2021). This metric error monitoring system is also impervious to social influence (Oztel et al., 2021).

Participants performed time reproductions and made judgements while a third-party observer watched yet their temporal error monitoring activity remained intact (Oztel et al., 2021).

Alternative Hypothesis: Metacognitive Readout

Other investigations of the neural basis of temporal metacognition have described an alternative mechanism to temporal error monitoring – temporal metacognitive readout. This alternate theory proposes that there is a secondary representation of internal durations that allow for evaluations of internal timing. It is based on the previously described beta power and its tendency to linearly scale with self-evaluation of the interval and the self-generation of the interval duration (Kononowicz and Wasserhove, 2019). Testing these two hypotheses involved a simultaneous M/EEG study in which participants were requested to produce a duration (always 1.45 seconds) and report the signed magnitude for how far they were from the target (Kononowicz and Wasserhove, 2019). No changes were observed in the amplitudes of the error positivity and error-related negativity, two event-related potentials that profile errors, despite the varying short, medium, and long self-produced and self-evaluated durations. However, a single trial time-frequency analysis of the time after producing the temporal duration but prior to its self-evaluation revealed an additional higher alpha power for shorter durations and lower alpha power for longer durations. Notably, beta power during the same interval predicted the emergence of this additional oscillatory power, the post-interval alpha power, reflective of the signal strength of the alpha oscillation for the readout coding for

the duration estimates and the signed magnitude difference between the target and produced interval, again lending support to the metacognitive readout hypothesis (Kononowicz & Wasserhove, 2019). The new post interval alpha power could be indicative of reorienting attentional focus after self-generation and evaluation of durations that are long. It could also relate to the alpha-beta coupling responsible for ensuring that durations are produced with precision (Grabot et al., 2019).

Metacognition and Confidence

Despite the debate as to what hypothesis – temporal error detection or metacognitive readout is better suited -- understanding the anatomy underlying temporal metacognition is critical. The neural substrates for decision confidence, a marker to evaluate decisions and guide future behavior are linked to metacognitive ability and have been associated with an array of brain regions. Proposed areas to represent confidence determined by single unit recordings included the orbitofrontal cortex in rodents (Kepecs et al., 2008,), dorsal pulvinar neurons (Komura et al., 2013) supplementary eye fields (Middlebrooks et al., 2012) and lateral intraparietal area of monkeys (Kiani & Shadlen, 2009), and the amygdala and the hippocampus in humans (Ruthishauser et al., 2015). Human fMRI studies point towards the ventromedial prefrontal cortex, the rostral medial

prefrontal cortex (Lebreton et al., 2015), and the ACC and dorsomedial cortex (Sarafyazd & Jazayeri, 2019) as regions for encoding confidence (Pouget & Kepecs, 2016).

An imaging study which employed cognitive tasks on belief judgements based on semantic knowledge of geography and history and another on time estimation recruited anatomically separate regions of the brain. However, confidence-related behavioral measures including accuracy, reaction time, confidence of preceding trial shared the same architecture and a domain-general network representing confidence (Roualt et al., 2022). With regards to anatomy, regardless of the type of cognitive task, the imaging results indicated that confidence was positively correlated with activity in the ventromedial prefrontal cortex and negatively correlated with the pre-fronto-parietal network (Roualt et al., 2022).

Clinical Conditions and Metacognitive Disruptions

Clinical conditions highlight the impairments in temporal metacognition when time perception is disrupted. A cohort of autism spectrum disorder (ASD) patients performed an auditory temporal reproduction task with no feedback but had confidence ratings and self-assessments of under or over-reproductions. Performance-wise, ASD children achieved the task objectives, and their mean reproduction accuracy and coefficient of variation were similar to neurotypical children (Doenyas et al., 2019). However, there was a mismatch between the level of subjective self-confidence and the actual objective performance in ASD children, suggesting that ASD children were unaware of their own temporal errors (Doenyas et al., 2019).

Another study of confidence and temporal metacognition investigated schizophrenics tested on a temporal order judgement (TOJ) task where they had to determine which movie clip came first in an encoded video sequence and produce a retrospective confidence judgement (Zheng et al., 2022). While they were able to confidently determine whether their selection was correct or not, schizophrenics relied more on their prior confidence history then the actual objective TOJ performance history to make the decision, suggesting a difference in metacognitive processing and use of a different processing schematic from that of neurotypicals (Zheng et al., 2022).

Our self-awareness of our own timing ability has been the topic of both behavioral and electrophysiological studies. This evaluative ability integrated error detection mechanisms and suggested the existence of a common metric error monitoring system for magnitude representations (line, space, numerosity, time). Also, the capacity to self-assess and evaluate timing behavior has been connected to confidence, which can be linked to specific brain areas. Additionally, temporal metacognition can be impaired, as observed by many clinical conditions with timing deficits.

Importantly, knowing that a timing error has occurred depends on first learning how to time interval durations. Learning to time relies on a trial-and-error reinforcement learning algorithm, which is the subject of the next section.

REINFORCEMENT LEARNING AND TIME PERCEPTION

Reinforcement Learning (RL) is a trial-and-error behavioral algorithm that describes how we make predictions about the consequences of our actions by incorporation of previous experiences into future scenarios to improve outcomes and maximize future rewards (Lee et al., 2012). The process of learning is fraught with errors, particularly when there is a mismatch between an expected and actual outcome, which signals a reward prediction error (RPE) (Hollerman & Schultz, 1998) and can be characterized by a loss function which maps the subjective cost of individual errors (Acerbi et al., 2012). A positive RPE results from an outcome that is better than expected whereas a negative RPE arises from an outcome that is worse than expected (Schultz, 2016). No error results when the outcome matches the expectation and RPEs update the value of the potential actions that lead to the outcome (Schultz, 2016). The computation underlying the RPE is coded by phasic dopamine (DA) release and is usually associated with an element of surprise and uncertainty (Hollerman & Schultz,1998). Positive RPEs are accompanied with an increase in phasic DA and are linked to striatal, medial prefrontal cortex, or ACC activity. Negative RPEs have reduced phasic DA in response to omitted rewards and are connected to insula and habenula activity (Garrison et al., 2013).

Notably, a recent study indicated how the shared striatal dopaminergic circuitry in timing and reinforcement learning may impact one another. Here, participants were shown two images with the latter image superimposed with positive or negative monetary value and were requested to determine which image was presented for a longer time (Toren et

al., 2020). Behavioral and imaging results revealed that positive RPEs yielded duration overestimates (perceived time dilation) and negative RPEs produced duration underestimates (perceived time compression), respectively with activity linked to the putamen (Toren et al., 2020).

When learning is complete, surprise diminishes between the expected and actual outcome (less RPEs) and the phasic DA returns to pre-learning levels during the response and back-propagates so that it is released at the cue-predicting event rather than during response (Schultz et al., 1997). This is important because it demonstrates that the brain documents the time interval between the cue and reward and that dopamine has access to this temporal prediction information throughout the learning process (Schultz et al., 1997; Fung et al., 2021).

Dopamine, Clock Speed, and Precision

Dopamine is central to reinforcement learning algorithms and has been known to modulate our internal clocks (Hollerman & Schultz, 1998), thus shaping and frequently distorting our time perception by increasing or decreasing clock speeds (Soares et al., 2016). For example, DA agonist drugs lead to over-estimations of temporal intervals (Pastor et al., 1992), whereas DA antagonists lead to temporal under-estimations (Buhusi & Meck, 2005; Gershman et al., 2014).

Dopamine also has a role in modulating precision of timing behavior, in readying for motor preparation for an action, and in encoding the internal representation of elapsed time. Pharmacological disruptions have solidified dopamine's role in these domains. When

a group of healthy participants were administered haliperdol (D1/D2 receptor blocker) and sulpride (D2 blocker) and performed the variable foreperiod task, they presented with impairments in temporal precision (Tomassini et al., 2015).

Dopamine, Reward, and Time

In addition to its role in RL, DA is implicated in the intersection of time perception with reward system (Fung et al., 2021) due to its modulation of clock speed. Whether the direction is an increase or decrease is dependent on whether DA is involved prior to or after reward delivery (Fung et al., 2021). Earlier than expected time delivery produces a higher pacemaker rate while later delivery elicits a reduction (Petter & Meck, 2018; Mikhael & Gershman, 2019). The RPE can also signal early or late reward arrivals and inform the subsequent behavioral output. Finally, similarly to its involvement in RL, dopamine can signal action initiation and ramp up the signal to a certain threshold depending on reward proximity.

From a computational perspective, predicting an action's value in RL paradigm in order to maximize rewards requires a precise measurement of time (Petter & Meck, 2018). Process-wise, model-free algorithms have been proposed to use time representations directly and linear temporal basis functions to predict rewards while model-based paradigms rely on training the algorithm to "what happens when" through a non-linear reward structure in conjunction with environmental simulations rather than direct environmental interaction (Petter & Meck, 2018). Regardless of the algorithm used, the rapid learning of time is hypothesized to have a biological substrate, the newly discovered

time cells in the striatum, supplementary motor area (SMA), and hippocampus that quantitatively encode and are preferably tuned to respond to a specific interval time durations (Petter & Meck, 2018). Time cells can be rescaled and receptive fields adjust swiftly when durations to reward change (Petter & Meck, 2018; Mikhael & Gershman, 2019) as with RL and after feedback. DA neurons mediate this rescaling in the corticostriatal synapses, by modulating the firing rate and altering the timing of the tonic dopamine signal and reward delivery (Petter & Meck, 2018; Mikhael & Gershman, 2019).

Tonic Dopamine, Reward, RL and Time

Interestingly, all of these effects also rely on tonic DA release, suggesting a dissociation between timing and RL across firing patterns (Soares et al., 2016; Simen & Matell, 2016). Tonic DA has been traditionally associated with response vigor and motivation (Niv et al., 2005) but it is also tied to both interval timing and RL. The theory of rational inattention connects these two functionalities together by linking tonic DA's role in average reward and heightened precision (Mikhael et al., 2021). DA controls precision, which, when higher, indicates more certainty about the environment, intensifying the ability to accumulate reward but at a cognitive cost. Whether that cost is worthwhile depends on the average reward size. The larger the average reward size, the greater the likelihood that the agent has the incentive to pay the cost. Tonic DA levels can bias behavior with high DA tipping the balance towards exploitation and low DA tilting towards exploration (Mikhael et al., 2021). The temporal estimates derived from

low DA have low precision and are context-dependent whereas high DA state responses are not based on context and are undertaken with more confidence (Mikhael et al., 2021).

Reinforcement learning uses the trial-and-error process coupled with an introspection of past experiences to improve behavioral outcomes when action selection occurs. Similarly, when learning to time an interval duration, this reflection on the past experiences can facilitate the decision for determining the duration of an interval. In particular, dopamine has a pivotal role in RL paradigms due to its affiliation with reward prediction errors, its ability to increase or decrease clock speed, its involvement in reward delivery and in enhancement of temporal precision. Notably, the influence of dopamine in RL is impacted by individual differences since genetic polymorphisms of the dopaminergic system may impact the level of dopamine in the brain and elicit differential effects on time perception.

IMPACT OF INDIVIDUAL DIFFERENCES ON TIME

An important factor to consider when learning to time are individual differences. In this realm, the discussion will be center upon cognitive styles, personality and genetics.

Cognitive Styles

Cognitive styles that delineate an individual's approach to learning and processing information play an important role since the strategy for acquiring, organizing and manipulating material can preferentially impact timing behavior (Farmaki et al., 2019). Field independent style learners derive patterns from complex visual images and investigate individual parts of the image while the field dependent style learners need contextual cues to comprehend the holistic image and is less able to distinguish objects from background images (Farmaki et al., 2019). These visual processing differences translate to varied behaviors and disparate impacts on temporal learning (Teghll et al., 2022). In a recent study of cognitive styles, participants were tested on a novel temporal learning task that expected them to learn and reproduce a stimulus duration that was internally or externally-based. In the internally based condition (IBL), the stimulus duration was fixed but the events demarcating the duration in a trial varied, while in the externally based condition (EBL), the stimulus duration varied but the number of events within a trial was constant. Field independent learners were significantly more accurate than field dependent learners in the internally based condition (IBL) and both groups

were more variable (less precise) in the EBL condition compared to the IBL. Error scores were more elevated in the internally-based conditions for both types of learners (Teghill et al., 2022). These results revealed the extent to which cognitive styles and task context can control suprasecond temporal learning.

Personality

The interaction of personality with temporal learning can also influence timing accuracy and metacognitive judgements. Past research has demonstrated that neuroticism did not have any relationship to absolute or directional timing errors in a time reproduction task with intervals ranging from 5-40 seconds (Rammsayer, 1997). In this same study, extroverts, when compared to introverts were more likely to over-estimate and inaccurately assess time (Rammsayer, 1997). High scorers on the psychopathy scale also exhibited time over-estimation (Rammsayer, 1997). More recently, participants were tested on a modified temporal bisection task were administered a schizoptypy personality test from the O-Life questionnaire (Corcoran et al., 2018). Higher scores on this assessment for impulsivity, unusual experiences, and cognitive disorganization negatively correlated with accuracy and metacognitive judgements, illustrating that personality can partially explain certain timing behaviors (Corcoran et al., 2018).

Genetic Differences

Genetic differences due to single nucleotide polymorphisms of genes impacting the dopaminergic system are another individual-level feature that effects subjective time

perception. Two polymorphisms--one associated with reduced D2 striatal receptor density (DRD/ANKK1-Taq1a) and another, the COMT Val158Met, a gene linked to increased activity of the COMT enzyme which metabolizes dopamine, have shown lower precision of time estimates (Wiener et al., 2011). This is related to BOLD activity in the basal ganglia and prefrontal cortex (Wiener et al., 2014). Also, of relevance, DA polymorphisms have been shown to alter the impact of reward magnitude on temporal estimates (Balci et al., 2013). One possible explanation for these effects is that increased DA tone leads to a "sharpening" effect on the temporal basis functions used for estimating time (Michael & Gershman, 2019) and is represented by duration tuned neurons occurring throughout the brain, but most notably in the SMA (Protopapa et al., 2019; Wiener et al., 2010).

Individual differences may influence the learning of interval durations in conjunction with cognitive styles and the type of learners. Personality type may also modulate time perception and timing awareness. Notably, extroverts are more likely to exhibit timing errors and over-reproduction and individuals higher on the impulsivity and disorganization on schizoptypy questionnaires perform poorly on timing accuracy and metacognitive judgement. Genetic differences due to DA polymorphisms from enzymes that metabolize dopamine to changes in striatal receptor density can impact temporal precision or modify the effect of reward on temporal estimation.

With a solid foundation of individual level variations that impact time perception and time awareness, the focus may shift to how we measure what transpires on an electrophysiological level as we time durations. An important electrophysiological

signature that profiles time perception is the contingent negative variation, the topic of the next section.

CONTINGENT NEGATIVE VARIATION

Event-related potentials (ERPs) can give us the temporal resolution of events and function by time-locking to cognitive events, supplying us with insight on the influence of learning and feedback in guiding timing behavior. Critical to the narrative on time perception is the contingent negative variation (CNV), an endogenous, slow, negative-deflecting cortical signature due to its strong involvement in temporal expectation, interval timing, and memory encoding of interval durations (Macar, 2002;2003). It is response-locked signal with a frontocentral distribution whose appearance depends on a behavioral response following a warning (S1) and target stimulus (S2) and was thought to reflect motor preparation and expectation (Walter et al., 1964; Falkenstein, Hoormann, Hohnsbein, & Kleinsorge, 2003) and attention (Rohrbaugh & Gaillard, 1983). An initial orienting wave, seen in early response selection, is referred to as the initial CNV (iCNV) while a later expectancy wave profiles the motor preparation prior to the S2 is known as the terminal CNV (tCNV) (Sahai & Tandon, 2000). Importantly, the waveform transitions to a biphasic wave after two seconds (Sahai & Tandon, 2000).

CNV and Time Perception

The CNV shows a characteristic ramping up pattern of activity (Casini, 2011; Kononowicz et al., 2014; van Rijn et al., 2011) associated with the accumulator in the centralized clock model of timing and is linked to the supplementary motor area (SMA) (Casini, 2011; Kononowicz et al., 2014; Macar et al., 1999) an area that is strongly

implicated in time perception (Wiener et al., 2010) and has exhibited temporally tuned neurons (Protopapa, 2019; Merchant et al., 2013). The CNV has also been linked to duration encoding and duration discrimination in a visual temporal discrimination task in which the morphology of the waveforms varied for the different comparison durations and was the most easily identifiable for the longest duration (Tarantino et al., 2010). The CNV's role in duration discrimination extends to both sub and supra-second intervals and increasingly higher negative amplitudes and longer peak latencies are seen as it approaches the standard memorized interval (Zhang et al., 2021). This suggests that the CNV amplitude profiles the comparison of durations while the latency represents the decision-making feature (Zhang et al., 2021).

CNV and Error Monitoring

Furthermore, this ERP has been connected to a timing study focused on error correction. In a time frequency study, the CNV's peak latency coincided with subsequent behavioral adjustment for tapping stimuli that were either shifted forwards or backward in time (Jang et al., 2016). Other studies on the confluence between timing and performance monitoring with the CNV have focused on tool use in sports activities (eg. bats in baseball) and have used a coincident timing task to model this real-world application. Participants use force-sensitive keys to move a rotating stimulus in an angular direction around a clock face for a target interval duration while a CNV was recorded simultaneously (Masaki et al., 2012). In this task, the CNV amplitudes were higher for faster velocities and longer

time-to-peak force conditions, likely because more pre-programming attentional resources and conscious effort was needed (Masaki et al., 2012).

Dopamine Tone and the CNV

The CNV is also a sensitive index of the levels of DA in the brain or DA tone, and neuropharmacological evidence centers on the finding that higher negative amplitudes are associated with greater DA levels (Linssen et al., 2011). Increased CNV amplitudes were seen when healthy volunteers were given placebo, 10, 20, or 40 mg of methylphenidate, showcasing a dose-dependent impact of the drug (Linssen et al., 2011). L-dopa and bromocriptine (a DA-like chemical in the brain) administered to Parkinson's Disease (PD) patients led to increased CNV amplitudes (Amablie et al.,1986). In an implicit timing study with variable stimulus onset times, moderate to severe PD patients that were off-medications for one day displayed reduced CNV amplitudes, absence of an anticipatory negative wave, and no temporal preparation (Praamstra & Pope, 2007).

Due to its ubiquitous presence in the basal ganglia, its role in timing and reward, and its association with the striatal beat frequency model, dopamine can also indirectly influence the contingent negative variation (Kononowicz, 2015). Starting from the onset of any to-be-timed interval, the ventral tegmental area releases dopamine to reset the phase of cortical oscillations to the striatum (Kononowicz, 2015). This action, dubbed as the "start gun" ensures that all of the cortical oscillations will initiate from the same phase, enabling coincident detection to occur and readout of the duration code (Kononowicz, 2015). Any disturbance of dopamine via pharmacological means could

cause variability in resetting and coincident detection, thereby reducing timing precision (Kononowicz, 2015).

fMRI-EEG Studies of the CNV

As a neural signature that can link together the subcortical and cortical structures, the CNV is a good candidate for fMRI-EEG studies. For example, a fMRI-EEG reward anticipation study profiled the CNV in this context using connectivity analysis (eg: mediation, dynamic causal modeling) (Plichita et al., 2013). Thalamic BOLD activation mediated the CNV signal and the BOLD activity in both the SMA and the ventral striatum, presenting evidence that thalamic BOLD can predict the CNV and operate as a top-down signal from SMA to the VS and the SMA to the thalamus (Plichita et al., 2013). This builds on an earlier fMRI-EEG study probing CNV-linked neural activity related to peripheral autonomic arousal through galvanic skin response (Nagai et al., 2004). Here, Nagai and colleagues (2004) described how trial-by-trial CNV amplitudes modulated BOLD activity in the bilateral thalamus, anterior cingulate and the SMA, again uncovering the importance of thalamocortical interactions in modulating the CNV.

The CNV is an essential ERP for tracking durations and discerning between different durations and it has been shown that the SMA is the source generator for the accumulator in the clock time model. In addition to its affiliation with time perception, the CNV is also associated with error monitoring and is heavily modulated by the level of dopamine, which may impact RL and learning of interval durations. There is also evidence to show CNV amplitudes can be used to predict BOLD activity in simultaneous fMRI-EEG

studies, notably in the SMA. It follows from this that the CNV is a critical ERP that appears in the estimation and reproduction phases of my time reproduction task. However, what transpires during the feedback phase? Another event related potential, the reward positivity, chronicles feedback related events and is discussed more extensively in the next chapter.

REWARD POSITIVITY (REW P)

A decision-related ERP that tracks feedback is integral to comprehending how feedback impacts human time estimation and learning to time. In this regard, to assess an outcome as rewarding or aversive (Gehring, 2002), a useful ERP and evaluative biomarker is the Reward positivity (RewP), which is a positive deflection elicited post-feedback in probabilistic trial-and-error learning tasks (Holroyd & Coles; 2002 Heydari & Holroyd, 2016). The RewP indexes RPEs and exhibits larger amplitudes for unexpected positive (rewarding) events compared to unexpected negative events, with more positivity on correct feedback trials and less on incorrect feedback trials (Holroyd & Coles; 2002; Heydari & Holroyd, 2016). By monitoring reward prediction errors (RPE) (Holroyd & Coles, 2002), the RewP, generated by the ACC, ventral striatum and medial frontal cortex, uses these contextually sensitive RPEs and dopaminergic signals from the basal ganglia (Heydari & Holroyd, 2016; Holroyd et al., 2008) to "learn" the value of actions via reinforcement learning and the midbrain phasic dopamine (Umemoto, 2017; Holroyd & Coles, 2002).

Reward Positivity and Learning

Fittingly, the strength of the RewP response is reflective of learning-related changes over time (Krigolson, 2018), due to its association with RPEs and because learning provides an opportunity for the performance monitoring system to shift focus from using external to internal information to track performance (Luft, 2014). As learning

occurs, the amplitude of the FRN/RewP wanes (Krigolson, Pierce, Tanaka, and Holroyd, 2009; Krigolson et al., 2014; Bellebaum and Colosio, 2014; Bellebaum and Daum, 2008; Eppinger et al., 2008; Luque et al., 2012; Sailer et al., 2010; Walsh and Anderson, 2012; Krigolson, 2018). Diminished RewP amplitudes can also be seen with individuals who learn at different rates (fast and slow learners) or who encounter varying task difficulty (easy vs. difficult) (Krigolson, 2018).

The RewP is an ideal feedback marker for tracking positive and negative outcomes and for indexing RPEs. RewP amplitudes are sensitive to learning-related changes and exhibit diminished amplitudes as individuals progressively learn a task. This is particularly relevant to my paradigm for rapid, one trial learning of interval durations.

Equipped with an understanding of the biomarkers for measuring temporal learning, we shift focus to more of a behavioral level of how feedback modulates time perception, feedback delivery methods, and clinical conditions in which feedback is affected.

FEEDBACK AND TIME PERCEPTION

There is behavioral and electrophysiological evidence to demonstrate human self-awareness of time but there are questions about what this entails (Akdogan & Balci, 2017; Kononowicz et al., 2018). Evaluating timing aptitude in the context of feedback and learning may broaden our comprehension of internal metacognitive process and its role in time perception. Management of errors related to early or late timing with or without external feedback are not fully understood. Studies on the impact of feedback on time perception have produced conflicting results, particularly due to the variability in the type of feedback delivery. Experimental timing paradigms offer a broad array of options ranging from no feedback, magnitude and directional feedback, magnitude-based feedback only, or directional-only feedback.

The Many Purposes of Feedback in Time Estimation

My design was based on the fact that feedback has a variety of purposes. In addition to simply supplying knowledge and guidance about the behavioral response (Salmoni et al., 1984), feedback has numerous other uses. It reduces response drifts over the experimental trajectory (Salmoni et al., 1984; Riemer et al. 2019) and may be erroneous or correct, but my study concentrates on correct feedback that tends to positively adjust behavioral responses (Salmoni et al., 1984). Its delivery may be absolute—after every trial or on a percentage of trials (relative). Additionally, feedback can be a motivational factor and act as an implicit reward for behavioral learning

(Salmoni et al., 1984; Tsukamoto et al., 2006). Feedback can be true or false and imaging studies of true feedback have shown activation in the thalamus, insula and striatum in a time estimation task (Tsukamoto et al., 2006). Post-error feedback can also facilitate the learning of time intervals (Ryan & Robey 2002). Feedback may be processed differently depending on the quality of the learners and is reflected in a well-functioning performance monitoring system (Luft et al., 2013).

Feedback's role in reducing noise in order to enhance precision and reduce behavioral variability is a noteworthy benefit. Recently, researchers showed that the rewarding or nonrewarding nature of the previous trial outcome causally controls the current trial behavioral variability in a ready-set-go paradigm, a motor context-dependent timing task where subjects were required to flexibly produce timing intervals using either a keypress or eye movement (Wang et al., 2020). When given probabilistic feedback, the participants' timing variability was higher for incorrect trials than correct trials regardless of the error size (Wang et al., 2020). This finding aligned well with my own past behavioral study's results (included here as Experiment I) demonstrating that the second trial performance following previous on-target feedback improved temporal precision (Bader & Wiener, 2021). Further evidence of feedback's beneficial effect on precision comes from a study that examined bias and variance changes for three time estimation tasks with a single interval design—motor reproduction, auditory comparison (duration discrimination), and auditory reproduction—and found that in all three tasks, participants overestimated time durations (Shi et al., 2013). Auditory feedback, included as a component of the auditory reproduction task, produced a lower overestimation bias and

variance than the motor reproduction task, although the bias still surpassed the auditory comparison task. In this same study, the signal to noise (SNR) ratios were determined by varying the decibel levels of the comparison and feedback tones thus altering the comparison/feedback ratio and simultaneously introducing pink noise to produce a varied SNR. This was later manipulated to yield low and high SNR conditions, and the variances on the reproduced interval, measured by standard deviations, were reduced in the high SNR condition compared with the low SNR in the same auditory reproduction task (Shi et al., 2013). Similar benefits of auditory feedback have also been observed in an experiment performed by Mitani and Kashino (2018), which required participants to reproduce the duration of a single tone after hearing it twice successively. Feedback was then delivered, and participants indicated whether they were early or late in responding. Bias and variability improved, self- judgement of timing error matched the actual temporal reproductions, and serial dependency was dampened but only for subsecond rather than suprasecond intervals (Mitani and Kashino 2018). My previous behavioral study (included as Experiment I here) extends the findings of these two studies to the visual modality and demonstrates a benefit in reducing timing variability in the longer suprasecond range (Bader & Wiener, 2021).

In addition to supplying informational content to update behavioral responses, the provision of feedback can be rehabilitative and therapeutic in clinical conditions characterized by aberrant temporal processing. Recently, a group of PD patients were tested on a time production task and other cognitive tasks (Homna et al., 2021). Feedback, given over the course of four weeks, involved viewing the digital stopwatch to

record the actual duration and compare it to the target duration. This type of feedback delivery provided advantages to both time perception and non-temporal domains. In addition to improved duration estimates, better accuracy in the Go/No Go and Stroop tasks and lowered impulsivity in other cognitive batteries were observed (Homna et al., 2021), illustrating that learning-related feedback effects could be transferred to other cognitive processes.

Comparison with other Feedback & Time Perception Studies

A landmark study in temporal error monitoring involved using a temporal reproduction task to assess how subjects reproduced a range of suprasecond intervals; their findings demonstrated that humans are aware of both the magnitude and direction (early/late) of their timing errors despite not receiving any external feedback (Akdogan & Balci, 2017). Another recent behavioral study used a temporal production task, in which subjects were asked to repeatedly produce a single duration (3 sec) and compared performance during a condition when only the magnitude of the error was given (absolute) against another condition in which both the magnitude and direction (signed) were given (Riemer et al., 2019). Signed feedback delivery yielded more behavioral adjustments in opposition to the direction of the error in subsequent trials, reduced bias in temporal estimates, and produced a more accurate and better calibrated performance when compared with absolute feedback. This study illustrated that directional information was not intrinsically accessible to the subject and that the participant's internal timing error representation failed to include that error direction. Furthermore,

subjects assigned to the absolute feedback group also tended to report an overreproduction of the interval duration when in reality, they were under-reproducing (Riemer et al., 2019). A key difference should be noted between these two studies, notably that feedback and retrospective self-judgments respectively were given following an entire block (Riemer et al., 2019) rather than trial by trial as in the Akdoğan and Balcı (2017) experiment. Task context also played a crucial role, as different tasks were used for the two studies; Akdoğan and Balcı (2017) used a temporal reproduction with a mixed set of intervals while Riemer et al. (2019) used a temporal production task with a singly presented interval.

Methodological Issues with Past Feedback and Time Studies

Methodologically, using an appropriate feedback technique is pivotal to fully understanding the complexities of self-timing awareness. The traditional feedback structure in psychophysics studies is best suited for single interval reproductions because the same interval is successively reproduced; therefore, the majority of the studies described above are single interval experiments. Challenges arise when reproducing a random set of a mixed range of intervals because corrective guidance is given on one interval duration, yet the next interval may be of a different duration (Ryan, 2016). This is problematic since there is no opportunity to use the feedback from the previous trial to the new trial, so the feedback is frequently misapplied to an entirely different duration (Ryan, 2016). To rectify this issue, our past behavioral study introduced a “redo” trial, which allows the subject to use the original feedback from the first trial in a second trial

of the same duration (Bader & Wiener, 2021). I hypothesized that the redo trials will be beneficial to subjects for improving performance and for minimizing the Vierordt effect (underestimation of long intervals and overestimation of short intervals) (Ryan, 2016). It is for this reason our past behavioral study (Experiment I) also incorporated absolute (nondirectional) feedback: to assess whether subjects possess awareness of the direction of the timing errors (Bader & Wiener, 2021). If there is a substantial directional awareness of timing error, then the central tendency would be reduced (Bader & Wiener, 2021).

Clinical Conditions and Feedback

Disruption in timing and learning to time are observed in children with clinical conditions involving impairments in dopaminergic pathways, such as Attention Deficit Hyperactivity Disorder (ADHD) and Neurofibromatosis (NF1). Prochnow and colleagues (2021) compared both patient groups to healthy control children and found that the patient participants presented with deficits in feedback-based learning of time estimation. Children in all groups were instructed to press a key 1-2 seconds following the appearance of a white square in a time production task. For responses from 1000-1400 ms, a smiley face and written feedback indicating it was correct were given. Early responses (400-1000 ms) and late responses (1400-3000 ms) were met with written feedback and sad faces. Data from the on-time trials for three blocks were analyzed to examine learning-related effects stemming from feedback. For ADHD patients, the reaction times were unstable amongst the three blocks, while the NF1 group was characterized by steady high reaction times but no fluctuation across the blocks. Both findings reiterated an absence of learning-based

adjustments of the temporal estimates in the NF1 and ADHD groups, unlike the healthy controls who exhibited appropriate feedback-based learning and steadily approached the target duration across the three blocks (Prochnow et al., 2021).

Lessons Learned Applied to Current fMRI-EEG study

Holistically, these historical studies on feedback have informed our experiments. Insight gleaned on methodology, experimental design, and the numerous uses of feedback were valuable during our current investigation of what transpires on the neural level when participants are given a second opportunity to generate a temporal estimate and how feedback modulates the resultant temporal responses.

METHODS

Three experiments were conducted for this study. Experiment I was behavior-only study which was not conducted in the scanner and involved a between subjects design and two groups: an on/off and no feedback condition. Data from this first experiment has been published (Bader & Wiener, 2021). Experiment II had a within subjects fMRI-EEG design with the on/off condition. Experiment III was another behavior-only study but it varied in the frequency of single or double trials and compared a group with a high frequency of double trials (initial+ redo) with a group of low frequency of double trials.

Table 1. Experimental Set-up

	Experiment I	Experiment II	Experiment III
Context	Behavior only	fMRI-EEG	Behavior-only
Feedback Conditions (Sample Size)	1. On/Off (17) 2. No Feedback (19)	1. On-Off (23)	1. Low double (19) 2. High double (18)
Ages	1. 20.8 ± 3.84 SD 2. 19.6 ± 1.53 SD	1. 23.17 ± 4.58 SD	1. 21± 4.58 SD 2. 20.6± 3.50 SD
Gender	1. 5 males, 12 females 2. 6 males, 13 females	1. 12 males, 11 females	1. 14 males, 5 females 2. 14 males, 4 females

Subjects

For experiments I and III, George Mason University undergraduates were recruited via a research studies database or flyers. For the fMRI-EEG experiment (Experiment II), participants were recruited solely through fliers around the GMU

campus to target students. Eligible participants who completed the research study received undergraduate psychology course credit for their participation or were paid for their time. For both experiments, researchers gave each subject a questionnaire to determine eligibility prior to beginning the experiment. Participants with any neurological and psychological disorders, hospitalization for a psychological disorder, or diagnosis or treatment for substance abuse were excluded.

Experiment I

Twenty subjects each were originally recruited for the on/off target condition. For the final analysis, data from only 17 right-handed neurologically healthy subjects (average age 20.8±3.84 SD yr, five males, 12 females) in experiment I were analyzed. Two subjects did not fully understand the task parameters and one recruited subject later informed us that she had a concussion so these three were excluded. Another twenty right-handed subjects were also recruited for the no feedback condition; however, for the final data analysis, 19 right-handed subjects (average age 19.6±1.53 SD yr, six males, 13 females) were analyzed because one subject had outlier responses that varied three standard deviations from the average mean responses. The difference in ages between the on/off and the no feedback groups was also not significant $t(34) = 1.196$, $p = 0.245$. Additionally, a Pearson $\chi 2$ revealed that the gender ratio was not significantly different between the on/off and no feedback groups $\chi(1) = 0.020$, $p = 0.888$ in Experiment I.

Experiment II:

Twenty-seven neurologically healthy, right-handed subjects were recruited for the fMRI-EEG experiment (Experiment II). Four participants were removed from the sample for technical reasons. EEG event markers failed to load for all stages of the task for three subjects thus leading to missing and insufficient trial counts. Another subject was unable to complete the entirety of the temporal reproduction task inside the scanner. The final data analysis included twenty-three right-handed neurologically healthy subjects (average age 23.17±4.58 SD yrs, 12 males, 11 females).

Experiment III:

Forty subjects were recruited for Experiment III (behavior-only); however, for the final analysis, 37 right-handed and neurologically health subjects (average age 20.81±4 SD, 28 males, 9 females) were included. Two subjects were unable to finish the entirety of the behavioral experiment and there was a data loss for another subject due to a technical issue related to the computer. Nineteen subjects were assigned to the low double group (average age of 21±4.58 SD, 14 males, 5 males). Eighteen subjects were assigned to the high double group (average age of 20.6±3.5 SD, 14 males, 4 females).

An independent t-test revealed that the ages between the low double and the high double were not significantly different $t(35)=0.291$, $p<0.772$ CI:-2.321-3.098. The Pearson's chi square $\chi(1)=0.084$, $p=0.772$ for the gender ratios was also not significantly different between the low double and high double groups.

Behavioral Paradigm

Experiment I and III, both behavior-only studies, were conducted outside of the scanner and did not involve EEG or imaging. The same temporal reproduction task was delivered via Psychopy2 on a 27-in Mac desktop while subjects sat ~ 60 cm from a computer screen (Dell S2716DGR, 120 Hz refresh rate) in the lab.

For the fMRI-EEG study (Experiment II) the temporal reproduction task was delivered via Psychopy2 from a Dell (120 Hz refresh rate) desktop and projected to Cambridge Research Systems BOLD Screen 32" 1920x1080 resolution screen situated ~1.5 meters outside of the MRI Bore. Participants with EEG electrodes attached to their scalp were laid inside the MRI bore and observed the experimental stimuli from a mirror inside the bore.

Experiment II started with the MRI scanner sending repetition time pulses to the stimulation PC (Dell) via the trigger box and also to the EEG computer through Psychopy's clock synchronization component. The task structure of the temporal reproduction task was comprised of three phases: estimation, reproduction, and feedback for all three experiments. These three phases were performed twice for each duration. Each trial initiated with a centrally presented fixation cross for a randomly presented duration of 2–6 s. In the estimation phase, a blue square was visually shown to the participant for one of five logarithmically spaced, randomly presented intervals (1.5–6 s). Until the square was on-screen, the participant was instructed to encode the duration in memory and to not use counting as a method to determine the elapsed time, which has

been demonstrated as an effective means of eliminating counting strategies (Rattat &Droit-Volet, 2012). Following the estimation phase, there was a 4- to 8-s gap prior to the reproduction phase. Then, the blue square reappeared on-screen in the reproduction phase and the participant was asked to press any number key when the blue square has remained on-screen for the same time duration as the time elapsed in the estimation phase. The subjects' keypress using the button box inside the scanner caused the square to disappear, signaling interval termination.

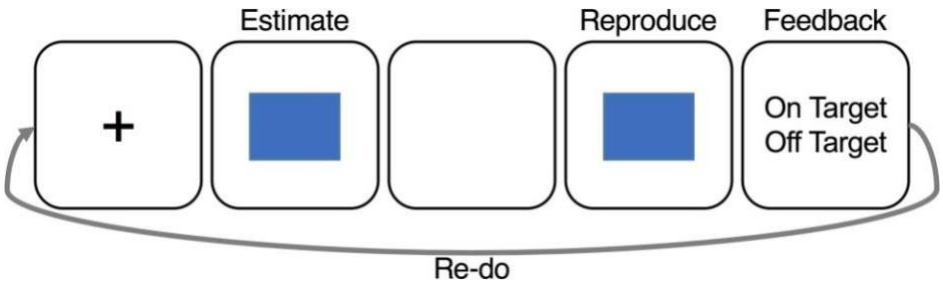

Figure 1. Task schematic of the Temporal Reproduction Task

After every trial in Experiment II and in the on/off condition of Experiment I, adaptive feedback (duration = 1 second) was delivered 2–4 s after the disappearance of the square and informed the participant whether the response was on-target or off-target; notably, this feedback provided no index of direction. On each trial, a feedback constant (k), starting with an initial value of 3.5 was adjusted such that that the reproduced interval had to be within the window [interval/k] and was updated according to the 1-up/1-down rule with a step size of 0.015 (Jazayeri & Shadlen 2010). If the participant's reproduced

interval was either 15% above or below the target duration, on-target feedback would be delivered; otherwise, off-target feedback was delivered. Critically, after each trial in Experiment II and the on/off condition in Experiment I, participants had a second opportunity (essentially a redo trial) to perform the entire sequence of phases (estimation, reproduction, and feedback) again, ensuring feedback was applied to the appropriate duration. After the second feedback in Experiment II, Psychopy waited for an amount of time specified by a random floating-point number with an exponential distribution before starting the next full trial (initial and redo). This was done to jitter the inter-stimulus intervals so that the trial durations and ISIs for all of the trials were within the total trial sequence time.

In total, Experiment II had 120 trials (10 durations/block × 6 blocks × two trials, initial and redo). Participants were given a break after each block for a total of six blocks. EEG triggers for each onset and offset of the estimation and reproduction phases for each of the five durations were sent from Psychopy via the trigger box from the stimulation PC to the EEG recording computer. The delivery of the on-target and off-target feedback markers for the initial and redo feedbacks were also sent from the button box which the subject pressed and trigger box to the EEG computer.

Subjects participating in Experiment I were assigned to either a condition with no feedback at all or an on/off condition. Similarly, to Experiment II, there are 120 trials (10 durations/block × 6 blocks × two trials) and participants were given a break after each block. Two groups performed the study with one experimental condition that delivered on/off feedback and another experimental condition that did not deliver feedback at all. A

different set of participants were used for each condition. In the on/off condition, on and off-feedback was provided for both trials while the no feedback condition still had two trials per duration but lacked any feedback for either the initial or redo trial.

Subjects participating in Experiment III did not always receive a second, redo trial and were randomly assigned to one of two groups with varying ratios of double (initial + redo) and single (initial only) trials. The two groups in Experiment III had a different set of participants for each condition. Experiment III had a low double group comprised of 80% of total trials with only one opportunity to perform the trial. The other 20% of total trials consisted of both an initial and redo trial. In the high double group, 80% of the total trials had a second chance (initial+ redo) whereas the other 20% of the total trials were single trials. Participants were blinded to the group assignment and to whether a specific trial would be a single or double trial as they performed the experiment. Experiment III had 250 trials total and five blocks and breaks following each block.

Experiments I and III were behavior-only and differed from the fMRI-EEG (Experiment II) in its absence of a clock synchronization component, no jittering after the second feedback in the double trials, and no EEG event markers for the onset and offset of each task phase.

Data Acquisition

Simultaneous raw EEG was recorded at 5000 Hz (Range: 16.384 mV, resolution: 0.5 uV and 10-250 bandpass filter) with a MR-compatible 64-channel (Brain Products) Ag/AgCl passive electrodes system as the participant was imaged inside the 3T Siemens Magnetom Prisma MR scanner. Electrode positioning (or the electrode montage) on the participants' scalps were based on the 10/20 system.

Online and ground references during the recording were FCz and AFz, respectively and impedances were maintained at 20kΩ. Gel specifically designed for a MR-compatible system was applied to the subjects' scalps. Head circumferences were measured, and the appropriately sized cap was selected when fitting the participant. The smaller 56-centimeter cap contained an additional vertical and horizontal electrooculograms (EOG). One vertical EOG was placed below the eye and the horizontal EOG was positioned at the outer canthus of the eyes. An ECG electrode (20kΩ) was also attached on the back of the participant close to the heart to record the electrocardiogram for all of the participants.

EEG data was transmitted from the cap via BrainAmp amplifiers (Brain Products) over fiber optic cables and a wave guide to the console room. EEG event markers for the various phases of the behavioral task including the first and second trial estimation onset and offset, reproduction onset and offsets, and the on and off-feedback were relayed via the Brain Products trigger box from the stimulus computer where the Psychopy experiment originated and received through a BNC connector from the button box (Current Design, 932 Interface) and delivered to the EEG computer (Dell). The scanner gradient and the EEG clocks were synchronized using a Brain Vision syncbox. The Psychopy experiment

was projected onto a Cambridge Research Systems BOLD Screen 32" 1920x1080 resolution screen situated outside of the MRI Bore. Visual stimuli were observed by the participant via a mirror in the MRI bore.

EEG Analysis

The Brain Vision Analyzer 2 (Brain Products) software was used for the initial EEG processing steps. Initially, the EEG data was segmented into six sections corresponding to the six BOLD runs using the magnetic resonance (MR) volume markers. Each EEG segment was then corrected for the MR gradient using template drift detection based on the Allen method (2000) and was downsampled to 256 Hz. Brain Vision Analyzer's baseline correction options enabled correction to the average and was computed over the whole artifact. The segments were then corrected for the cardio-ballistic artifact (Allen et al., 1998) using a combination of both automation and visual inspection of R-peak detection using Brain Vision Analyzer 2. Noisy EEG channels, detected through visual inspection, were corrected through topographic interpolation (spherical splines). Data was re-referenced to the mastoids (TP9/TP10) and low pass filtered at 30 Hz. Infomax-based independent component analysis (ICA) was used to remove blinks and movement artifacts. The six pre-processed EEG segments were stitched and appended together to reflect the chronological order of the runs. The newly stitched EEG data for each subject was fed into EEGLAB and further processed using the clean_raw EEGLAB plug in for detecting and separating noisy channels, drifts and flatlines from the data (Kothe et al., 2019). It applied

ASR (automated subspace removal) to detect and reject remaining artifacts produced by blinks, motion and muscle activity (Kothe et al., 2019).

Event Related Potentials (ERPs)

In-house MATLAB scripts using EEGLAB, as noted in the Appendix, were used to calculate and extract single trial ERP amplitude data both individually and across the group of all participants from the processed EEG data (see Appendix). The EEG data was segmented into separate epochs for the estimation phase, reproduction phase, on- and off-feedbacks using the event markers and the in-house scripts. The estimation and reproduction epochs were baseline corrected 1000 ms pre-stimulus whereas on- and off-feedback were baseline corrected from 500 millisecond prior. For the contingent negative variation (CNV), single trial frontocentral mean amplitudes were extracted from the following electrode arrays: FCz, Fz, Cz, FC1, FC2, F1, F2, C1, and C2. The mean CNV amplitudes from the initial and redo estimation and reproduction onset phases for an a-priori window from 430-598 milliseconds (Robinson & Wiener, 2020) were examined. To capture the Reward Positivity (RewP), the same electrode array was inspected and the amplitudes corresponding to the initial and redo trial and on and off feedback responses were extracted from a window of 400-550 ms.

fMRI Acquisition

A Siemens Magnetom 3T whole-body MR scanner was used to acquire all imaging sequences. First, a localizer was performed to identify the brain's position in space followed by a field map to measure the magnetic field inhomogeneity. Field mapping parameters were TE1=4.92ms and TE2=7.38 ms, TR=731 ms, FOV=208 mm, matrix (104x104) voxel size=2x2x2 mm and 72 slices were collected with a 2 mm thickness. Next, a structural magnetization-prepared gradient-echo-planar image (MP-RAGE) T1* was performed with the following values: repetition time (TR)=2300, echo time (TE)=2.23 ms, flip angle 8 degrees, field-of-view (FOV)=256 mm, matrix (256x256) 192 slices at a thickness of 0.88 mm were acquired with MP-RAGE sequence. The helium pump was turned off prior to the acquisition of the echo planar images (EPI) images. EPI T2* scans were then collected with the following parameters (TR=2390 ms, TE=30 ms, 90-degree flip angle, FOV: 192 mm, matrix: 94x94). Forty interleaved slices with a transverse orientation, a slice thickness of 3 millimeters and 2x3x3 mm voxel size were taken. Each participant underwent one localizer, one field map, one MP-RAGE and six BOLD EPI sessions.

fMRI Pre-Processing Steps

All pre-processing steps were performed in SPM 12 on 3D nifti files generated from the MP-RAGE, field map, and the six EPI T2 sequences. First, voxel displacement was calculated using the magnitude and phase images from the field map, followed by a slice

timing correction, realignment and calculation of six affine rigid movement parameters related to head movement and unwarping. Images were then normalized to standard Montreal Neurological Institute (MNI) anatomical space and mean BOLD values were computed, written, and smoothed. Behavioral data on onset times and durations for each of the various phases (estimation, reproduction, feedback) in both the initial and redo trials were extracted and loaded by an in-house batch processing Matlab script which then estimated and wrote a first order General Linear Model (GLM) for each individual participant using the BOLD images.

fMRI-EEG Processing

In-house MATLAB scripts, as noted in the Appendix, using SPM 12 loaded the extracted CNV and RewP amplitude EEG data, the behavioral onset and durations for all of the phases (estimation, reproduction, and feedback) for the initial and redo trials from each of the subjects, with the six processed BOLD images from each participant (see Appendix). The ERP amplitude regressors were parametrized and convolved with the hemodynamic response function so that the covaried EEG signal could be coupled with the mean BOLD activation. For each subject, a separate first-level general linear model for the combined fMRI-EEG datasets was estimated and written. Next, SPM's contrast manager was used to create contrasts to examine changes in BOLD activation between the task phases and between the initial and redo trials of those phases in this combined dataset. The specified contrasts and weights were then fed into an additional in-house Matlab script and

a second-level group GLM was estimated and written. Afterwards in SPM, one-sample t-test was performed for each contrast and whole brain group level results were displayed with a familywise error correction for multiple comparisons at the cluster level.

Statistics

JASP 0.16 (JASP team, 2021) was used to analyze the behavioral data from the temporal reproduction task in the two experimental groups independently. For all the experiments, the data was normally distributed and passed the Shapiro–Wilks test of normality for the absolute temporal error, accuracy, and precision (as measured by the coefficient of variation (CV)). The absolute temporal error was calculated as the reproduced duration – target duration for Experiments II and III. The CVs was calculated as the standard deviation of the mean reproduced durations/participant's mean reproduced durations and two separate CV values were generated for the initial and redo trials. A linear mixed model (fixed effects: duration, trial designation, target duration; random effects: subjects) was used to detect changes in absolute temporal error between initial and redo trials in Experiment II and between the low double and high double groups in Experiment III.

RESULTS

Behavioral Results

In this section, behavioral results for Experiments I-III are presented with a focus on initial and redo trials. Behavioral measures tested include accuracy which reveals how close the reproduced duration is to target duration; and precision, which is an indication of timing variability, and is measured by the coefficient of variation. The absolute temporal error at the single trial level, calculated as the absolute value of the difference between the target and reproduced durations, was also measured. Experiment I will have an additional set of results examining the second trial CVs based on first trial status of whether feedback was on or off along. Second trial slopes based on first trial status of on or off feedback are also displayed.

Experiment I:

Subjects administered the on/off feedback version of the temporal reproduction task exhibited central tendency with overestimation of short durations and underestimations of long durations. The accuracy of the reproduced times for the first and second trials was compared and a significant main effect of duration ($F_{(2.12,33.92)}$ = 291.655, $p < 0.001$, $\eta = 0.948$), of the trial ($F_{(1,16)} = 12.134$, $p = 0.03$, $\eta = 0.431$) and a trial × duration interaction ($F_{(2.297,36.758)} = 3.527$, $p = 0.034$, $\eta = 0.181$) were observed. Second trial estimates were more accurate and closer to the target durations, and there was less uncertainty in time estimation, as revealed by nearer estimations to the reference line or identity line.

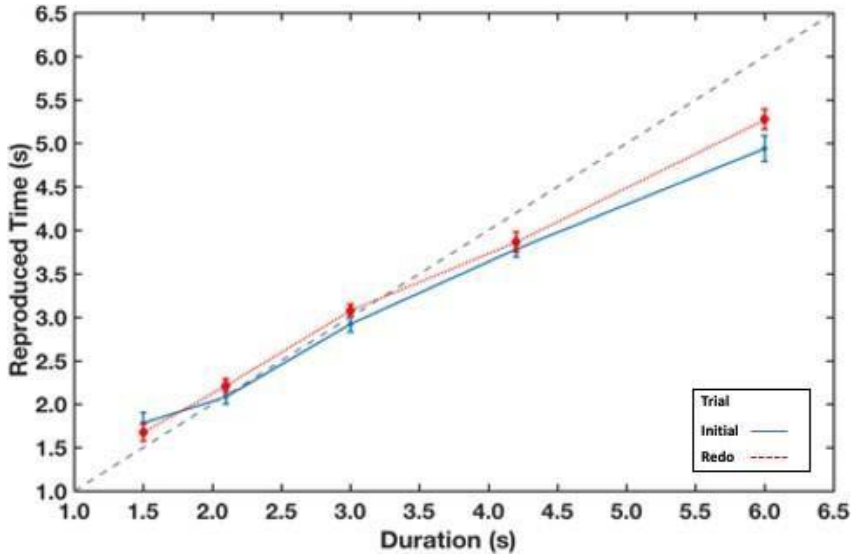

Figure 2. Accuracy of Reproduced Durations in On/Off condition by trial type. The initial trial is represented by the blue solid line and the redo trial is represented by the red dotted line. Data are expressed as reproduced duration in seconds ±SEM.

The second trial time estimates were also more precise ($F_{(1,16)} = 9.398$, $p = 0.007$, $\eta = 0.370$), as measured by the lower coefficient of variation in the second trial estimates. Similar to accuracy, precision also exhibited a main effect of duration ($F_{(1.553, 24.841)} = 8.862$, $p = 0.002$, $\eta = 0.356$).

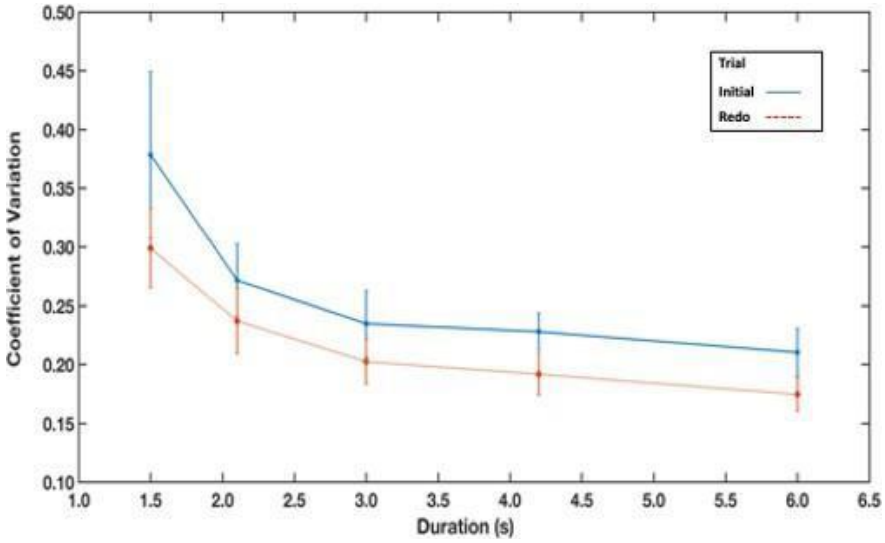

Figure 3. Temporal Precision in the On/Off Feedback Condition. The initial trial is represented by the blue solid line and the redo trial is represented by the red line. Data are expressed as the coefficient of variation ±SEM.

Similar to the on-off feedback condition, the subjects in the no-feedback group exhibited central tendency with subjects overestimating short time intervals and underestimating long time intervals. More accurate reproduced temporal estimates in the second trial for the no-feedback group signaled that they were reproducing the time closer to the target duration with significant differences between the original and redo trials ($F_{(1,18)} = 6.2$, $p = 0.023$, $\eta = 0.256$). Duration ($F_{(1.49,26.92)} = 123.03$, $p < 0.01$, $\eta = 0.872$) and the duration × trial interaction ($F_{(3.353,60.346)} = 2.786$, $p = 0.043$, $\eta = 0.134$) also varied significantly between the trials despite the lack of feedback.

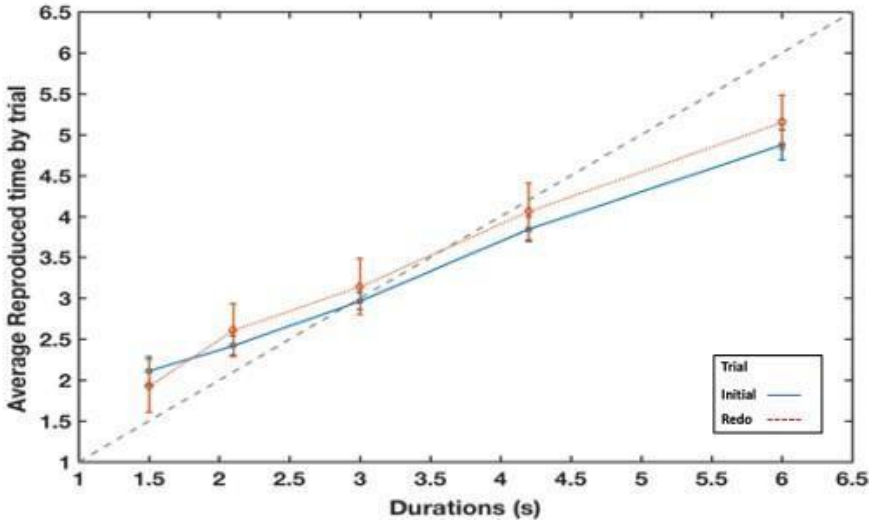

Figure 4. Reproduction Accuracy in the No Feedback Condition. The initial trial is represented by the blue solid line and the redo trial is represented by the red dotted line. Data are expressed as reproduced duration in seconds ±SEM.

Although more temporally accurate, subjects failed to show greater temporal precision, as evidenced by CVs in the redo trials of the no-feedback version of the task $F_{(1,18)} = 1.672$, $p = 0.212$, $\eta = 0.085$. No significant differences in precision were observed in the duration ($F_{(4,72)} = 1.921$, $p = 0.116$, $\eta = 0.096$) or duration × trial ($F_{(2.93,52.73)} = 2.583$, $p = 0.064$, $\eta = 0.125$).

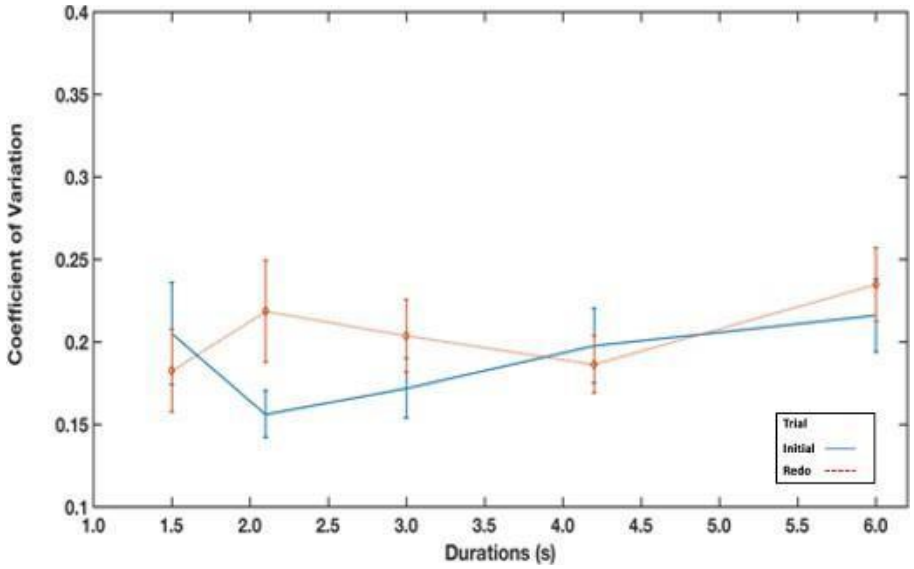

Figure 5. Temporal Precision in the No Feedback Condition.
The initial trial is represented by the blue solid line and the redo trial is represented by the red line. Data are expressed as the coefficient of variation ±SEM.

The delta precision was also calculated for each subject ($CV_{trial2} - CV_{trial1}$) in both the on/off and no feedback conditions. Notably, participants in the on/off conditions exhibited significantly reduced CV (higher precision) than the no-feedback condition $t_{(34)} = 3.234$, $p = 0.003$ (CI: 0.0223–0.09784).

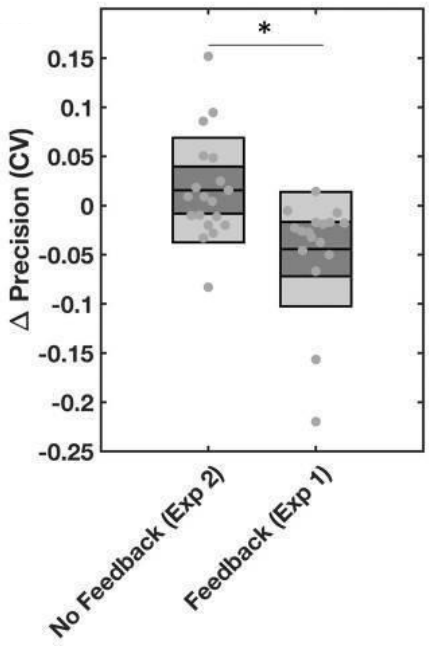

Figure 6. CV difference between No Feedback and Feedback
95% confidence intervals are represented by the outer boxes, and ±one standard deviation are represented by the inner boxes. Individual dots represent both sets of participants from the two conditions. The asterisk indicates a significant difference at $p < 0.05$.

An additional analysis of Experiment I involved dissecting the second trial CVs according to whether the first trial was on-target or off-target. Positive (on-target) feedback in the first trial resulted in significantly more precise estimates (lower CVs) in the second trial ($F_{(1,16)} = 8.106$, $p = 0.012$, $\eta = 0.336$) performance than negative feedback

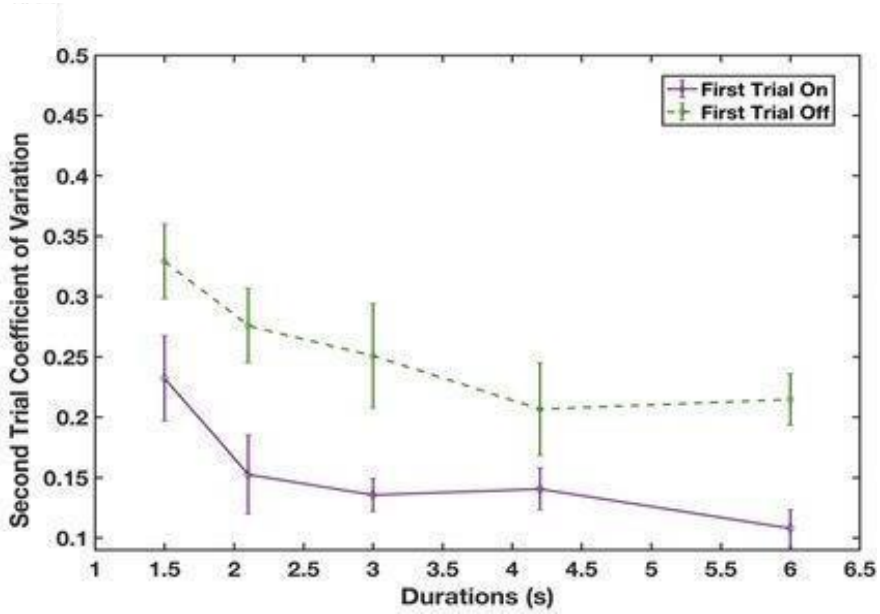

Figure 7. Second Trial CVs based on First Trial Feedback Status. The solid purple line represents the on-target responses whereas the green dotted line represents off-target responses. Data are expressed as the coefficient of variation ±SEM.

The second trial slopes which measure how certain the temporal estimates were also dissected into whether the first trial was on-target or off-target. The individual slopes of the redo trials $t_{(16)} = 4.699$, $p < 0.001$ between the first trial positive (on) and negative feedback (off) also varied significantly, demonstrating more certainty in temporal estimation following positive feedback

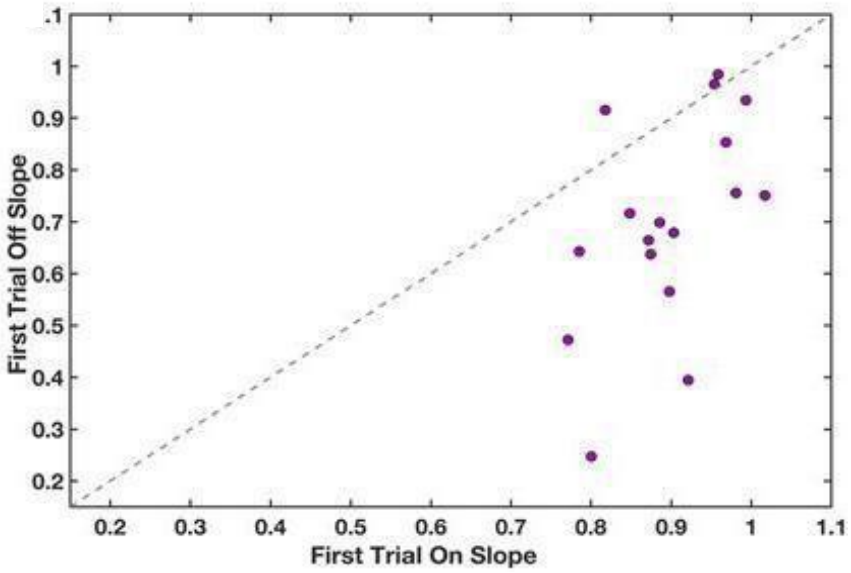

Figure 8. Second trial slope based on first trial feedback status.
Data is represented by a scatter plot with x and y coordinates corresponding to on- and off-target slopes, respectively of each individual. The reference line represents a slope=1.

Experiment II:

A linear mixed model was performed on the absolute temporal error, showing a significant reduction in the redo trial when compared to the initial trial ($p<0.015$, $F(1,190.7)=6.039$. Essentially, timing performance improved when provided a second chance.

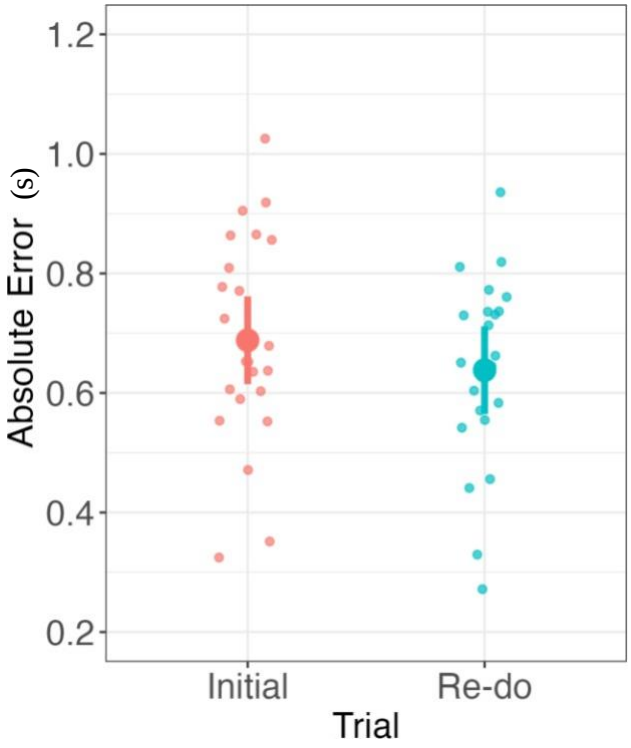

Figure 9. Absolute temporal error by trial type in fMRI-EEG.
The initial trial is represented by the pink dots and the redo trial is represented by blue dots. Data are expressed as target duration-reproduced duration ± 95% confidence interval.

A repeated measures ANOVA revealed that the participants' reproduced durations for the redo trials were also more accurate, thus nearer to the target duration and the identity line when compared to the initial trial $p<0.001$, $F(1,22) = 14.146$, $\eta=0.001$, again showing an improvement in temporal estimates. There was also a main effect duration $p<0.001$, $F(1.83, 41.422)=680.058$), $\eta=0.957$.

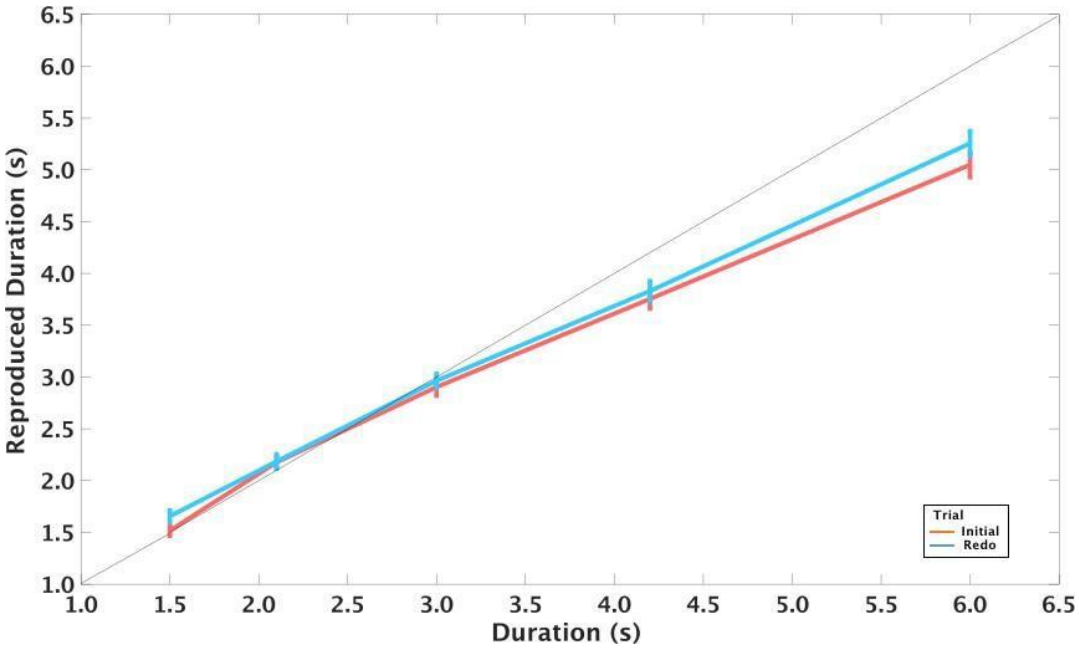

Figure 10. Accuracy of Reproduced Durations by trial type in fMRI-EEG. The initial trial is represented by the red solid line and the redo trial is represented by the blue solid line. Data are expressed as reproduced duration in seconds ±SEM.

Participants, however, did not display significantly better precision (lower coefficient of variation) in their redo trials $p<0.225$, $F(1,1.562)$, but did exhibit a main effect of duration $F(4,26.239)$ $p<0.001$.

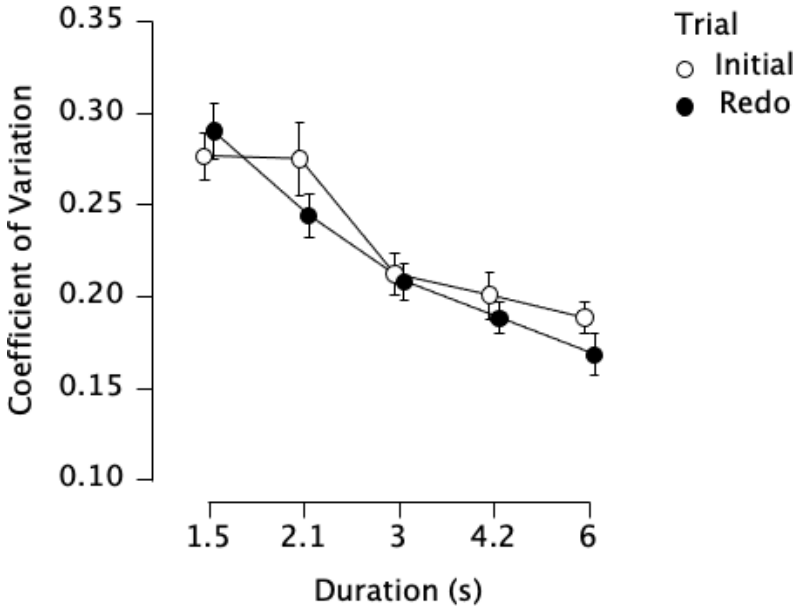

Figure 11. Temporal precision by trial type in fMRI-EEG.
The initial trial is represented by open circles and the redo trial is represented by solid circles. Data are expressed as the coefficient of variation ±SEM.

Experiment III:

Another linear mixed model was performed to compare the absolute temporal error between the low double (20 single:80 double) trial and high double (80 single:20 double) trial groups. Low-double group participants had significantly lower absolute temporal errors overall $F(1,35.06) = 6.433$, $p < 0.016$ than high-double group, demonstrating that when given only one chance, participants are more likely to exert more effort than when provided with two opportunities. Also, participants may be learning the underlying structure of the environment, adapting and anticipating either having a single or double trial. Similarly, to experiment I, both groups had significantly

reduced absolute temporal errors in the redo trial F (1,35.92) =15.326, p<0.001 and a main effect of duration F(1, 36.46)=68.285, p<0.001.

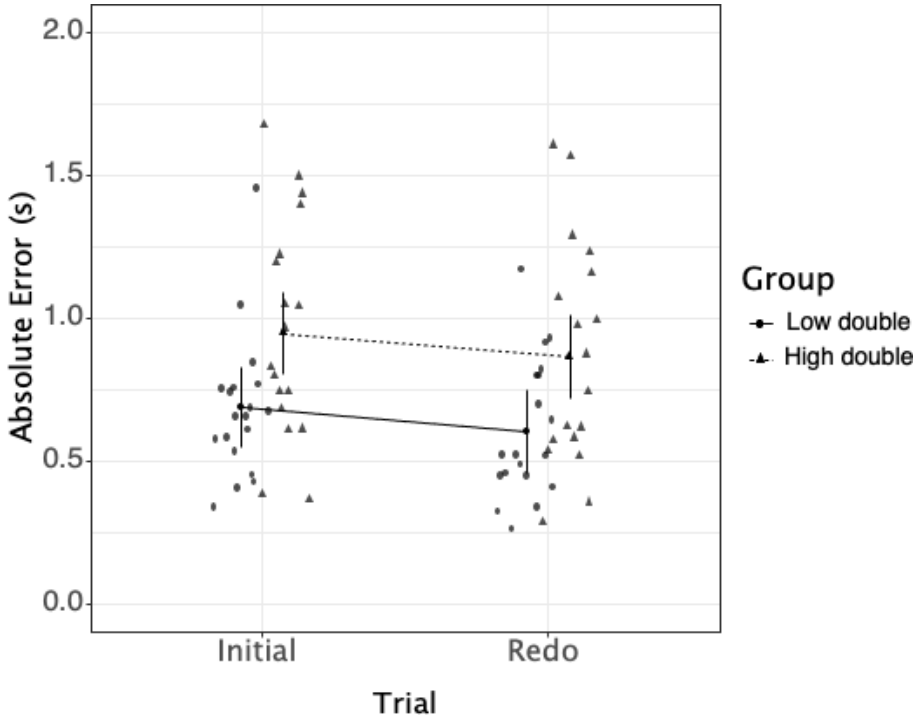

Figure 12. Absolute temporal error by trial and group type in uncertain environments. Low double group participants are represented by solid dots and high double group participants by solid triangles. Data are expressed as target duration – reproduced duration ± 95% confidence interval.

Accuracy, computed as the mean reproduced durations, did not significantly differ between the low-double or the high-double groups F (1,35) =0.173, p<0.680. Regardless of which group a participant was assigned, there was a main effect of trial with significantly more accurate redo trial estimates F (1,35) =15.121, p<0.001, η=0.008 and

duration F(4,140)=3.972, p<0.004 η=0.864 in concert with a duration x group interaction F(4,140)=3.972, p<0.004, η=0.007.

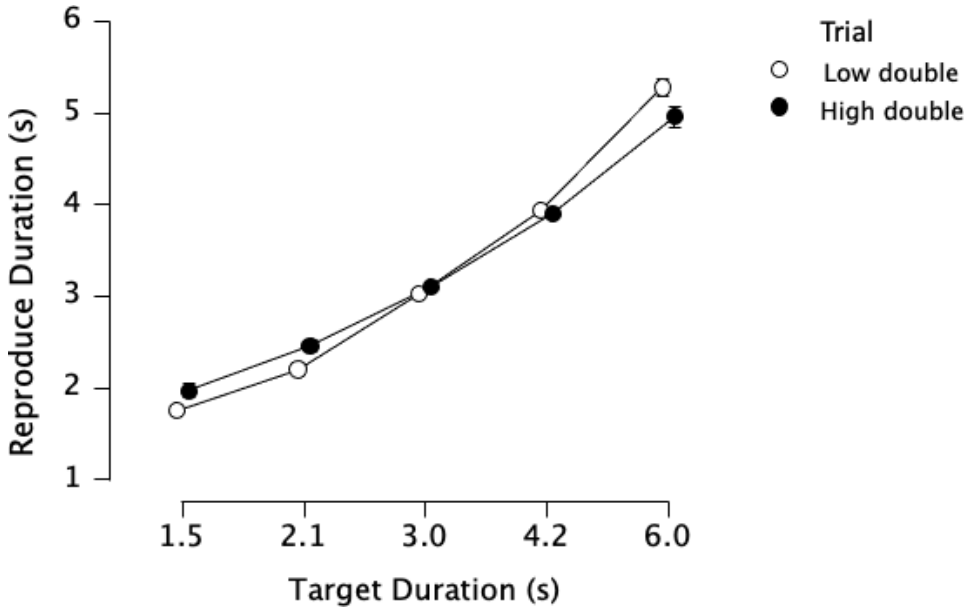

Figure 13. Accuracy of reproduced duration in uncertain environments by group type. Low double group participants are represented by open circles and high double group participants are represented by closed circles. Data are expressed as reproduced duration ± SEM.

Participants in the low double group exhibited significantly more precise (lower) estimates than those in the high double group F (1,35) =8.69, p<0.006, η=0.114, indicating that an environment with less opportunities to make a second temporal estimate will reduce the sensory noise. Lowered CVs and enhanced precision were observed in the redo trials F (1, 35) =19.678, η=0.012.

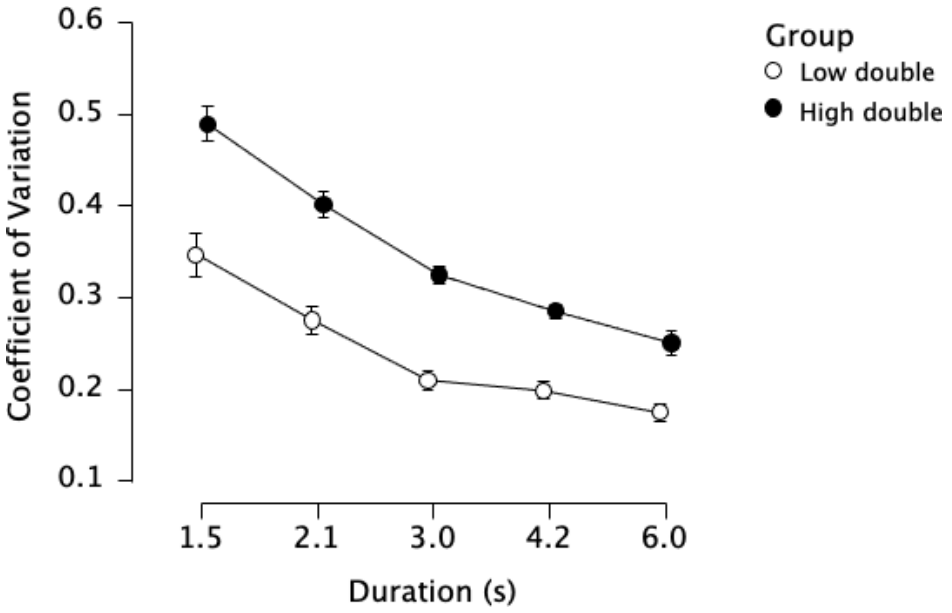

Figure 14. Temporal precision in uncertain environments by group type. The low double group is represented by open circles and the high double group is represented by solid circles. Data are expressed as the coefficient of variation ±SEM.

Electrophysiology Results

Contingent Negative Variation

The mean subject CNV ERP (window: 430-598 ms) for the Estimate phase of the task were plotted and waveforms were dissected into initial and redo trials for all of the durations. Since the data was not normally distributed according to the Shapiro-Wilks test, the Wilcoxon rank sum test was performed and no significant differences in Estimation phase mean amplitudes were observed between the initial and redo trials collapsed across the durations W=151, z=0.395, p<0.709 (CI: -0.356-0.509).

Initial and redo trials during the reproduction phase of the CNV were also plotted. A paired t-test demonstrated that there were no significant differences in the mean reproduction phase amplitudes collapsed across durations between the initial and redo trials t (22) =1.058, p<0.302 (CI: -1.116-3.441). A local peak between 3000-3500 ms in the reproduction phase, although not significant between the initial and redo trials, is of note because the CNV usually tracks the average of the target durations and the mean duration for this study is 3360 milliseconds.

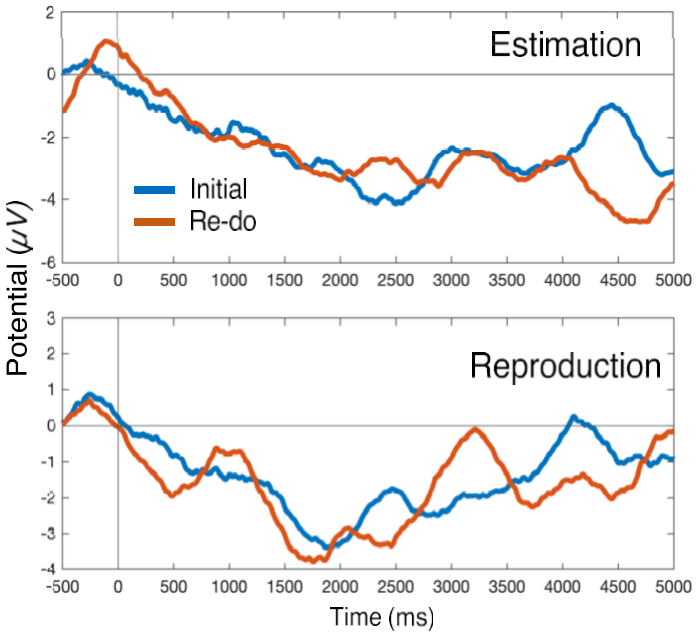

Figure 15. Mean Subject CNV for Estimation and Reproduction Phases initial and redo trials. The initial trial is represented by a blue line whereas the redo trial is represented by a red line. Data are expressed in µV.

Reward Positivity

The mean subject RewP ERP (window: 400-550 ms) for the On-Target and Off-Target feedbacks were plotted for both feedback conditions. On- and Off-target ERPs were separated into the initial and redo trials for the aggregate durations (data not shown). No significant differences in amplitudes were seen between redo and initial trials for either the On- or Off-target conditions.

Imaging Results

The fMRI only and the EEG-informed fMRI peak activation contrasts were all cluster corrected at $p<0.05$ and voxel wise at $p<0.001$, with the exception of the Reproduce Redo-Reproduce Initial contrast which was uncorrected with a voxel wise $p<0.001$, $k=10$. All contrasts had a familywise error correction for multiple comparisons at the cluster level.

Estimate Initial – Estimate Redo Contrast

EEG-Informed fMRI Peak activations in the Estimate Initial – Estimate Reproduce contrast were derived from the mean subject CNV amplitudes parametrized onto the BOLD signal. Neural activations were seen bilaterally in the supplementary motor area (SMA), the middle cingulate gyrus, and a low activation of the right precentral gyrus medial segments. The SMA was likely involved in the initial encoding of the interval durations whereas the precentral gyrus was activated to ready for movement preparation.

Estimate Redo- Estimate Initial Contrast

The fMRI Peak activations for the contrast Estimate Redo – Estimate Initial displayed high BOLD activations in the bilateral calcarine cortex, bilateral lingual gyrus, left cuneus, left occipital pole, and the left occipital fusiform gyrus. These are all visual processing areas and indicate that the subject is observing and fixating on the blue square in order to encode it.

Table 2. Estimate {Initial -Redo} and Estimate {Redo-Initial} fMRI Activations

Contrast Condition	Location	Hemisphere	x	y	z	t-score	Cluster size
Estimate {Initial - Redo}-EEG Informed	Supplementary Motor Cortex,	L,R	-6	-6	53	5.21	125
	Middle Cingulate Gyrus	L	0	-6	38	4.58	
	Middle Cingulate Gyrus	R	2	-14	41	4.40	
	Supplementary area	R					
	Precentral gyrus medial segment	R					
Estimate {Redo-Initial}	Calcarine cortex	L,R	-2	-92	-4	5.45	116
	Lingual Gyrus	L,R					
	Cuneus	L					
	Occipital Pole	L					
	Lingual Gyrus	L	-12	-83	-7	4.96	
	Occipital fusiform gyrus	L					

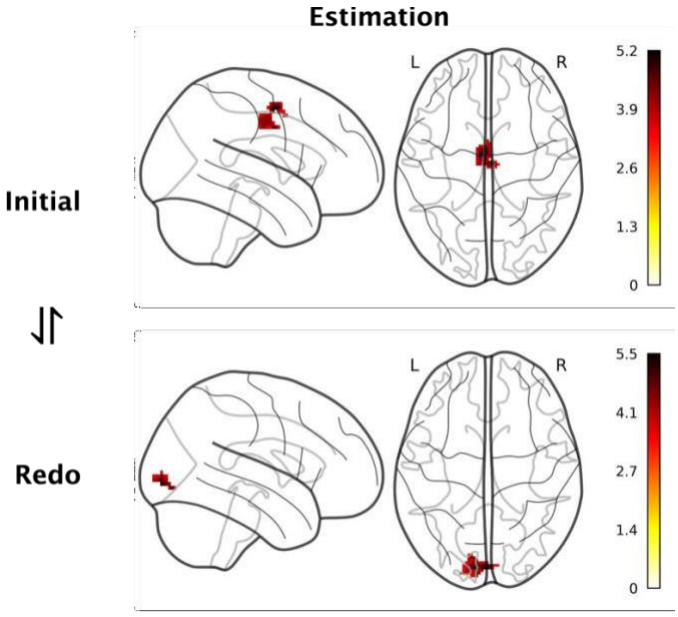

Figure 16. High BOLD in Estimate {Initial-Redo} and Estimate {Redo–Initial} Contrasts. Arrows are bidirectional. Neural activation in Estimate Initial – Estimate Redo is an EEG-Informed fMRI Peak activation whereas the Estimate Redo-Estimate Initial is an imaging only contrast. Cluster corrected at p<0.05 and voxel wise at p<0.001, FWE corrected.

Reproduce Initial – Reproduce Redo

Neural activations in the Reproduce Initial – Reproduce Redo contrasts were detected in the bilateral SMA (mainly right hemisphere), the exterior cerebellum, right superior frontal gyrus, the right anterior cingulate gyrus, left postcentral gyrus, left supramarginal gyrus, right calcarine cortex, bilateral thalamus, posterior insula, bilateral caudate, right putamen, right hippocampus, right posterior insula, right pallidum, right accumbens. Here, in addition to time-perception related areas (SMA, supramarginal gyrus, basal ganglia), and interoceptive awareness (insula), activation was observed in memory related regions (hippocampus) as the encoded time is recalled and performance

is monitored (superior frontal gyrus and anterior cingulate cortex) when decisions about the duration are made in the initial and redo trials. Notably, activation was also exhibited in the cerebellum, a region that has been associated with error learning. Previously, higher cerebellar activity has been viewed in fMRI studies in trials with sensory errors than trials without errors (Diedrichsen et al., 2005; Schlerf et al., 2012). The cerebellum also plays a role in performance monitoring, error processing, and feedback learning (Peterburs & Desmond, 2017) in conjunction with predictive timing and the regulation of trial-by-trial variation in self-timing (Tanaka et al., 2020), particularly due to connections with the frontoparietal cortices (Tanaka et al., 2020).

Reproduce Redo-Reproduce Initial Contrast

Task-related BOLD activations in the Reproduce Redo-Initial contrast were observed in the bilateral medial frontal cortex, bilateral gyrus rectus, bilateral superior frontal gyrus medial segment and the left medial orbital gyrus. Recruitment of brain regions in performance monitoring (medial frontal cortex) and working memory (superior frontal gyrus) (Algapan et al., 2019) are displayed in the reproduction phase, demonstrating a mechanism for error detection and correction.

Table 3. Reproduce {Initial -Redo} and Reproduce {Redo-Initial} fMRI Activation

Contrast Condition	Location	Hemisphere	x	y	z	t-score	Cluster size
Reproduce {Initial – Redo}	Calcarine Cortex	R	19	-71	8	6.13	1228
	Cerebellum Exterior	R	19	-59	-16	5.67	
	Supplementary motor cortex	R, L	4	27	56	6.88	363
	Superior frontal gyrus	R					
	Superior frontal gyrus medial segment	R, L	0	37	32	5.34	
	Anterior Cingulate Gyrus	R	4	29	35	5.17	
	Caudate	R	9	4	-1	5.33	248
	Pallidum	R					
	Thalamus	R	9	-2	5	5.32	
	Accumbens Area	R					
	Caudate	L	-10	-2	20	4.48	
	Thalamus	L					
	Hippocampus	R	33	-24	-4	5.50	108
	Putamen	R					
	Posterior Insula	R					
	Thalamus	L	-22	-22	14	6.04	85
	Postcentral gyrus	L	-55	-26	50	6.37	84
	Supramarginal gyrus	L					
Reproduce {Redo-Initial}	Medial frontal cortex	L, R	-2	47	-16	5.07	107
	Gyrus Rectus	L					
	Medial frontal cortex	L, R	-2	58	-7	4.43	
	Superior Frontal Gyrus Medial Segment	L, R					
	Gyrus Rectus	L, R	-2	45	-25	3.78	
	Medial Orbital gyrus	L					

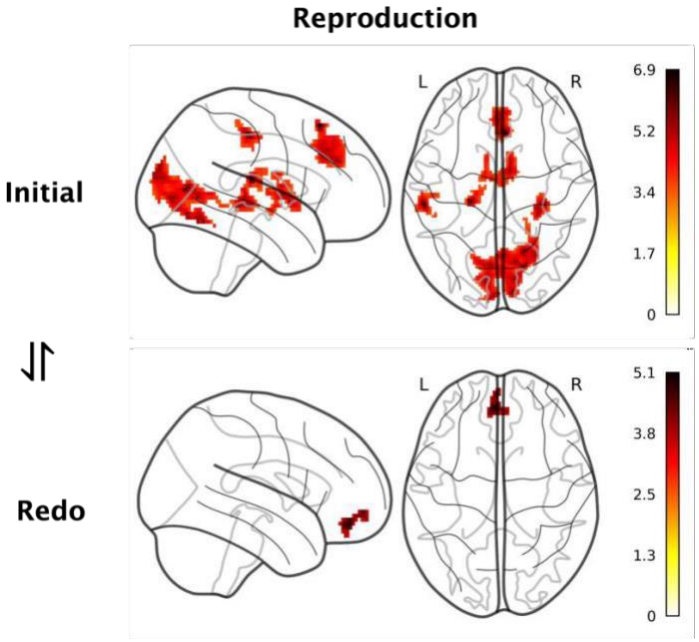

Figure 17. High BOLD in Reproduce{Initial-Redo} and Reproduce{Redo-Initial} Contrast. Note that the top contrast is cluster corrected at p<0.05 and voxel wise at p<0.001 but the bottom is uncorrected, p<0.001, k=10. Both are FWE corrected.

Estimation Initial – Reproduction Initial Contrast

BOLD activations were seen in the bilateral superior frontal gyrus, right middle frontal gyrus, left middle occipital gyrus, right post- and pre-central gyrus, left angular and supramarginal gyrus (SMG), left and right precuneus, bilateral posterior cingulate gyrus. In this inter-phase contrast, more parietal involvement for time perception (angular gyrus and SMG) along with pre-central gyrus for motor movement was observed in conjunction with the recruitment of structures associated with the default mode network (posterior cingulate gyrus) and metacognition (precuneus).

Reproduction Initial – Estimation Initial Contrast

Neural activations were observed in the left pre- and postcentral gyrus; bilateral SMA; bilateral middle cingulate gyrus; bilateral superior frontal gyrus, left central operculum, left parietal operculum, left supramarginal gyrus, right occipital pole, right cuneus, right calcarine and lingual cortex, and superior occipital gyrus. The SMA is recruited again when re-creating the interval duration jointly with timing-related, parietal brain areas to include the SMG, left central, or parietal operculum. High detection of activity in the superior frontal gyrus also reiterates the brain's performance monitoring system is online. Visual processing of the stimuli is emphasized again due to the eliciting of the BOLD signal in the occipital lobe.

Table 4. Estimate and Reproduce Initial fMRI Activations

Contrast Condition	Location	Hemisphere	x	y	z	t-score	Cluster size
Estimate$_{initial}$ - Reproduce$_{initial}$	Superior frontal gyrus	L	-18	43	47	7.82	2353
	Middle frontal gyrus	R	33	29	53	6.72	
	Superior frontal gyrus	R					
	Angular gyrus	L	-53	-61	38	5.28	276
	Supramarginal gyrus	L					
	Middle occipital gyrus	L	-49	-67	26	5.26	
	Precentral gyrus	R	35	-20	53	5.70	118
	Postcentral gyrus	R					
	Precuneus	R,L	0	-55	23	4.72	129
	Posterior Cingulate gyrus	R,L					

Reproduce$_{initial}$ -Estimate$_{initial}$	Precentral gyrus	L	-40	-16	53	8.85	1083
	Postcentral gyrus	L					
	Supplementary motor area	L	-4	-2	53	7.96	588
	Middle cingulate	L, R					
	Superior frontal gyrus	L	-6	-4	74	7.16	
	Superior frontal gyrus	R	6	-2	74	4.82	
	Supplementary Area	R					
	Occipital pole	R	15	-92	14		225
	Cuneus	R					
	Calcarine cortex	R					
	Superior occipital gyrus	R					
	Lingual gyrus	R	9	-87	-4		
	Central operculum	L	-57	-20	20		154
	Postcentral gyrus	L					
	Parietal operculum	L					
	Supramarginal gyrus	L					

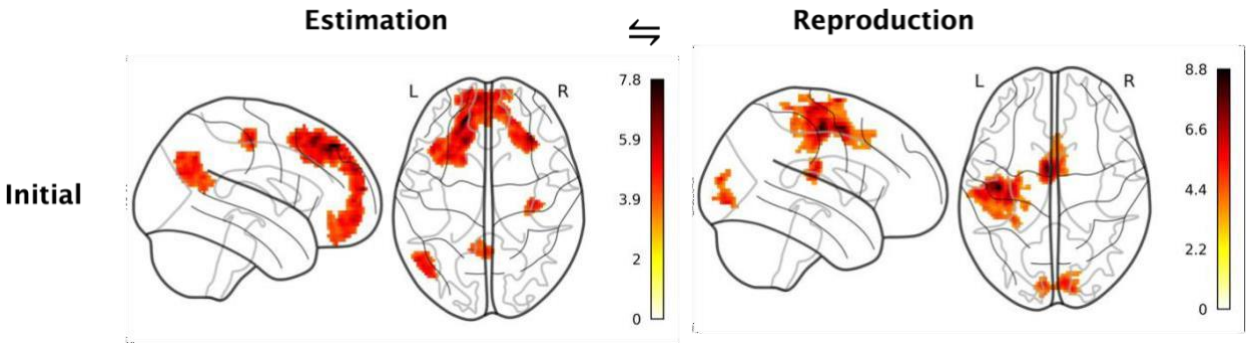

Figure 18. High BOLD in Estimate-Reproduce{Initial} & Reproduce-Estimate {Initial}. Cluster corrected at p<0.05 and voxel wise at p<0.001,FWE corrected

Estimation Redo-Reproduction Redo Contrast

Task related activations were witnessed in the bilateral posterior cingulate, bilateral middle cingulate gyrus, right middle frontal gyrus, right triangular and opercular part of the inferior frontal gyrus, right inferior temporal gyrus, right middle and superior temporal gyrii, left cuneus and bilateral precuneus respectively, right superior frontal gyrus, bilateral superior frontal gyrus medial segment, anterior cingulate cortex, right frontal pole, bilateral angular gyrus, and left supramarginal gyrus. Regions related to forming duration judgements (inferior frontal gyrus, bilateral angular gyrus and SMG) along with self-awareness (precuneus) and the default mode network (posterior cingulate cortex) have high BOLD activation when comparing the redo trials between phases.

Reproduction Redo – Estimation Redo Contrast

BOLD activations were seen in the bilateral SMA and the right superior frontal gyrus, signaling the sharpening of temporal estimates in the second (redo) trials in conjunction with invoking the brain's performance monitoring system (superior frontal gyrus).

Table 5. Estimate and Reproduce Redo fMRI Activations

Contrast Condition	**Location**	**Hemisphere**	**x**	**y**	**z**	**t-score**	**Cluster size**
$Estimate_{redo}$-$Reproduce_{redo}$	Frontal Pole	R	15	66	17	5.39	971

	Superior frontal gyrus medial segment	L,R	-2	49	17	5.01	
	Anterior cingulate gyrus	L,R					
	Superior frontal gyrus	R	9	39	53	4.98	
	Middle frontal gyrus	R	49	31	22	6.13	453
	Triangular part of the inferior frontal gyrus	R					
	Opercular part of the inferior frontal gyrus	R	45	13	26	4.94	
	Precentral gyrus	R					
	Precuneus	L	-6	-73	32	6.02	432
	Superior occipital gyrus	L	-14	87	35	4.89	
	Cuneus	L					
	Precuneus	R	13	-67	44	4.85	
	Posterior cingulate	L, R	-2	-36	29	7	297
	Middle cingulate gyrus	R,L	0	-28	23	5.31	
	Precuneus	R,L	2	-45	35	3.69	
	Angular gyrus	R	53	-61	38	4.74	296
	Middle occipital gyrus	R	43	-65	26	4.33	
	Angular gyrus	L	-51	-61	35	5.36	255
	Supramarginal gyrus	L	-55	-53	44	4.31	
	Inferior temporal gyrus	R	56	-43	-13	6.08	253
	Middle temporal gyrus	R	47	-36	-7	4.89	
	Superior temporal gyrus	R	43	-22	-7	4.41	
Reproduce$_{redo}$-Estimate$_{redo}$	Supplementary Motor area	L	-6	-2	56	6.34	261
	Supplementary Motor area	R	4	-2	56	6.34	
	Superior frontal gyrus	R	15	2	68	4.90	

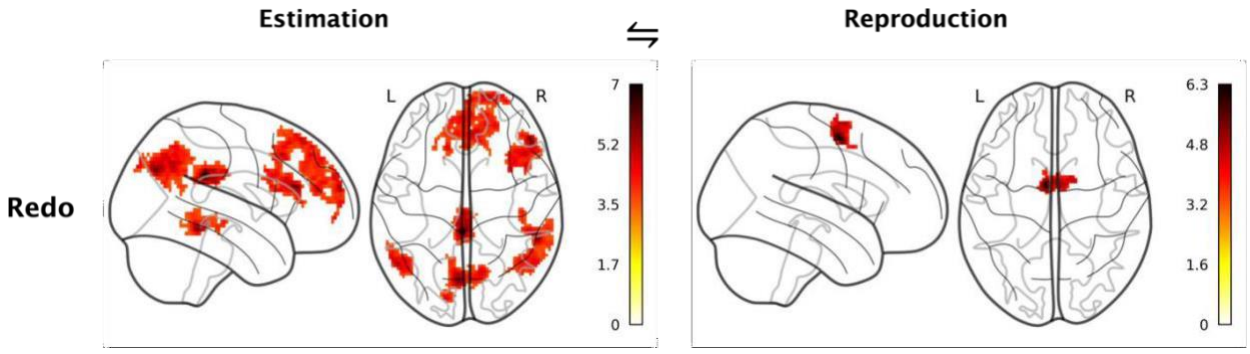

Figure 19. High BOLD in Estimate-Reproduce{Redo} and Reproduce-Estimate {Redo}Cluster corrected at p<0.05 and voxel wise at p<0.001, FWE corrected.

On Feedback redo- On Feedback initial Contrast

Positive feedback associated activations were observed in the pre- and postcentral gyrus, left superior parietal lobe, right precuneus, bilateral anterior and posterior insula, left planum temporale, right entorhinal area, left putamen, left hippocampus, left pallidum, left calcarine cortex and bilateral cuneus. On-target feedback recruited the basal ganglia areas for reward (putamen and pallidum), memory related regions (hippocampus and entorhinal area), the insula (interoceptive awareness of time) and the superior parietal lobe (spatial awareness and visual attention). Detection of activity in the precuneus also showed an awareness of successful timing performance.

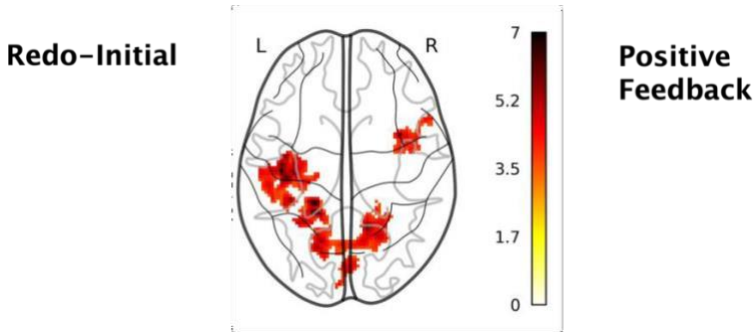

Figure 20. High BOLD activation in the On-Target{Redo-Initial}trial phases. Cluster corrected at p<0.05 and voxel wise at p<0.001, FWE corrected

Off Feedback Redo-Off Feedback Initial Contrast

Negative feedback related activations were seen in the following areas: left calcarine gyrus, left lingual gyrus, bilateral precuneus, left post- and precentral gyrus, left parietal operculum, planam temporal, left supramarginal gyrus, left posterior insula, left transverse temporal gyrus, and left putamen. Off-target feedback activated more visual processing areas (calcarine and lingual gyrus), metacognition (precuneus) and parietal timing related areas (parietal operculum and supramarginal gyrus) in concert with fewer basal ganglia areas (putamen). The transverse temporal gyrus, an auditory region, also showed heightened BOLD response, indicating the temporal representation occurs via the auditory cortex because it is optimized for time perception (Amadeo et al., 2020).

Table 6. Positive and Negative Feedback fMRI Activations

Contrast Condition	Location	Hemisphere	x	y	z	t-score	Cluster size
On_{redo}-$On_{initial}$	Precuneus	R	15	-55	8	6.65	548
	Cuneus	L	-18	-69	20	5.42	

	Calcarine cortex	L	-16	-65	8	5.37	
	Precentral gyrus	L	-43	-18	62	6.98	418
	Postcentral gyrus	L	-36	-36	65	5.52	
	Superior parietal lobe	L					
	Anterior Insula	R	37	6	-13	6.03	201
	Posterior Insula	R					
	Entorhinal area	R					
	Central operculum	R	41	4	8	4.75	
	Frontal operculum	R					
	Putamen	L	-32	-20	4	6.02	154
	Posterior insula	L					
	Hippocampus	L					
	Planum polare	L					
	Pallidum	L					
	Posterior insula	L	-40	14	8	5.59	
	Central operculum	L					
	Transverse temporal gyrus	L					
	Anterior insula	L					
	Postcentral gyrus	L	-20	-38	71	6.73	150
	Superior parietal lobe	L	-30	-53	65	5.26	
	Cuneus	L, R	0	-83	26	4.75	88
	Occipital Pole	L	-4	-94	23	4.50	
Off_{redo}-$Off_{initial}$	Postcentral gyrus	L	-43	-22	50	6.60	416
	Precentral gyrus	L	-34	-8	65	5.84	
	Supramarginal gyrus	L	-45	-26	32	5.30	
	Calcarine	L	-22	-65	2		202
	Lingual gyrus	L					
	Precuneus	L					
	Cuneus	L	-14	-67	11		
	Posterior cingulate	L	-14	-57	-1		
	Parietal operculum	L	-49	-28	20		83
	Planum temporale	L	-57	-30	11		

	Central operculum	L	-57	-20	20		
	Posterior Insula	L	-32	-20	2		72
	Putamen	L					
	Transverse Temporal gyrus	L					
	Planum polare	L	-45	-16	-1		
	Lingual gyrus	R	13	-63	2		67
	Calcarine cortex	R	25	-63	2		
	Precuneus	R	23	-63	11		

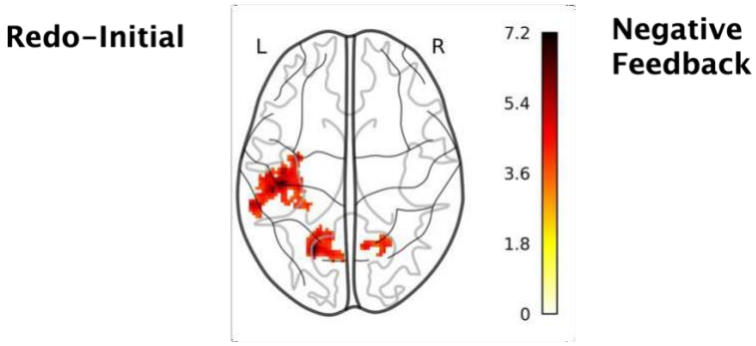

Figure 21. High BOLD activation in Off-target{Redo-Initial} trial phases. Cluster corrected at p<0.05 and voxel wise at p<0.001, FWE corrected.

Estimate – Reproduce Contrast

EEG-Informed fMRI Peak activations for the contrast Estimate – Reproduce contrasts (not separated by redo or initial trials) were derived from the mean subject CNV amplitudes parametrized into the BOLD signal and were cluster level corrected at p<0.05 and voxel wise 0<0.001 (data not shown). Time-related activations were seen in the left opercular and triangular part of the inferior frontal gyrus, left middle gyrus, and the left precentral gyrus. Activation of the IFG, which is implicated in time perception provides further biological evidence for the CNV's role in modulating duration judgements. The

left precentral gyrus is activated due to movement from the right-hand keypress of the button box.

Estimate – Contrast

EEG-Informed fMRI Peak activations for the contrast Estimate (not fractionated by redo or initial trials) were also derived from the mean subject CNV amplitudes parametrized into the BOLD signal and were cluster level corrected at $p<0.05$ and voxel wise $0<0.001$ (data not shown). Neural activations were seen in the right transverse temporal gyrus, right parietal and central operculum, right posterior insula, right planum temporale and right thalamus proper, and the right putamen. Basal ganglia, insular, and parietal involvement related to time perception in association with the transverse temporal gyrus, an auditory region. The activation of the transverse temporal gyrus aligned with the finding that auditory cortex may also represent complex visual stimuli due to its supra-modal, privileged role in temporal representation and the finding that early visual processing of time recruits the temporal cortex (Amadeo et al., 2020).

DISCUSSION

Behavioral and electrophysiological evidence suggest that humans and rodents can monitor errors during timing behavior (Akdogan & Balci, 2017; Kononowicz et al., 2019; 2022). Studies reveal that subjects are cognitively aware of the timing errors they make, particularly when learning to time interval durations, which happens rapidly and within one trial (Simen et al., 2011). In Experiment I, I demonstrated that when allowed to "re-do" a trial, humans can incorporate non-directional feedback to improve timing estimates both in accuracy and in precision (Bader & Wiener, 2021). Novel in using a mixed range of interval durations rather than a single duration, this experiment also showed that in the absence of feedback, the accuracy of time reproductions improved whereas the precision did not. These results revealed that humans are aware of the direction of their timing error; however, feedback was needed to make timing more precise. Next, a simultaneous fMRI-EEG paradigm (Experiment II) was used to determine the neural regions underlying this improvement in timing estimation. Afterwards, an additional follow-up behavioral experiment (III) using the same time reproduction paradigm further informed how temporal judgement responses were performed in uncertain environments.

The behavioral results of the fMRI-EEG were also highly illuminating. The redo trial integrated the feedback and improved timing, the absolute temporal error decreased, and the accuracy of the temporal estimates was improved with reproduced targets approaching their target durations. In contrast to our earlier behavior-only study using this

same paradigm, temporal precision was not enhanced (Bader & Wiener, 2021) in the fMRI-EEG study. This may have stemmed from participants' immersion in the scanner environment and the more involved set-up with application and recording from EEG electrodes.

Benefits gained from the second redo trial were also observed in Experiment III despite its varying ratio of single and double trials in the two groups. Both the high double and low double groups had reduced absolute temporal error and more accurate temporal judgements during the redo trial. Regardless of the group assignments, precision also improved with the second opportunity to recreate the interval duration. Notably, the low double group had more significant reduction in the absolute temporal error and enhanced precision, which may indicate that the participants in both groups were learning the underlying structure of the initially uncertain environment and adapting to it. This finding aligns with a study showing that participants can learn the temporal statistics and trial structure of a novel, uncertain environment and adapt its timing processes accordingly (Jazayeri & Shadlen, 2010). In the high double group, participants may have realized that there would be another opportunity by the preponderance of double trials and tracking of reward history. High double group participants failed to perform their best in the initial trial, secure in the knowledge that they would have another opportunity in the later redo trial to optimize their performance. Conversely, in the low double group, participants exhibited metacognitive awareness that they would have only one chance; therefore, their first opportunity would have to count more. Expectedly, low double group members contributed more effort and produced better timing estimates.

Revisiting the baseball analogy from the beginning, in situations with a 100% of a second chance swing (Experiment II), batting improved in the second try. In situations of uncertainty (Experiment III) the probability of attaining that second chance altered the performance. In conditions where there was a high probability of a second opportunity, batters decided that if the first swing fails to count, why give it your best? However, if second redo swings are a rare occurrence, then that first swing needed to be optimized as it had to be the most successful.

Our imaging results reinforced the behavioral results but also reiterated the importance of the supplementary motor area in representing temporal information and measuring time, which has been demonstrated repeatedly in the time perception literature (Ferrandez et al., 2003; Coull et al., 2004; Pouthas et al., 2005; Macar et al., 2006). The initial recruitment of the SMA indicated that the duration was encoded in the estimation phase and was invoked again in the redo trials during reproduction. The EEG-informed fMRI activations during the Estimate initial – redo contrast further confirmed the SMA's pivotal role and showcased the covariation of both the BOLD signal and the electrophysiological signals in the time course of the CNV. This finding aligned with the behavioral data and the sharpening of temporal responses and was reflected by a reduction in temporal errors and an improvement in accuracy in the second, redo trial in the fMRI-EEG experiment.

Neural activation in performance monitoring network structures (superior frontal cortex, medial frontal cortex, anterior cingulate cortex) suggested the co-occurrence of temporal error detection and correction in concert with the activation of the timing

network. A high BOLD signal displayed in these regions was linked with tracking and correcting errors, behavioral inhibition, feedback evaluation and cognitive control (Van Noordt & Segalowitz, 2012) and was witnessed when the participants recreated the duration using a keypress during reproduction. Performance monitoring tended to come online when learning a new task; therefore, the co-activation of the two networks was not unexpected. Also, the basal ganglia are activated throughout the task, a common biological substrate for both time perception networks and performance monitoring.

Learning to time when given a second opportunity involved the default mode network (posterior cingulate) as humans mentalized time to improve their estimates, as indicated by PCC activation. Structures associated with metacognition (precuneus) that have connections with the DMN showed enhanced activity during temporal reproduction in our experiment, indicating a self-awareness of timing ability and performance. Studies addressing the interaction of time perception with the DMN are sparse; however, an experiment using a temporal expectation task of periodic and non-periodic motion to test temporal attention showed recruitment of the DMN during the periodic motion condition (Carvallho et al., 2016). Study authors attributed this recruitment to increased familiarity and predictability of the stimulus and a reduction in task difficulty following successful learning of a novel task, resulting in attenuated attentional engagement (Carvallho et al., 2016). Applying this explanation to our temporal reproduction task would lead to the conclusion that as a participant learned to make accurate duration judgements and the task became more habitual, the resting state network become more engaged.

Alternatively, the length of an interval duration to be tracked (short or long) can determine whether the DMN will become involved (Morillon et al., 2009). A time discrimination study in which participants had to report the longer duration or hue between two sequentially presented circles recruited the DMN when there were temporal errors for longer durations exceeding two seconds while the motor system tracked time for less than two seconds (Morillon et al., 2009). BOLD activity in the SMA decreased after two seconds whereas activity in the posterior cingulate cortex increased after two seconds, substantiating this finding. Additionally, heightened activity in the DMN was not limited to only the medial prefrontal cortex and the posterior cingulate cortex but also the inferior temporal cortex, particularly in response to under-reproduction of time (Morillon et al., 2009). Since our current study employs four target durations over two seconds, it is not surprising that the DMN is invoked. Future studies can examine the interaction of the DMN network and time perception network more deeply.

A comparison and contrast of the positive or negative feedback brain responses is also important to address. Aside from the greater visual processing area recruitment and heightened activity in the occipital lobe in the off-target condition which was likely due to enhanced visual attention to the stimuli in an incorrect trial, there is little to distinguish the profiles between the two conditions. Basal ganglia and insular activation are witnessed in both feedback conditions while less so in the off-target condition which only has putamen activation whereas on-target included both the putamen and pallidum activity. The positive feedback condition displayed more memory-related activity with the hippocampus and the entorhinal cortex. It was also puzzling to note the lack of

frontal cortical activity in either condition as the medial frontal cortex has been implicated as one of the source generators of the RewP (Carlson et al., 2011; Foti et al., 2011; Becker et al., 2014).

In a future iteration of this study, we can measure the awareness of temporal errors more directly and the neural regions implicated therein. Using the absolute temporal error from our behavioral data as a regressor and parametric modulator in the general linear model for BOLD activity is a method devised to demonstrate how the magnitude of the error modulates hemodynamic activity in networks related to timing, performance monitoring, and the resting state/default mode network. A dissection and separate analysis of each of the five durations used in the study with this temporal error regressor, or alternatively, the ERPs, the imaging, and the EEG-informed fMRI BOLD activations would also be enlightening, given different brain areas and networks are recruited depending on the length of the time duration.

With reference to event-related potentials, another ERP that we could examine is the Pe, or error positivity, a biomarker of conscious error awareness that has been linked to metacognition (Boldt & Yeung, 2015; Charles et al., 2013; Yeung & Summerfield, 2012). The ERP functions as a marker of evidence accumulation of knowledge for error commission (Steinhauser & Yeung, 2010; Ullsperger et al., 2014). As a post-decisional ERP, the Pe is also associated with confidence levels. In future studies, the error positivity (Pe), an ERP biomarker of error awareness, can also be related to confidence levels since higher Pe amplitudes are linked to lower confidence in simple decision task performance (Boldt & Yeung, 2015).

While the EEG-informed component of this study was focused on extracting data from event-related potentials, an extension of this study may integrate more time-frequency components. Inclusion of these time frequency components may be able to tease out more EEG-informed fMRI results from our study particularly from the feedback conditions, as this has been an ongoing limitation. Timing errors have been linked to oscillatory activity; therefore, a power spectral analysis of oscillatory components related to timing and metacognitive could yield additional regressors for the GLM to predict BOLD activity in time perception networks. Frontal theta oscillations are a good candidate due to their involvement in error processing and cognitive control (Ullsperger et al., 2014; Cavanagh & Frank, 2014). Studies show that inter-trial phase reset of the theta band can be modulated by both error magnitude (higher reset with larger errors) and incorrect temporal prediction (Barne et al., 2017).

The delta oscillation is another frequency band implicated in error processing stemming from studies that have linked delta with error corrections, anticipatory responses, and future behavioral adjustments following an incorrect trial (Barne et al., 2017; Arnal et al., 2014; Arnal & Giraud, 2012). Delta oscillations also have a role in temporal prediction and response accuracy in temporal judgement tasks (Barne et al., 2017; Arnal et al., 2014; Arnal & Giraud, 2012). Beta oscillations are yet another suitable choice as higher beta power (13-30Hz) has also been associated with encoding longer temporal durations and ability to self-deduce timing errors (Kononowicz et al., 2019) while alpha-beta phase coupling has been connected to precision in self-generated time intervals (Grabot et al., 2019). Beta power is also predictive of the post-interval alpha

power metacognitive readout coding for the duration estimate (Kononowicz and Wasserhove, 2019). Alpha power is yet another candidate because it is a BOLD correlate of EEG synchronization associated with resting state network activity (Jann et al., 2009). With an array of oscillatory components to choose from, any of these bands would be a valued biomarker for further exploratory analysis.

Another time-frequency decomposition analysis involves exploring event related spectral perturbation (ERSPs) in order to examine synchrony and desynchrony in brain areas. Comparing the ERSPs of the CNV between the initial and redo trials during the estimation and reproduction phases may offer insights on the neural substrates of time awareness. Again, this measure can once again be fed into the GLM model to determine if it can modulate BOLD responses in timing networks. Incorporating the initial and redo ERSPs for the feedback phases can also demystify our feedback results along with enhancing our understanding of what happens neuronally when offered a second opportunity to encode and recreate a temporal duration.

Behaviorally, another future research direction would integrate a self-reporting tool to rate confidence in temporal estimates post-judgement, a feature seen in many temporal metacognition studies (Akdogan & Balci, 2017; Kononowicz et al., 2019). The confidence measure may also include a self-evaluation of magnitude and direction to describe proximity to the target duration. These confidence values can be compared to the actual performance to provide an estimate of timing self-awareness. Furthermore, including this component whilst inside the scanner would confirm the neural regions involved in self-appraisal of timing and of confidence.

CONCLUSIONS

With the rich repository of data gathered from these experiments, there are a multitude of exploratory options to further comprehend the neural substrates of temporal learning and metacognition. Each avenue reveals a new facet of learning how to time. The sheer speed at which we learn to time visual durations is notable. Regardless of the feedback condition (adaptive, non-directional or none) and context (scanner or behavior only) or the frequency in type of trials (high single or high double), participants excelled at learning to infer the pattern of interval durations, incorporated the guidance supplied by the feedback, and improved their time reproductions by the second try. This confirmed the robustness of human learning of time estimation and re-emphasized that it can be done rapidly and in one trial as proposed by Simen et al. (2011).

My fMRI-EEG experiments demonstrated that timing systems co-activated with performance monitoring and error detection systems at various stages of time reproduction. To more thoroughly investigate this co-activation and subsequent interaction, we may analyze the fMRI connectivity patterns between the various brain areas involved in time perception and performance monitoring using graph theory, a technique where cortical or subcortical regions are represented by nodes and the direct or indirect connections between them are symbolized by edges (Bullmore & Sporns, 2012; Farhani et al., 2019). This method would supply further insight into the patterns,

clustering, path length distances, and strength and number of connections between the two brain systems (Bullmore & Sporns, 2012).

Network analysis using graph theory can also unravel the interaction between traditionally timing related areas to that of resting state network brain regions. Bridging the gap between mentalizing time and then accurately reproducing it, a dual DMN and time perception network analysis may pave the path for further probing how we formulate and maintain an awareness of time.

Timing self-awareness, while witnessed behaviorally in accuracy and precision improvements in time reproductions, may also be surmised through activation of structures associated with metacognition, including the precuneus or the posterior cingulate. Metacognition can be confirmed by incorporating measures of confidence (e.g., P_e). Another fMRI-EEG study using these advanced fMRI connectivity techniques to tie the neural activations between the confidence-related structures to the metacognitive regions would generate further evidence, and supplemented by behavioral self-report, solidify our findings.

Learning to time, knowing when we make a timing error, and adjusting to and learning from that error in the future are fundamental to the acts of daily living. These abilities are necessary for performance of any discrete motor action that permits multiple tries whether it be from hitting a baseball to performing day-to-day tasks (e.g., driving through traffic lights) to enacting a timing decision that employs a redo. The delivery of correct feedback aids and abets these abilities, but what if the feedback regime is incorrect or skewed? A future study exploring this possibility can evaluate how altered

feedback impacts time perception by shifting the distribution away from the reproduced intervals, akin to motor adaptation studies. An example would be to test how altered visual feedback impacts performance on a reaching task (Gaffin-Cahn et al., 2019) with a time perception component. In that same regard to modulating feedback, future studies can also modulate the cost associated with error correction, particularly in timing studies related to sensorimotor learning (Sedhagat-Nejad & Shedmahr, 2021). An error incurs a time and energy cost to rectify it; therefore, adjusting the error cost can influence learning rate so that larger error costs increase the brain's learning rate (Sedhagat-Nejad & Shedmahr, 2021).

While the three experiments comprising this study clearly enrich the narrative on temporal processing and the impact of feedback on neurotypical populations, they also provide a window into what may occur when timing mechanisms are impaired, particularly in relationship to temporal metacognition and learning. When extended to clinical conditions, the possibilities for identifying and understanding timing disruptions are replete with boundless new possibilities for research inquiry.

APPENDIX

List of MATLAB code that was used:

batch_dicom2nifti_fMRIEEG.m

```
% Script to convert dicom imaging files to .nii
base_dir = '/Users/sladmin/Desktop/Farah/ImagingOnly/';    %%% Where the subjects' data is kept

%%
subj_dirs = { ...

};

subj_subdirs = { ...

   '/EP2D_BOLD_GMU_1/' ...
   '/EP2D_BOLD_GMU_2/' ...
   '/EP2D_BOLD_GMU_3/' ...
   '/EP2D_BOLD_GMU_4/' ...
   '/EP2D_BOLD_GMU_5/' ...
   '/EP2D_BOLD_GMU_6/' ...
   '/T1_MPRAGE_SAG_P2_ISO/'...
   '/GRE_FIELD_MAPPING_2MM_0001/'...
   '/GRE_FIELD_MAPPING_2MM_0002/'...


    };


%%

num_subjs=length(subj_dirs); %how many subjects are there?
num_sub_dir=length(subj_subdirs); %how many sub-directories are there?

%%
for subj_num=1:num_subjs, %for each subject

   this_subj_dir = subj_dirs{subj_num};
   disp(['Processing subject ' num2str(subj_num) ': ' this_subj_dir ]);

   for cur_dir=1:num_sub_dir, %for each sub-directory
```

```
      dicm2nii([base_dir this_subj_dir subj_subdirs{cur_dir}], [base_dir this_subj_dir
subj_subdirs{cur_dir}],'.nii 3D');
   end
end
```

Batch_PreprocessingfMRIEEG.m
%% Batch Preprocessing script for each individual imaging file

```
base_dir = '/Users/sladmin/Desktop/Farah/ImagingOnly/';    %%% Where the subjects'
data is kept
template_dir = '/Users/sladmin/Desktop/Farah/Scripts/fMRI_Analysis_Scripts/'; %%%
Where the templates are stored
cd(base_dir);  %%% Where the Subjects' data is kept
%%

subj_dirs = { ...

    };

Bold_subdirs = { ...


   '/EP2D_BOLD_GMU_1/' ...
   '/EP2D_BOLD_GMU_2/' ...
   '/EP2D_BOLD_GMU_3/' ...
   '/EP2D_BOLD_GMU_4/' ...
   '/EP2D_BOLD_GMU_5/' ...
   '/EP2D_BOLD_GMU_6/'  ...


    };

fmap_subdirs = { ...

   '/GRE_FIELD_MAPPING_2MM_0001/'...
   '/GRE_FIELD_MAPPING_2MM_0002/'...


    };

%%
```

```
num_subjs = size(subj_dirs,2); %how many subjects are there?
num_runs=6; %how many runs are there?

%% Perform batch preprocessing


for subj_num = 1:num_subjs,

   for curr_run=1:num_runs,


       this_subj_bold_dir = [base_dir subj_dirs{subj_num} Bold_subdirs{curr_run}];
       disp(['Running batch preprocessing on subject ' subj_dirs{subj_num} ]);

       %%% Load in batch pipeline
       load([template_dir 'Batch_PreprocessorfMRIEEG.mat']);

       %%% Add in phase image

matlabbatch{1,1}.spm.tools.fieldmap.calculatevdm.subj.data.presubphasemag.phase=cell
str([base_dir subj_dirs{subj_num} fmap_subdirs{2}
'gre_field_mapping_2mm_phase.nii']);

       %%% Add in Magnitude image

matlabbatch{1,1}.spm.tools.fieldmap.calculatevdm.subj.data.presubphasemag.magnitude
=cellstr([base_dir subj_dirs{subj_num} fmap_subdirs{1}
'gre_field_mapping_2mm_00001.nii']);

       %%% The only thing we need to change is that we are going to
       %%% load in a different subject's data for slice timing
       bold_files_from_manual_job = matlabbatch{1,2}.spm.temporal.st.scans;

       image_filenames_without_dir_path =
spm_select('List',this_subj_bold_dir,['^ep2d*.*']);
       num_TR_per_run=length(image_filenames_without_dir_path);
       copies_of_directory_path = repmat(this_subj_bold_dir,num_TR_per_run,1);
       image_filenames_with_path = cellstr([ copies_of_directory_path
       image_filenames_without_dir_path ]);



      matlabbatch{1,2}.spm.temporal.st.scans{1} = cellstr(image_filenames_with_path);
```

```
        %%% Run the realign job
        spm_jobman('run',matlabbatch);


    end;


end
```

Batch_GLM_fMRIOnly.m

```
% Estimating Individual GLM for only the imaging files
base_dir = '/Users/sladmin/Desktop/Farah/ImagingOnly/';    %%% Where the subjects' data is kept
template_dir = '/Users/sladmin/Desktop/Farah/Scripts/fMRI_Analysis_Scripts/'; %%% Where the templates are stored
log_dir = '/Users/sladmin/Desktop/Farah/Behavior data/Log files only/'; %%% Where the log files are
behav_dir='/Users/sladmin/Desktop/Farah/Behavior data'; %%% where the behavioral data are
cd(base_dir);  %%% Where the Subjects' data is kept
%%

subj_dirs = { ...



  };

Bold_subdirs = { ...


    '/EP2D_BOLD_GMU_1/' ...
    '/EP2D_BOLD_GMU_2/' ...
    '/EP2D_BOLD_GMU_3/' ...
    '/EP2D_BOLD_GMU_4/' ...
    '/EP2D_BOLD_GMU_5/' ...
    '/EP2D_BOLD_GMU_6/'  ...
```

```
    };

Behav_dirs= { ...

    };


%%

num_subjs = length(subj_dirs); %how many subjects are there?
num_runs=6; %how many runs are there?

cd(log_dir);
loglist=dir('*.log');
loglist={loglist.name};
%loglist={loglist{5:6}};%delete this line once it's done.  It selects only the last two
subjects for log files.

%% Perform batch preprocessing

for subj_num = 1:num_subjs,


     this_subj_GLM_directory = [base_dir subj_dirs{subj_num} ];
     disp(['Running batch preprocessing on subject ' subj_dirs{subj_num} ]);

    %load in the SPM Template
    load ([template_dir 'GLMTemplatefMRIonlysubj2mod.mat']);
    matlabbatch{1,1}.spm.stats.fmri_spec.dir = cellstr(this_subj_GLM_directory);
%update to the current subject directory

    cd(log_dir);
    [VarName1 text]=LogfileImporter(loglist{subj_num});%import the log file
    [EstOnsetTimes RepOnsetTimes EstOnset2Times RepOnset2Times OnTargetTimes
    OffTargetTimes OnTargetTimes2 OffTargetTimes2] =
    PrototypeLogExtractor(VarName1,text);

    cd([behav_dir Behav_dirs{subj_num}]);
    file=dir('*.csv');
    subj_data=readtable(file.name);

    for curr_run = 1:num_runs,
```

```
%load up the appropriate files
this_subj_bold_dir1=[this_subj_GLM_directory Bold_subdirs{curr_run}];
image_filenames_without_dir_path =
spm_select('List',this_subj_bold_dir1,['^swua*.*']);
num_TR_per_run=length(image_filenames_without_dir_path);
copies_of_directory_path1 = repmat(this_subj_bold_dir1,num_TR_per_run,1);
image_filenames_with_path1 = [ copies_of_directory_path1
image_filenames_without_dir_path ];
matlabbatch{1,1}.spm.stats.fmri_spec.sess(curr_run).scans =
cellstr(image_filenames_with_path1);

%Put in all the log file data.  Note: we still need to put in
%duration information for estimation and reproduction phases, which
%can only be extracted by analyzing the behavioral data.

matlabbatch{1,1}.spm.stats.fmri_spec.sess(curr_run).cond(1).onset =
EstOnsetTimes(:,curr_run);
matlabbatch{1,1}.spm.stats.fmri_spec.sess(curr_run).cond(1).duration =
subj_data.intervals_1(subj_data.runs_thisN==(curr_run-1));

matlabbatch{1,1}.spm.stats.fmri_spec.sess(curr_run).cond(2).onset =
RepOnsetTimes(:,curr_run);

matlabbatch{1,1}.spm.stats.fmri_spec.sess(curr_run).cond(2).duration =
subj_data.Endreproductionkey_rt(subj_data.runs_thisN==(curr_run-1));

matlabbatch{1,1}.spm.stats.fmri_spec.sess(curr_run).cond(3).onset =
OnTargetTimes(curr_run);

matlabbatch{1,1}.spm.stats.fmri_spec.sess(curr_run).cond(4).onset =
OffTargetTimes(curr_run);

 matlabbatch{1,1}.spm.stats.fmri_spec.sess(curr_run).cond(5).onset =
EstOnset2Times(:,curr_run);
matlabbatch{1,1}.spm.stats.fmri_spec.sess(curr_run).cond(5).duration =
subj_data.intervals_1(subj_data.runs_thisN==(curr_run-1));

matlabbatch{1,1}.spm.stats.fmri_spec.sess(curr_run).cond(6).onset =
RepOnset2Times(:,curr_run);

matlabbatch{1,1}.spm.stats.fmri_spec.sess(curr_run).cond(6).duration =
subj_data.repro_2key_rt(subj_data.runs_thisN==(curr_run-1));
```

```
        matlabbatch{1,1}.spm.stats.fmri_spec.sess(curr_run).cond(7).onset =
OnTargetTimes2(curr_run);

        matlabbatch{1,1}.spm.stats.fmri_spec.sess(curr_run).cond(8).onset =
OffTargetTimes2(curr_run);


        %lastly, load in the multiple regressors for each run


        cd(this_subj_bold_dir1); %go to BOLD directory
        file=dir('*00001.txt');


        matlabbatch{1,1}.spm.stats.fmri_spec.sess(curr_run).multi_reg =
cellstr([this_subj_bold_dir1 file.name]);

    end

    %Now generate the GLM
    spm_jobman('run',matlabbatch);

    %% Now estimate the model
    load ([template_dir 'EstimateSPM12Template.mat']);
    matlabbatch{1,1}.spm.stats.fmri_est.spmmat = cellstr([this_subj_GLM_directory
'/SPM.mat']);
    %%% Run the GLM-estimate job
    spm_jobman('run',matlabbatch);

end;  % End of loop through subjects
```

Batch_GLM_fMRIEEG.m

```
%% Batch Preprocessing script for fMRI-EEG data

base_dir = '/Users/sladmin/Desktop/Farah/ImagingOnly/';    %%% Where the subjects' data is kept
template_dir = '/Users/sladmin/Desktop/Farah/Scripts/fMRI_Analysis_Scripts/'; %%% Where the templates are stored
log_dir = '/Users/sladmin/Desktop/Farah/Behavior data/Log files only/'; %%% Where the log files are
behav_dir='/Users/sladmin/Desktop/Farah/Behavior data'; %%% where the behavioral data are
EEG_dir='/Users/sladmin/Desktop/Farah/Brain Vision Processed fMRI_EEG_files_cleanrawdata/';%%% Where EEG data are
cd(base_dir);  %%% Where the Subjects' data is kept
%%

subj_dirs = { ...

    };

Bold_subdirs = { ...


'/EP2D_BOLD_GMU_1/'  ...
'/EP2D_BOLD_GMU_2/'  ...
'/EP2D_BOLD_GMU_3/'  ...
'/EP2D_BOLD_GMU_4/'  ...
'/EP2D_BOLD_GMU_5/'  ...
'/EP2D_BOLD_GMU_6/'  ...


    };

Behav_dirs= { ...

    };

EEG_dirs={...


    };


%%
```

```
%%%

num_subjs = length(subj_dirs); %how many subjects are there?
num_runs=length(Bold_subdirs); %how many runs are there?


%loglist={loglist{5:6}};%delete this line once it's done.  It selects only the last two
subjects for log files.

%% Perform batch preprocessing

for subj_num = 1:num_subjs,


    this_subj_GLM_directory = [base_dir subj_dirs{subj_num} ];
    disp(['Running batch preprocessing on subject ' subj_dirs{subj_num} ]);

   %load in the SPM Template
   load ([template_dir 'GLMTemplatefMRIEEG.mat']);
   matlabbatch{1,1}.spm.stats.fmri_spec.dir = cellstr([this_subj_GLM_directory
'/FMRIEEG']); %update to the current subject directory



   cd([behav_dir Behav_dirs{subj_num}]);
   loglist=dir('*.log');
   loglist={loglist.name};

   [VarName1 text]=LogfileImporter(loglist{1});%import the log file
   [EstOnsetTimes RepOnsetTimes EstOnset2Times RepOnset2Times
FirstFeedbackTimes SecondFeedbackTimes FirstFeedbackOnOff
SecondFeedbackOnOff] = PrototypeLogExtractor(VarName1,text);

   %cd([behav_dir Behav_dirs{subj_num}]);
   file=dir('*.csv');
   subj_data=readtable(file.name);

   cd([EEG_dir EEG_dirs{subj_num}]);
   fname=dir('*EstRep*.mat');
   load(fname.name);
   fname=dir('*OnOff*.mat');
   load(fname.name);
```

```
   %Reshape the amplitudes into array by runs (6)

OnOffAmplitudes=reshape(OnOffAmplitudes,20,6);%OnOffAmplitudes=[zeros(20,1),O
nOffAmplitudes];

OnOffIndices=reshape(OnOffIndices,20,6);%OnOffIndices=[zeros(20,1),OnOffIndices];

EstAmplitudes=reshape(EstAmplitudes,20,6);%EstAmplitudes=[zeros(20,1),EstAmplitu
des];

RepAmplitudes=reshape(RepAmplitudes,20,6);%RepAmplitudes=[zeros(20,1),RepAmpl
itudes];

% %     %Re-Order Everything (this is just for the wrongly stitched ones)
% %      OnOffAmplitudes=[OnOffAmplitudes(:,5:6),fliplr(OnOffAmplitudes(:,1:4))];
% %      OnOffIndices=[OnOffIndices(:,5:6),fliplr(OnOffIndices(:,1:4))];
% %     EstAmplitudes=[EstAmplitudes(:,5:6),fliplr(EstAmplitudes(:,1:4))];
% %     RepAmplitudes=[RepAmplitudes(:,5:6),fliplr(RepAmplitudes(:,1:4))]

   %Divide into first and second trials
   EstAmplitudes_1=EstAmplitudes(1:2:end,:);
   EstAmplitudes_2=EstAmplitudes(2:2:end,:);
   RepAmplitudes_1=RepAmplitudes(1:2:end,:);
   RepAmplitudes_2=RepAmplitudes(2:2:end,:);
   OnOffAmplitudes_1=OnOffAmplitudes(1:2:end,:);
   OnOffAmplitudes_2=OnOffAmplitudes(2:2:end,:);
   OnOffIndices_1=OnOffIndices(1:2:end,:);
   OnOffIndices_2=OnOffIndices(2:2:end,:);

%    EstOnsetTimes=EstOnsetTimes(:,2:end);
%    EstOnset2Times=EstOnset2Times(:,2:end);
%    RepOnsetTimes=RepOnsetTimes(:,2:end);
%    RepOnset2Times=RepOnset2Times(:,2:end);
%    FirstFeedbackOnOff=FirstFeedbackOnOff(:,2:end);
%    FirstFeedbackTimes=FirstFeedbackTimes(:,2:end);
%    SecondFeedbackOnOff=SecondFeedbackOnOff(:,2:end);
%    SecondFeedbackTimes=SecondFeedbackTimes(:,2:end);
%


   for curr_run = 1:num_runs,

      %load up the appropriate files
      this_subj_bold_dir1=[this_subj_GLM_directory Bold_subdirs{curr_run}];
```

```
        image_filenames_without_dir_path =
spm_select('List',this_subj_bold_dir1,['^swua*.*']);
        num_TR_per_run=length(image_filenames_without_dir_path);
        copies_of_directory_path1 = repmat(this_subj_bold_dir1,num_TR_per_run,1);
        image_filenames_with_path1 = [ copies_of_directory_path1
image_filenames_without_dir_path ];
        matlabbatch{1,1}.spm.stats.fmri_spec.sess(curr_run).scans =
cellstr(image_filenames_with_path1);


        %Put in all the log file data.  Note: we still need to put in
        %duration information for estimation and reproduction phases, which
        %can only be extracted by analyzing the behavioral data.

        %Estimation Onset
        matlabbatch{1,1}.spm.stats.fmri_spec.sess(curr_run).cond(1).onset =
        EstOnsetTimes(:,curr_run);
        matlabbatch{1,1}.spm.stats.fmri_spec.sess(curr_run).cond(1).duration =
        subj_data.intervals_1(subj_data.runs_thisN==(curr_run-1));

        matlabbatch{1,1}.spm.stats.fmri_spec.sess(curr_run).cond(1).pmod.param=EstAmpl
        itudes_1(:,curr_run);
        %Reproduction Onset
        matlabbatch{1,1}.spm.stats.fmri_spec.sess(curr_run).cond(2).onset =
        RepOnsetTimes(:,curr_run);
        matlabbatch{1,1}.spm.stats.fmri_spec.sess(curr_run).cond(2).duration =
        subj_data.Endreproductionkey_rt(subj_data.runs_thisN==(curr_run-1));

      matlabbatch{1,1}.spm.stats.fmri_spec.sess(curr_run).cond(2).pmod.param=RepAmpl
      itudes_1(:,curr_run);

        %On Target Feedback
      matlabbatch{1,1}.spm.stats.fmri_spec.sess(curr_run).cond(3).onset =
      FirstFeedbackTimes(FirstFeedbackOnOff(:,curr_run)==1,curr_run);

      matlabbatch{1,1}.spm.stats.fmri_spec.sess(curr_run).cond(3).pmod.param=OnOffA
      mplitudes_1(OnOffIndices_1(:,curr_run)==1,curr_run);
        %Off Target Feedback
      matlabbatch{1,1}.spm.stats.fmri_spec.sess(curr_run).cond(4).onset =
      FirstFeedbackTimes(FirstFeedbackOnOff(:,curr_run)==2,curr_run);

      matlabbatch{1,1}.spm.stats.fmri_spec.sess(curr_run).cond(4).pmod.param=OnOffA
      mplitudes_1(OnOffIndices_1(:,curr_run)==2,curr_run);
        %Estimation 2 Onset
```

```
 matlabbatch{1,1}.spm.stats.fmri_spec.sess(curr_run).cond(5).onset =
EstOnset2Times(:,curr_run);
matlabbatch{1,1}.spm.stats.fmri_spec.sess(curr_run).cond(5).duration =
subj_data.intervals_1(subj_data.runs_thisN==(curr_run-1));

matlabbatch{1,1}.spm.stats.fmri_spec.sess(curr_run).cond(5).pmod.param=EstAmpli
tudes_2(:,curr_run);
%Reproduction 2 Onset
 matlabbatch{1,1}.spm.stats.fmri_spec.sess(curr_run).cond(6).onset =
 RepOnset2Times(:,curr_run);
 matlabbatch{1,1}.spm.stats.fmri_spec.sess(curr_run).cond(6).duration =
 subj_data.repro_2key_rt(subj_data.runs_thisN==(curr_run-1));

 matlabbatch{1,1}.spm.stats.fmri_spec.sess(curr_run).cond(6).pmod.param=RepAmp
 litudes_2(:,curr_run);
 %On Target Feedback 2
 matlabbatch{1,1}.spm.stats.fmri_spec.sess(curr_run).cond(7).onset =
 SecondFeedbackTimes(SecondFeedbackOnOff(:,curr_run)==1,curr_run);

 matlabbatch{1,1}.spm.stats.fmri_spec.sess(curr_run).cond(7).pmod.param=OnOffA
 mplitudes_2(OnOffIndices_2(:,curr_run)==1,curr_run);
 %Off Target Feedback 2
 matlabbatch{1,1}.spm.stats.fmri_spec.sess(curr_run).cond(8).onset =
 SecondFeedbackTimes(SecondFeedbackOnOff(:,curr_run)==2,curr_run);

 matlabbatch{1,1}.spm.stats.fmri_spec.sess(curr_run).cond(8).pmod.param=OnOffA
 mplitudes_2(OnOffIndices_2(:,curr_run)==2,curr_run);

 %lastly, load in the multiple regressors for each run


 cd(this_subj_bold_dir1); %go to BOLD directory
 file=dir('*00001.txt');


 matlabbatch{1,1}.spm.stats.fmri_spec.sess(curr_run).multi_reg =
 cellstr([this_subj_bold_dir1 file.name]);

end

%Now generate the GLM
spm_jobman('run',matlabbatch);

%% Now estimate the model
```

```
   load ([template_dir 'EstimateSPM12Template.mat']);
   matlabbatch{1,1}.spm.stats.fmri_est.spmmat = cellstr([this_subj_GLM_directory
   '/FMRIEEG/SPM.mat']);
   %%% Run the GLM-estimate job
   spm_jobman('run',matlabbatch);

  end;  % End of loop through subjects
```

Contrast_Batch_fMRI_Only.m
%% Batch Contrasts for First-level fMRI only

```
base_dir = '/Users/sladmin/Desktop/Farah/ImagingOnly/';    %%% Where the subjects'
data is kept
template_dir = '/Users/sladmin/Desktop/Farah/Scripts/fMRI_Analysis_Scripts/'; %%%
Where the templates are stored
cd(base_dir);  %%% Where the Subjects' data is kept
%%

subj_dirs = { ...

   };

%%

num_subjs = size(subj_dirs,2); %how many subjects are there?

%% Perform batch preprocessing
for subj_num = 1:num_subjs,


    this_subj_GLM_directory = [base_dir subj_dirs{subj_num} ];
    disp(['Running contrast batch preprocessing on subject ' subj_dirs{subj_num} ]);

   %load in the SPM Template
   load ([template_dir 'fMRIEEGBatchTemplateFeb2022v2spec.mat']);
   matlabbatch{1,1}.spm.stats.con.spmmat = cellstr([this_subj_GLM_directory
'/FMRIEEG/SPM.mat']);

   load([this_subj_GLM_directory '/FMRIEEG/SPM.mat']); %load in SPM.mat file for
subject
   feedbacktest=sum(SPM.xX.X)==0; %are any of the covariates empty? (this indicates
no feedback of a particular type)
```

```
   feedbacktest=feedbacktest(1:104);%cut out the extra covariates for session,change if
BOLD runs are cut out
   for con=1:37 %for each contrast (hard coded)

matlabbatch{1,1}.spm.stats.con.consess{1,con}.tcon.weights(find(feedbacktest==1))=0;
       %set the weights to zero if there was a run without any events
   end

   %Now generate the GLM
   spm_jobman('run',matlabbatch);

 end;  % End of loop through subjects
```

fMRIEEGProcessorv3.m

%% Script for processing EEG data for combined fMRI analysis

```
base_dir='/Users/sladmin/Desktop/Farah/Brain Vision Processed
fMRI_EEG_files_NOcleanrawdata/';

subj_dirs = { ...

   };

num_subj=length(subj_dirs);

%%

for subj_num=1:num_subj,

   %Go to the subject directory

   cd([base_dir subj_dirs{subj_num}]);
   fname=dir('*.eeg');
   fname={fname.name};

   EEG=pop_fileio(fname{1}); %load in data

   channel=dir('*.bvef');
   channel={channel.name};

   EEG.chanlocs=loadbvef(channel{1}); %update channel information
   EEG.chanlocs(1) = [];
   EEG.chanlocs(1).labels = 'FCz';
```

```
    if length(EEG.chanlocs)>65,
       EEG = pop_select( EEG,'nochannel',{'ECG' 'IO' 'HEOG'});

    end

    EEG = pop_reref( EEG, [30 31] ); %Re-reference to the mastoids

    %This is for the weird ones where the bvef file doesn't work.
%     EEG=pop_chanedit(EEG,
'lookup','/Users/sladmin/Desktop/eeglab14_1_2b/plugins/dipfit2.3/standard_BESA/stand
ard-10-5-cap385.elp','insert',64,'changefield',{64 'labels'
'FCz'},'lookup','/Users/sladmin/Desktop/eeglab14_1_2b/plugins/dipfit2.3/standard_BESA
/standard-10-5-cap385.elp');
%     EEG = pop_reref( EEG, [29 30]
,'refloc',struct('labels',{'FCz'},'type',{''},'theta',{0},'radius',{0.12662},'X',{32.9279},'Y',{0
},'Z',{78.363},'sph_theta',{0},'sph_phi',{67.208},'sph_radius',{85},'urchan',{64},'ref',{''},'
datachan',{0}));

      %%
    %Remove bad channels
    %EEG = pop_rejchan(EEG, 'elec',[1:60]
,'threshold',5,'norm','on','measure','spec','freqrange',[1 125] );


    %Or, alternatively, use clean_rawdata (comment out above line if you
    %want to try)


EEG=clean_artifacts(EEG,'FlatlineCriterion',5,'ChannelCriterion',0.8,'LineNoiseCriterion
',4,'Highpass','off','BurstCriterion',20,'WindowCriterion','off','BurstRejection','off','Distanc
e','Euclidian');

    %Low-pass filter at 30Hz
    EEG =  pop_eegfiltnew(EEG,  [],30,110,0,[],0);

    %Epoching for Estimation
    EEG1 = pop_epoch( EEG, {  'S  1'  'S  2'  'S  3'  'S  4'  'S  5'  'S 23'  'S 24'  'S 25'  'S 26'
'S 27'  }, [-1  7], 'newname', 'Estimation', 'epochinfo', 'yes');
    EEG1 = pop_rmbase( EEG1, [-1000     0]);
    EEG1.setname='Estimation';
%     %EEG1=pop_runica(EEG1,'extended',1,'interupt','off');
   EEG1=pop_saveset(EEG1,'filename',[subj_dirs{subj_num}
'Estimation.set'],'filepath',[base_dir   subj_dirs{subj_num}]);
```

```
%     %Epoching for Reproduction
    EEG2 = pop_epoch( EEG, {  'S  6'  'S  7'  'S  8'  'S  9'  'S 10'  'S 33'  'S 34'  'S 35'  'S 36'
'S 37'  }, [-1  7], 'newname', 'Reproduction', 'epochinfo', 'yes');
   EEG2 = pop_rmbase( EEG2, [-1000     0]);
   EEG2.setname='Reproduction';
%     %EEG2=pop_runica(EEG2,'extended',1,'interupt','off');
   EEG2=pop_saveset(EEG2,'filename',[subj_dirs{subj_num}
'Reproduction.set'],'filepath',[base_dir  subj_dirs{subj_num}]);
  %Epoching for On-Feedback
  EEG3 = pop_epoch( EEG, {  'S 11' 'S 43'  }, [-0.5 1], 'newname', 'Off-feedback',
'epochinfo', 'yes');
  EEG3 = pop_rmbase( EEG3, [-500     0]);
  EEG3.setname='OnFeedback';
    %EEG3=pop_runica(EEG3,'extended',1,'interupt','off');
EEG3=pop_saveset(EEG3,'filename',[subj_dirs{subj_num}
'OnFeed.set'],'filepath',[base_dir subj_dirs{subj_num}]);
  %Epoching for Off-Feedback
   EEG4 = pop_epoch( EEG, {  'S 12'  'S 44'  }, [-0.5 1], 'newname', 'Off-feedback',
'epochinfo', 'yes');
   EEG4 = pop_rmbase( EEG4, [-500     0]);
   EEG4.setname='OffFeedback';
    %EEG4=pop_runica(EEG4,'extended',1,'interupt','off');
   EEG4=pop_saveset(EEG4,'filename',[subj_dirs{subj_num}
'OffFeed.set'],'filepath',[base_dir  subj_dirs{subj_num}]);
     %Epoching for On and Off-Feedback
   EEG5 = pop_epoch( EEG, {  'S 11' 'S 43' 'S 12'  'S 44'  }, [-0.5 1], 'newname', 'OnOff-
feedback', 'epochinfo', 'yes');
   EEG5 = pop_rmbase( EEG5, [-500     0]);
   EEG5.setname='OnOffFeedback';
    %EEG4=pop_runica(EEG4,'extended',1,'interupt','off');
   EEG5=pop_saveset(EEG5,'filename',[subj_dirs{subj_num}
'OnOffFeed.set'],'filepath',[base_dir subj_dirs{subj_num}]);

End
```

fMRIEEGamplitudeExtractoNewWindowsmar14_22r.m
%% Script for extracting amplitudes from EEG portion for fMRI

```
%%

%Set parameters and extract the data for frontocentral electrodes, single
%trials
STUDY = pop_statparams(STUDY, 'singletrials','on');
STUDY = pop_erpparams(STUDY,
'plotconditions','together','averagechan','on','topotime',[]);
STUDY = pop_erpparams(STUDY, 'filter',5,'topotime',[]);

[STUDY erpdata erptimes] = std_erpplot(STUDY,ALLEEG,'channels',{'FCz' 'Fz' 'Cz'
'FC1' 'FC2' 'F1' 'F2' 'C1' 'C2'},'plotstderr','on');

%% For Estimation-Reproduction Data

%average within 430-598ms window (358 - 401), using Bader & Wiener, 2021
timeframe

Estamps=mean(erpdata{1}(358:401,:));
Repamps=mean(erpdata{2}(358:401,:));

%Need an index of which points correspond to which trials

num_subj=length(STUDY.subject);
EstSubIndex=[];
RepSubIndex=[];

for s=1:num_subj, %for each subject

   Estindex=1:2:(num_subj*2);
   Repindex=2:2:(num_subj*2);

   EstSubIndex=[EstSubIndex;
ones(length(STUDY.datasetinfo(Estindex(s)).trialinfo),1)*s];
   RepSubIndex=[RepSubIndex;
ones(length(STUDY.datasetinfo(Repindex(s)).trialinfo),1)*s];

end

for s=1:num_subj,

   EstAmplitudes=Estamps(EstSubIndex==s);
```

```
   RepAmplitudes=Repamps(RepSubIndex==s);
   save(['EstRepAmplitudes_S' num2str(s)],'EstAmplitudes','RepAmplitudes');

end

%% For Off-On data
%note that I'm not sure if we want to use a frontocentral array, or just a
%single electrode, and also if I want to use the clean_rawdata bunch or or
%not

%average within 400-550ms window (226-263)

OnOffamps=mean(erpdata{1}(226:263,:));

%Need an index of which points correspond to which trials

num_subj=length(STUDY.subject);
OnOffSubIndex=[]; %empty matrix for subject index
OnOffIndex=[];%empty matrix for whether it's positive or negative feedback


for s=1:num_subj, %for each subject

   Onindex=1:num_subj;


   OnOffSubIndex=[OnOffSubIndex;
ones(length(STUDY.datasetinfo(Onindex(s)).trialinfo),1)*s];


end

for s=1:num_subj, %for each subject

   triggerindex={STUDY.datasetinfo(s).trialinfo.type};
   triggerindex=string(triggerindex);
   Onindex=contains(triggerindex,{'11' '43'});
   Offindex=contains(triggerindex,{'12' '44'});
   OnOffIndex=[OnOffIndex; (Onindex+(Offindex*2))'];
end


for s=1:num_subj,
```

```
    OnOffAmplitudes=OnOffamps(OnOffSubIndex==s);
    OnOffIndices=OnOffIndex(OnOffSubIndex==s);

    save(['OnOffAmplitudes_S'
STUDY.datasetinfo(s).filename(1:3)],'OnOffAmplitudes','OnOffIndices');

end
```

REFERENCES

Acerbi, L., Wolpert, D. M., & Vijayakumar, S. (2012). Internal Representations of Temporal Statistics and Feedback Calibrate Motor-Sensory Interval Timing. *PLoS Computational Biology*, *8*(11), e1002771. https://doi.org/10.1371/journal.pcbi.1002771

Akdoğan, B., & Balcı, F. (2017). Are you early or late?: Temporal error monitoring. *Journal of Experimental Psychology. General*, *146*(3), 347–361. https://doi.org/10.1037/xge0000265

Alagapan, S., Lustenberger, C., Hadar, E., Shin, H. W., & Fröhlich, F. (2019). Low-frequency direct cortical stimulation of left superior frontal gyrus enhances working memory performance. *NeuroImage*, *184*, 697–706. https://doi.org/10.1016/j.neuroimage.2018.09.064

Allen, P. J., Josephs, O., & Turner, R. (2000). A method for removing imaging artifact from continuous EEG recorded during functional MRI. *NeuroImage*, *12*(2), 230–239. https://doi.org/10.1006/nimg.2000.0599

Allen, P. J., Polizzi, G., Krakow, K., Fish, D. R., & Lemieux, L. (1998). Identification of EEG events in the MR scanner: The problem of pulse artifact and a method for its subtraction. *NeuroImage*, *8*(3), 229–239. https://doi.org/10.1006/nimg.1998.0361

Allman, M. J., & Meck, W. H. (2012). Pathophysiological distortions in time perception and timed performance. *Brain*, *135*(3), 656–677. https://doi.org/10.1093/brain/awr210

Amabile, G., Fattapposta, F., Pozzessere, G., Albani, G., Sanarelli, L., Rizzo, P. A., & Morocutti, C. (1986). Parkinson disease: Electrophysiological (CNV) analysis related to pharmacological treatment. *Electroencephalography and Clinical Neurophysiology*, *64*(6), 521–524. https://doi.org/10.1016/0013-4694(86)90189-6

Amadeo, M. B., Campus, C., & Gori, M. (2020). Visual representations of time elicit early responses in human temporal cortex. *NeuroImage*, *217*, 116912. https://doi.org/10.1016/j.neuroimage.2020.116912

Amiez, C., Joseph, J.-P., & Procyk, E. (2005). Anterior cingulate error-related activity is modulated by predicted reward. *The European Journal of Neuroscience*, *21*(12), 3447–3452. https://doi.org/10.1111/j.1460-9568.2005.04170.x

Arnal, L., Doelling, K., & Poeppel, D. (2014). Delta-Beta Coupled Oscillations Underlie Temporal Prediction Accuracy. *Cerebral Cortex (New York, N.Y. : 1991)*, *25*. https://doi.org/10.1093/cercor/bhu103

Arnal, L. H., & Giraud, A.-L. (2012). Cortical oscillations and sensory predictions. *Trends in Cognitive Sciences*, *16*(7), 390–398. https://doi.org/10.1016/j.tics.2012.05.003

Bader, F., & Wiener, M. (2021). Awareness of errors and feedback in human time estimation. *Learning & Memory (Cold Spring Harbor, N.Y.)*, *28*(5), 171–177. https://doi.org/10.1101/lm.053108.120

Baker, T. E., & Holroyd, C. B. (2011). Dissociated roles of the anterior cingulate cortex in reward and conflict processing as revealed by the feedback error-related

negativity and N200. *Biological Psychology*, *87*(1), 25–34. https://doi.org/10.1016/j.biopsycho.2011.01.010

Balcı, F., Wiener, M., Çavdaroğlu, B., & Branch Coslett, H. (2013). Epistasis effects of dopamine genes on interval timing and reward magnitude in humans. *Neuropsychologia*, *51*(2), 293–308. https://doi.org/10.1016/j.neuropsychologia.2012.08.002

Barne, L. C., Claessens, P. M. E., Reyes, M. B., Caetano, M. S., & Cravo, A. M. (2017). Low-frequency cortical oscillations are modulated by temporal prediction and temporal error coding. *NeuroImage*, *146*, 40–46. https://doi.org/10.1016/j.neuroimage.2016.11.028

Beatty, P. J., Buzzell, G. A., Roberts, D. M., & McDonald, C. G. (2018). Speeded response errors and the error-related negativity modulate early sensory processing. *NeuroImage*, *183*, 112–120. https://doi.org/10.1016/j.neuroimage.2018.08.009

Becker, M. P. I., Nitsch, A. M., Miltner, W. H. R., & Straube, T. (2014). A Single-Trial Estimation of the Feedback-Related Negativity and Its Relation to BOLD Responses in a Time-Estimation Task. *Journal of Neuroscience*, *34*(8), 3005–3012. https://doi.org/10.1523/JNEUROSCI.3684-13.2014

Bellebaum, C., & Colosio, M. (2014). From feedback- to response-based performance monitoring in active and observational learning. *Journal of Cognitive Neuroscience*, *26*(9), 2111–2127. https://doi.org/10.1162/jocn_a_00612

Bellebaum, C., & Daum, I. (2008). Learning-related changes in reward expectancy are reflected in the feedback-related negativity. *The European Journal of Neuroscience*, *27*(7), 1823–1835. https://doi.org/10.1111/j.1460-9568.2008.06138.x

Beudel, M., Renken, R., Leenders, K. L., & de Jong, B. M. (2009). Cerebral representations of space and time. *NeuroImage*, *44*(3), 1032–1040. https://doi.org/10.1016/j.neuroimage.2008.09.028

Bizo LA, White KG. The behavioral theory of timing: Reinforcer rate determines pacemaker rate. J Exp Anal Behav. 1994 Jan;61(1):19-33.

Block, R. A., & Zakay, D. (1997). Prospective and retrospective duration judgments: A meta-analytic review. *Psychonomic Bulletin & Review*, *4*(2), 184–197. https://doi.org/10.3758/BF03209393

Bluschke, A., Schuster, J., Roessner, V., & Beste, C. (2018). Neurophysiological mechanisms of interval timing dissociate inattentive and combined ADHD subtypes. *Scientific Reports*, *8*(1), 2033. https://doi.org/10.1038/s41598-018-20484-0

Boldt, A., & Yeung, N. (2015). Shared Neural Markers of Decision Confidence and Error Detection. *The Journal of Neuroscience : The Official Journal of the Society for Neuroscience*, *35*, 3478–3484. https://doi.org/10.1523/JNEUROSCI.0797-14.2015

Borght, L. V. der, Schevernels, H., Burle, B., & Notebaert, W. (2016). Errors Disrupt Subsequent Early Attentional Processes. *PLOS ONE*, *11*(4), e0151843. https://doi.org/10.1371/journal.pone.0151843

Botvinick, M. M., Braver, T. S., Barch, D. M., Carter, C. S., & Cohen, J. D. (2001). Conflict monitoring and cognitive control. *Psychological Review*, *108*(3), 624–652. https://doi.org/10.1037/0033-295X.108.3.624

Brocas, I., Carrillo, J. D., & Tarrasó, J. (2018). Self-awareness of biases in time perception. *Journal of Economic Behavior & Organization*, *148*, 1–19. https://doi.org/10.1016/j.jebo.2018.02.001

(Bud) Craig, & D, A. (2009a). How do you feel — now? The anterior insula and human awareness. *Nature Reviews Neuroscience*, *10*(1), 59–70. https://doi.org/10.1038/nrn2555

(Bud) Craig, & D, A. (2009b). How do you feel — now? The anterior insula and human awareness. *Nature Reviews Neuroscience*, *10*(1), 59–70. https://doi.org/10.1038/nrn2555

Bueti, D., & Walsh, V. (2009). The parietal cortex and the representation of time, space, number and other magnitudes. *Philosophical Transactions of the Royal Society of London. Series B, Biological Sciences*, *364*(1525), 1831–1840. https://doi.org/10.1098/rstb.2009.0028

Buhusi, C. V., & Meck, W. H. (2005). What makes us tick? Functional and neural mechanisms of interval timing. *Nature Reviews Neuroscience*, *6*(10), 755–765. https://doi.org/10.1038/nrn1764

Bullmore, E., & Sporns, O. (2012). The economy of brain network organization. *Nature Reviews Neuroscience*, *13*(5), 336–349. https://doi.org/10.1038/nrn3214

Buonomano, D. V., & Laje, R. (2010). Population clocks: Motor timing with neural dynamics. *Trends in Cognitive Sciences*, *14*(12), 520–527. https://doi.org/10.1016/j.tics.2010.09.002

Buzzell, G. A., Beatty, P. J., Paquette, N. A., Roberts, D. M., & McDonald, C. G. (2017). Error-Induced Blindness: Error Detection Leads to Impaired Sensory Processing and Lower Accuracy at Short Response–Stimulus Intervals. *Journal of Neuroscience*, *37*(11), 2895–2903. https://doi.org/10.1523/JNEUROSCI.1202-16.2017

Carlson, J. M., Foti, D., Mujica-Parodi, L. R., Harmon-Jones, E., & Hajcak, G. (2011). Ventral striatal and medial prefrontal BOLD activation is correlated with reward-related electrocortical activity: A combined ERP and fMRI study. *NeuroImage*, *57*(4), 1608–1616. https://doi.org/10.1016/j.neuroimage.2011.05.037

Carvalho, F. M., Chaim, K. T., Sanchez, T. A., & de Araujo, D. B. (2016). Time-Perception Network and Default Mode Network Are Associated with Temporal Prediction in a Periodic Motion Task. *Frontiers in Human Neuroscience*, *10*, 268. https://doi.org/10.3389/fnhum.2016.00268

Casini, L., & Vidal, F. (2011). The SMAs: Neural Substrate of the Temporal Accumulator? *Frontiers in Integrative Neuroscience*, *5*. https://www.frontiersin.org/article/10.3389/fnint.2011.00035

Cavanagh, J. F., & Frank, M. J. (2014). Frontal theta as a mechanism for cognitive control. *Trends in Cognitive Sciences*, *18*(8), 414–421. https://doi.org/10.1016/j.tics.2014.04.012

Charles, L., Van Opstal, F., Marti, S., & Dehaene, S. (2013). Distinct brain mechanisms for conscious versus subliminal error detection. *NeuroImage*, *73*, 80–94. https://doi.org/10.1016/j.neuroimage.2013.01.054

Cona, G., Wiener, M., & Scarpazza, C. (2021). From ATOM to GradiATOM: Cortical gradients support time and space processing as revealed by a meta-analysis of neuroimaging studies. *NeuroImage*, *224*, 117407. https://doi.org/10.1016/j.neuroimage.2020.117407

Corcoran, A. W., Groot, C., Bruno, A., Johnston, A., & Cropper, S. J. (2018). Individual differences in first- and second-order temporal judgment. *PLOS ONE*, *13*(2), e0191422. https://doi.org/10.1371/journal.pone.0191422

Coull, J., & Nobre, A. (2008). Dissociating explicit timing from temporal expectation with fMRI. *Current Opinion in Neurobiology*, *18*(2), 137–144. https://doi.org/10.1016/j.conb.2008.07.011

Coull, J. T., Hwang, H. J., Leyton, M., & Dagher, A. (2012). Dopamine precursor depletion impairs timing in healthy volunteers by attenuating activity in putamen and supplementary motor area. *The Journal of Neuroscience: The Official Journal of the Society for Neuroscience*, *32*(47), 16704–16715. https://doi.org/10.1523/JNEUROSCI.1258-12.2012

Coull, J. T., Vidal, F., Nazarian, B., & Macar, F. (2004). Functional anatomy of the attentional modulation of time estimation. *Science (New York, N.Y.)*, *303*(5663), 1506–1508. https://doi.org/10.1126/science.1091573

Craig, A. D. (Bud). (2009). Emotional moments across time: A possible neural basis for time perception in the anterior insula. *Philosophical Transactions of the Royal Society B: Biological Sciences*, *364*(1525), 1933–1942. https://doi.org/10.1098/rstb.2009.0008

Diedrichsen, J., Hashambhoy, Y., Rane, T., & Shadmehr, R. (2005). Neural correlates of reach errors. *The Journal of Neuroscience: The Official Journal of the Society for Neuroscience*, *25*(43), 9919–9931. https://doi.org/10.1523/JNEUROSCI.1874-05.2005

Doenyas, C., Mutluer, T., Genç, E., & Balcı, F. (2019). Error monitoring in decision-making and timing is disrupted in autism spectrum disorder. *Autism Research*, *12*(2), 239–248. https://doi.org/10.1002/aur.2041

Droit-Volet S, Izaute M. Improving time discrimination in children and adults in a temporal bisection task: the effects of feedback and no forced choice on decision and memory processes. Q J Exp Psychol (Hove). 2009 Jun;62(6):1173-88

Dušek, P., Jech, R., Sieger, T., Vymazal, J., Růžička, E., Wackermann, J., & Mueller, K. (2012). Abnormal Activity in the Precuneus during Time Perception in Parkinson's Disease: An fMRI Study. *PLOS ONE*, *7*(1), e29635. https://doi.org/10.1371/journal.pone.0029635

Duyan, Y. A., & Balcı, F. (2018). Numerical error monitoring. *Psychonomic Bulletin & Review*, *25*(4), 1549–1555. https://doi.org/10.3758/s13423-018-1506-x

Duyan, Y. A., & Balcı, F. (2019). Metric error monitoring in the numerical estimates. *Consciousness and Cognition*, *67*, 69–76. https://doi.org/10.1016/j.concog.2018.11.011

Duyan, Y. A., & Balcı, F. (2020). Monitoring line length reproduction errors. *Consciousness and Cognition*, *77*, 102831. https://doi.org/10.1016/j.concog.2019.102831

Eichenbaum, H. (2017). On the Integration of Space, Time, and Memory. *Neuron*, *95*(5), 1007–1018. https://doi.org/10.1016/j.neuron.2017.06.036

Eppinger, B., Kray, J., Mock, B., & Mecklinger, A. (2008). Better or worse than expected? Aging, learning, and the ERN. *Neuropsychologia*, *46*(2), 521–539. https://doi.org/10.1016/j.neuropsychologia.2007.09.001

Falkenstein, M., Hohnsbein, J., Hoormann, J., & Blanke, L. (1991). Effects of crossmodal divided attention on late ERP components. II. Error processing in choice reaction tasks. *Electroencephalography and Clinical Neurophysiology*, *78*(6), 447–455. https://doi.org/10.1016/0013-4694(91)90062-9

Falkenstein, M., Hoormann, J., Hohnsbein, J., & Kleinsorge, T. (2003). Short-term mobilization of processing resources is revealed in the event-related potential. *Psychophysiology*, *40*(6), 914–923. https://doi.org/10.1111/1469-8986.00109

Farahani, F. V., Karwowski, W., & Lighthall, N. R. (2019). Application of Graph Theory for Identifying Connectivity Patterns in Human Brain Networks: A Systematic

Review. *Frontiers in Neuroscience*, *13*. https://www.frontiersin.org/article/10.3389/fnins.2019.00585

Farmaki, C., Sakkalis, V., Loesche, F., & Nisiforou, E. A. (2019). Assessing Field Dependence–Independence Cognitive Abilities Through EEG-Based Bistable Perception Processing. *Frontiers in Human Neuroscience*, *13*. https://www.frontiersin.org/article/10.3389/fnhum.2019.00345

Ferrandez, A. M., Hugueville, L., Lehéricy, S., Poline, J. B., Marsault, C., & Pouthas, V. (2003). Basal ganglia and supplementary motor area subtend duration perception: An fMRI study. *NeuroImage*, *19*(4), 1532–1544. https://doi.org/10.1016/s1053-8119(03)00159-9

Fleming, S., & Dolan, R. (2012). The neural basis of metacognitive ability. *Philosophical Transactions of the Royal Society of London. Series B, Biological Sciences*, *367*, 1338–1349. https://doi.org/10.1098/rstb.2011.0417

FMRI design with jittered ISI. (n.d.). Retrieved June 20, 2022, from https://groups.google.com/g/psychopy-users/c/ZbV5t_MVvUk

Fontes, R., Ribeiro, J., Gupta, D. S., Machado, D., Lopes-Júnior, F., Magalhães, F., Bastos, V. H., Rocha, K., Marinho, V., Lima, G., Velasques, B., Ribeiro, P., Orsini, M., Pessoa, B., Leite, M. A. A., & Teixeira, S. (2016). Time Perception Mechanisms at Central Nervous System. *Neurology International*, *8*(1), 5939. https://doi.org/10.4081/ni.2016.5939

Foti, D., Weinberg, A., Dien, J., & Hajcak, G. (2011). Event-related potential activity in the basal ganglia differentiates rewards from nonrewards: Response to

commentary. *Human Brain Mapping*, *32*(12), 2267–2269. https://doi.org/10.1002/hbm.21357.

Freestone, D., Russell, Church. (2015). Optimal Timing. Current Opinions in Behavioral Science. 8:276-281.

Fu, Z., Beam, D., Chung, J. M., Reed, C. M., Mamelak, A. N., Adolphs, R., & Rutishauser, U. (2022). The geometry of domain-general performance monitoring in the human medial frontal cortex. *Science*, *376*(6593), eabm9922. https://doi.org/10.1126/science.abm9922

Fung, B. J., Sutlief, E., & Hussain Shuler, M. G. (2021). Dopamine and the interdependency of time perception and reward. *Neuroscience and Biobehavioral Reviews*, *125*, 380–391. https://doi.org/10.1016/j.neubiorev.2021.02.030

Gaffin-Cahn, E., Hudson, T. E., & Landy, M. S. (2019). Did I do that? Detecting a perturbation to visual feedback in a reaching task. *Journal of Vision*, *19*(1), 5. https://doi.org/10.1167/19.1.5

Garrison, J., Erdeniz, B., & Done, J. (2013). Prediction error in reinforcement learning: A meta-analysis of neuroimaging studies. *Neuroscience & Biobehavioral Reviews*, *37*(7), 1297–1310. https://doi.org/10.1016/j.neubiorev.2013.03.023

Gehring, W. J., Goss, B., Coles, M. G. H., Meyer, D. E., & Donchin, E. (1993). A Neural System for Error Detection and Compensation. *Psychological Science*, *4*(6), 385–390. https://doi.org/10.1111/j.1467-9280.1993.tb00586.x

Gehring, W. J., & Willoughby, A. R. (2002). The Medial Frontal Cortex and the Rapid Processing of Monetary Gains and Losses. *Science*, *295*(5563), 2279–2282. https://doi.org/10.1126/science.1066893

Genovesio, A., Tsujimoto, S., & Wise, S. P. (2009). Feature- and Order-Based Timing Representations in the Frontal Cortex. *Neuron*, *63*(2), 254–266. https://doi.org/10.1016/j.neuron.2009.06.018

Gershman, S., Moustafa, A., & Ludvig, E. (2014). Time representation in reinforcement learning models of the basal ganglia. *Frontiers in Computational Neuroscience*, *7*. https://www.frontiersin.org/article/10.3389/fncom.2013.00194

Gibbon, J., Church, R. M., & Meck, W. H. (1984). Scalar Timing in Memory. *Annals of the New York Academy of Sciences*, *423*(1), 52–77. https://doi.org/10.1111/j.1749-6632.1984.tb23417.x

Goel, A., & Buonomano, D. V. (2014). Timing as an intrinsic property of neural networks: Evidence from in vivo and in vitro experiments. *Philosophical Transactions of the Royal Society of London. Series B, Biological Sciences*, *369*(1637), 20120460. https://doi.org/10.1098/rstb.2012.0460

Grabot, L., Kononowicz, T. W., Tour, T. D. la, Gramfort, A., Doyère, V., & Wassenhove, V. van. (2019). The Strength of Alpha–Beta Oscillatory Coupling Predicts Motor Timing Precision. *Journal of Neuroscience*, *39*(17), 3277–3291. https://doi.org/10.1523/JNEUROSCI.2473-18.2018

Grondin, S. (2010). Timing and time perception: A review of recent behavioral and neuroscience findings and theoretical directions. *Attention, Perception, & Psychophysics*, *72*(3), 561–582. https://doi.org/10.3758/APP.72.3.561

Gu, B.-M., & Meck, W. H. (2011). New Perspectives on Vierordt's Law: Memory-Mixing in Ordinal Temporal Comparison Tasks. In A. Vatakis, A. Esposito, M. Giagkou, F. Cummins, & G. Papadelis (Eds.), *Multidisciplinary Aspects of Time and Time Perception: COST TD0904 International Workshop, Athens, Greece, October 7-8, 2010, Revised Selected Papers* (pp. 67–78). Springer. https://doi.org/10.1007/978-3-642-21478-3_6

Harrington, D. L., Zimbelman, J. L., Hinton, S. C., & Rao, S. M. (2010). Neural Modulation of Temporal Encoding, Maintenance, and Decision Processes. *Cerebral Cortex*, *20*(6), 1274–1285. https://doi.org/10.1093/cercor/bhp194

Hayden, B. Y., Pearson, J. M., & Platt, M. L. (2011). Neuronal basis of sequential foraging decisions in a patchy environment. *Nature Neuroscience*, *14*(7), 933–939. https://doi.org/10.1038/nn.2856

Heydari, S., & Holroyd, C. B. (2016). Reward positivity: Reward prediction error or salience prediction error? *Psychophysiology*, *53*(8), 1185–1192. https://doi.org/10.1111/psyp.12673

Hollerman, J. R., & Schultz, W. (1998). Dopamine neurons report an error in the temporal prediction of reward during learning. *Nature Neuroscience*, *1*(4), 304–309. https://doi.org/10.1038/1124

Holroyd, C. B., & Coles, M. G. H. (2002). The neural basis of human error processing: Reinforcement learning, dopamine, and the error-related negativity. *Psychological Review*, *109*(4), 679–709. https://doi.org/10.1037/0033-295X.109.4.679

Holroyd, C. B., Pakzad-Vaezi, K. L., & Krigolson, O. E. (2008). The feedback correct-related positivity: Sensitivity of the event-related brain potential to unexpected positive feedback. *Psychophysiology*, *45*(5), 688–697. https://doi.org/10.1111/j.1469-8986.2008.00668.x

Honma, M., Murakami, H., Yabe, Y., Kuroda, T., Futamura, A., Sugimoto, A., Terao, Y., Masaoka, Y., Izumizaki, M., Kawamura, M., & Ono, K. (2021). Stopwatch training improves cognitive functions in patients with Parkinson's disease. *Journal of Neuroscience Research*, *99*(5), 1325–1336. https://doi.org/10.1002/jnr.24812

How to Generate Random Timings for a Poisson Process. (n.d.). Retrieved June 20, 2022, from https://preshing.com/20111007/how-to-generate-random-timings-for-a-poisson-process/#comment-33488

Jang, J., Jones, M., Milne, E., Wilson, D., & Lee, K.-H. (2016). Contingent negative variation (CNV) associated with sensorimotor timing error correction. *NeuroImage*, *127*, 58–66. https://doi.org/10.1016/j.neuroimage.2015.11.071

Jann, K., Dierks, T., Boesch, C., Kottlow, M., Strik, W., & Koenig, T. (2009). BOLD correlates of EEG alpha phase-locking and the fMRI default mode network. *NeuroImage*, *45*(3), 903–916. https://doi.org/10.1016/j.neuroimage.2009.01.001

Jazayeri, M., & Shadlen, M. N. (2010). Temporal context calibrates interval timing. *Nature Neuroscience*, *13*(8), 1020–1026. https://doi.org/10.1038/nn.2590

Jentzsch, I., & Dudschig, C. (2009). Short Article: Why do we slow down after an error? Mechanisms underlying the effects of posterror slowing. *Quarterly Journal of Experimental Psychology*, *62*(2), 209–218. https://doi.org/10.1080/17470210802240655

Jocham, G., & Ullsperger, M. (2009). Neuropharmacology of performance monitoring. *Neuroscience & Biobehavioral Reviews*, *33*(1), 48–60. https://doi.org/10.1016/j.neubiorev.2008.08.011

Jones, C. R. G., Rosenkranz, K., Rothwell, J. C., & Jahanshahi, M. (2004). The right dorsolateral prefrontal cortex is essential in time reproduction: An investigation with repetitive transcranial magnetic stimulation. *Experimental Brain Research*, *158*(3), 366–372. https://doi.org/10.1007/s00221-004-1912-3

Kennerley, S. W., Walton, M. E., Behrens, T. E. J., Buckley, M. J., & Rushworth, M. F. S. (2006). Optimal decision making and the anterior cingulate cortex. *Nature Neuroscience*, *9*(7), 940–947. https://doi.org/10.1038/nn1724

Kepecs, A., Uchida, N., Zariwala, H. A., & Mainen, Z. F. (2008). Neural correlates, computation and behavioural impact of decision confidence. *Nature*, *455*(7210), 227–231. https://doi.org/10.1038/nature07200

Kiani, R., & Shadlen, M. N. (2009). Representation of Confidence Associated with a Decision by Neurons in the Parietal Cortex. *Science*, *324*(5928), 759–764. https://doi.org/10.1126/science.1169405.

Killeen, P. R., & Fetterman, J. G. (1988). A behavioral theory of timing. *Psychological Review, 95*(2), 274–295.

Kimura, K., & Kimura, M. (2016). Temporal prediction restores the evaluative processing of delayed action feedback: An electrophysiological study. *NeuroReport, 27*(14), 1061–1067. https://doi.org/10.1097/WNR.0000000000000657

King, J. A., Korb, F. M., Cramon, D. Y. von, & Ullsperger, M. (2010). Post-Error Behavioral Adjustments Are Facilitated by Activation and Suppression of Task-Relevant and Task-Irrelevant Information Processing. *Journal of Neuroscience, 30*(38), 12759–12769. https://doi.org/10.1523/JNEUROSCI.3274-10.2010

Koch, G., Oliveri, M., Carlesimo, G. A., & Caltagirone, C. (2002). Selective deficit of time perception in a patient with right prefrontal cortex lesion. *Neurology*, *59*(10), 1658–1658. https://doi.org/10.1212/01.WNL.0000032504.45792.8F

Koch, G., Oliveri, M., Torriero, S., & Caltagirone, C. (2003). Underestimation of time perception after repetitive transcranial magnetic stimulation. *Neurology*, *60*(11), 1844–1846. https://doi.org/10.1212/WNL.60.11.1844

Komura, Y., Nikkuni, A., Hirashima, N., Uetake, T., & Miyamoto, A. (2013). Responses of pulvinar neurons reflect a subject's confidence in visual categorization. *Nature Neuroscience*, *16*(6), 749–755. https://doi.org/10.1038/nn.3393

Komura, Y., Tamura, R., Uwano, T., Nishijo, H., Kaga, K., & Ono, T. (2001). Retrospective and prospective coding for predicted reward in the sensory thalamus. *Nature*, *412*(6846), 546–549. https://doi.org/10.1038/35087595

Kononowicz, T. W. (2015). Dopamine-dependent oscillations in frontal cortex index "start-gun" signal in interval timing. *Frontiers in Human Neuroscience*, *9*, 331. https://doi.org/10.3389/fnhum.2015.00331

Kononowicz, T. W., Roger, C., & van Wassenhove, V. (2019). Temporal Metacognition as the Decoding of Self-Generated Brain Dynamics. *Cerebral Cortex*, *29*(10), 4366–4380. https://doi.org/10.1093/cercor/bhy318

Kononowicz, T. W., & van Rijn, H. (2014). Decoupling Interval Timing and Climbing Neural Activity: A Dissociation between CNV and N1P2 Amplitudes. *The Journal of Neuroscience*, *34*(8), 2931–2939. https://doi.org/10.1523/JNEUROSCI.2523-13.2014

Kononowicz, T. W., & van Wassenhove, V. (2019). Evaluation of Self-generated Behavior: Untangling Metacognitive Readout and Error Detection. *Journal of Cognitive Neuroscience*, *31*(11), 1641–1657. https://doi.org/10.1162/jocn_a_01442

Kononowicz, T. W., van Wassenhove, V., & Doyère, V. (2022). Rodents monitor their error in self-generated duration on a single trial basis. *Proceedings of the National Academy of Sciences*, *119*(9), e2108850119. https://doi.org/10.1073/pnas.2108850119

Kothe, A., Miyakoshi, Delorme, Christian, Makoto. (2019). *Clean_rawdata* (2.7) [MATLAB]. https://github.com/sccn/clean_rawdata (Original work published 2019)

Krigolson, O. E. (2018). Event-related brain potentials and the study of reward processing: Methodological considerations. *International Journal of Psychophysiology: Official Journal of the International Organization of Psychophysiology*, *132*(Pt B), 175–183. https://doi.org/10.1016/j.ijpsycho.2017.11.007

Krigolson, O. E., Hassall, C. D., & Handy, T. C. (2014). How We Learn to Make Decisions: Rapid Propagation of Reinforcement Learning Prediction Errors in Humans. *Journal of Cognitive Neuroscience*, *26*(3), 635–644. https://doi.org/10.1162/jocn_a_00509

Krigolson, O. E., Pierce, L. J., Holroyd, C. B., & Tanaka, J. W. (2009). Learning to become an expert: Reinforcement learning and the acquisition of perceptual expertise. *Journal of Cognitive Neuroscience*, *21*(9), 1833–1840. https://doi.org/10.1162/jocn.2009.21128

Lak, A., Okun, M., Moss, M. M., Gurnani, H., Farrell, K., Wells, M. J., Reddy, C. B., Kepecs, A., Harris, K. D., & Carandini, M. (2020). Dopaminergic and Prefrontal Basis of Learning from Sensory Confidence and Reward Value. *Neuron*, *105*(4), 700-711.e6. https://doi.org/10.1016/j.neuron.2019.11.018

Laming, D. (1979). Choice reaction performance following an error. *Acta Psychologica*, *43*(3), 199–224. https://doi.org/10.1016/0001-6918(79)90026-X

Lebreton, M., Abitbol, R., Daunizeau, J., & Pessiglione, M. (2015). Automatic integration of confidence in the brain valuation signal. *Nature Neuroscience*, *18*(8), 1159–1167. https://doi.org/10.1038/nn.4064

Lee, D., Seo, H., & Jung, M. W. (2012). Neural Basis of Reinforcement Learning and Decision Making. *Annual Review of Neuroscience*, *35*, 287–308. https://doi.org/10.1146/annurev-neuro-062111-150512

Leon, M. I., & Shadlen, M. N. (2003). Representation of time by neurons in the posterior parietal cortex of the macaque. *Neuron*, *38*(2), 317–327. https://doi.org/10.1016/s0896-6273(03)00185-5

Lewis, P. A., & Miall, R. C. (2003). Distinct systems for automatic and cognitively controlled time measurement: Evidence from neuroimaging. *Current Opinion in Neurobiology*, *13*(2), 250–255. https://doi.org/10.1016/s0959-4388(03)00036-9

Li, P., Peng, W., Li, H., & Holroyd, C. B. (2018). Electrophysiological measures reveal the role of anterior cingulate cortex in learning from unreliable feedback. *Cognitive, Affective & Behavioral Neuroscience*, *18*(5), 949–963. https://doi.org/10.3758/s13415-018-0615-3

Linssen, A. M. W., Vuurman, E. F. P. M., Sambeth, A., Nave, S., Spooren, W., Vargas, G., Santarelli, L., & Riedel, W. J. (2011). Contingent negative variation as a dopaminergic biomarker: Evidence from dose-related effects of methylphenidate. *Psychopharmacology*, *218*(3), 533–542. https://doi.org/10.1007/s00213-011-2345-x

Luft, C. D. B. (2014). Learning from feedback: The neural mechanisms of feedback processing facilitating better performance. *Behavioural Brain Research*, *261*, 356–368. https://doi.org/10.1016/j.bbr.2013.12.043

Luque, D., López, F. J., Marco-Pallares, J., Càmara, E., & Rodríguez-Fornells, A. (2012). Feedback-related Brain Potential Activity Complies with Basic Assumptions of Associative Learning Theory. *Journal of Cognitive Neuroscience*, *24*(4), 794–808. https://doi.org/10.1162/jocn_a_00145

Macar, F., Coull, J., & Vidal, F. (2006). The supplementary motor area in motor and perceptual time processing: FMRI studies. *Cognitive Processing*, *7*(2), 89–94. https://doi.org/10.1007/s10339-005-0025-7

Macar, F., & Vidal, F. (2002). Time processing reflected by EEG surface Laplacians. *Experimental Brain Research*, *145*(3), 403–406. https://doi.org/10.1007/s00221-002-1103-z

Macar, F., & Vidal, F. (2003). The CNV peak: An index of decision making and temporal memory. *Psychophysiology*, *40*(6), 950–954. https://doi.org/10.1111/1469-8986.00113

Macar, F., Vidal, F., & Casini, L. (1999). The supplementary motor area in motor and sensory timing: Evidence from slow brain potential changes. *Experimental Brain Research*, *125*(3), 271–280. https://doi.org/10.1007/s002210050683

Maier, M. E., Yeung, N., & Steinhauser, M. (2011). Error-related brain activity and adjustments of selective attention following errors. *NeuroImage*, *56*(4), 2339–2347. https://doi.org/10.1016/j.neuroimage.2011.03.083

Masaki, H., Sommer, W., Takasawa, N., & Yamazaki, K. (2012). Neural mechanisms of timing control in a coincident timing task. *Experimental Brain Research*, *218*(2), 215–226. https://doi.org/10.1007/s00221-012-3052-5

Matell, M. S., & Meck, W. H. (2000). Neuropsychological mechanisms of interval timing behavior. *BioEssays*, *22*(1), 94–103. https://doi.org/10.1002/(SICI)1521-1878(200001)22:1<94::AID-BIES14>3.0.CO;2-E

Matell, M. S., & Meck, W. H. (2004). Cortico-striatal circuits and interval timing: Coincidence detection of oscillatory processes. *Cognitive Brain Research*, *21*(2), 139–170. https://doi.org/10.1016/j.cogbrainres.2004.06.012

Matthews, W. J., & Meck, W. H. (20160519). Temporal cognition: Connecting subjective time to perception, attention, and memory. *Psychological Bulletin*, *142*(8), 865. https://doi.org/10.1037/bul0000045

Mauk, M. D., & Buonomano, D. V. (2004). The neural basis of temporal processing. *Annual Review of Neuroscience*, *27*, 307–340. https://doi.org/10.1146/annurev.neuro.27.070203.144247

McFarland, C. P., & Glisky, E. L. (2009). Frontal lobe involvement in a task of time-based prospective memory. *Neuropsychologia*, *47*(7), 1660–1669. https://doi.org/10.1016/j.neuropsychologia.2009.02.023

Meck, W. H. (2005). Neuropsychology of timing and time perception. *Brain and Cognition*, *58*(1), 1–8. https://doi.org/10.1016/j.bandc.2004.09.004

Meirhaeghe, N., Sohn, H., & Jazayeri, M. (2021). A precise and adaptive neural mechanism for predictive temporal processing in the frontal cortex. *Neuron*, *109*(18), 2995-3011.e5. https://doi.org/10.1016/j.neuron.2021.08.025

Merchant, H., Pérez, O., Zarco, W., & Gámez, J. (2013). Interval Tuning in the Primate Medial Premotor Cortex as a General Timing Mechanism. *Journal of*

Neuroscience, *33*(21), 9082–9096. https://doi.org/10.1523/JNEUROSCI.5513-12.2013

Middlebrooks, P. G., & Sommer, M. A. (2012). Neuronal Correlates of Metacognition in Primate Frontal Cortex. *Neuron*, *75*(3), 517–530. https://doi.org/10.1016/j.neuron.2012.05.028

Mikhael, J. G., & Gershman, S. J. (2019). Adapting the flow of time with dopamine. *Journal of Neurophysiology*, *121*(5), 1748–1760. https://doi.org/10.1152/jn.00817.2018

Mikhael, J. G., Lai, L., & Gershman, S. J. (2021). Rational inattention and tonic dopamine. *PLOS Computational Biology*, *17*(3), e1008659. https://doi.org/10.1371/journal.pcbi.1008659

Miltner, W. H. R., Braun, C. H., & Coles, M. G. H. (1997). Event-Related Brain Potentials Following Incorrect Feedback in a Time-Estimation Task: Evidence for a "Generic" Neural System for Error Detection. *Journal of Cognitive Neuroscience*, *9*(6), 788–798. https://doi.org/10.1162/jocn.1997.9.6.788

Mioni, G., Grondin, S., Bardi, L., & Stablum, F. (2020). Understanding time perception through non-invasive brain stimulation techniques: A review of studies. *Behavioural Brain Research*, *377*, 112232. https://doi.org/10.1016/j.bbr.2019.112232

Mioni, G., Stablum, F., McClintock, S. M., & Grondin, S. (2014). Different methods for reproducing time, different results. *Attention, Perception & Psychophysics*, *76*(3), 675–681. https://doi.org/10.3758/s13414-014-0625-3

Mita, A., Mushiake, H., Shima, K., Matsuzaka, Y., & Tanji, J. (2009). Interval time coding by neurons in the presupplementary motor areas. *Nature Neuroscience*, *12*, 502–507. https://doi.org/10.1038/nn.2272

Mitani, K., & Kashino, M. (2018). Auditory feedback assists post hoc error correction of temporal reproduction, and perception of self-produced time intervals in subsecond range. *Frontiers in Psychology*, *8*. https://doi.org/10.3389/fpsyg.2017.02325

Morillon, B., Kell, C. A., & Giraud, A.-L. (2009). Three Stages and Four Neural Systems in Time Estimation. *Journal of Neuroscience*, *29*(47), 14803–14811. https://doi.org/10.1523/JNEUROSCI.3222-09.2009

Muir, A. M., Eberhard, A. C., Walker, M. S., Bennion, A., South, M., & Larson, M. J. (2021). Dissociating the effect of reward uncertainty and timing uncertainty on neural indices of reward prediction errors: A reward positivity (RewP) event-related potential (ERP) study. *Biological Psychology*, *163*, 108121. https://doi.org/10.1016/j.biopsycho.2021.108121

Nagai, Y., Critchley, H. D., Featherstone, E., Fenwick, P. B. C., Trimble, M. R., & Dolan, R. J. (2004a). Brain activity relating to the contingent negative variation: An fMRI investigation. *NeuroImage*, *21*(4), 1232–1241. https://doi.org/10.1016/j.neuroimage.2003.10.036

Nagai, Y., Critchley, H. D., Featherstone, E., Fenwick, P. B. C., Trimble, M. R., & Dolan, R. J. (2004b). Brain activity relating to the contingent negative variation:

An fMRI investigation. *NeuroImage*, *21*(4), 1232–1241. https://doi.org/10.1016/j.neuroimage.2003.10.036

Nani, A., Manuello, J., Liloia, D., Duca, S., Costa, T., & Cauda, F. (2019). The Neural Correlates of Time: A Meta-analysis of Neuroimaging Studies. *Journal of Cognitive Neuroscience*, *31*(12), 1796–1826. https://doi.org/10.1162/jocn_a_01459

Nieuwenhuis, S., Slagter, H. A., Von Geusau, N. J. A., Heslenfeld, D. J., & Holroyd, C. B. (2005). Knowing good from bad: Differential activation of human cortical areas by positive and negative outcomes. *European Journal of Neuroscience*, *21*(11), 3161–3168. https://doi.org/10.1111/j.1460-9568.2005.04152.x

Niv, Y., Daw, N., & Dayan, P. (2005). How fast to work: Response vigor, motivation and tonic dopamine. In *Advances in Neural Information Processing Systems* (Vol. 18).

Notebaert, W., Houtman, F., Opstal, F. V., Gevers, W., Fias, W., & Verguts, T. (2009). Post-error slowing: An orienting account. *Cognition*, *111*(2), 275–279. https://doi.org/10.1016/j.cognition.2009.02.002

Oliveri, M., Koch, G., Salerno, S., Torriero, S., Gerfo, E. L., & Caltagirone, C. (2009). Representation of time intervals in the right posterior parietal cortex: Implications for a mental time line. *NeuroImage*, *46*(4), 1173–1179. https://doi.org/10.1016/j.neuroimage.2009.03.042

Onoe, H., Komori, M., Onoe, K., Takechi, H., Tsukada, H., & Watanabe, Y. (2001). Cortical networks recruited for time perception: A monkey positron emission

tomography (PET) study. *NeuroImage*, *13*(1), 37–45. https://doi.org/10.1006/nimg.2000.0670

Öztel, T., Eskenazi, T., & Balcı, F. (2021). Temporal error monitoring with directional error magnitude judgements: A robust phenomenon with no effect of being watched. *Psychological Research*, *85*(5), 2069–2078. https://doi.org/10.1007/s00426-020-01379-0

Pastor, M. A., Artieda, J., Jahanshahi, M., & Obeso, J. A. (1992). Time estimation and reproduction is abnormal in Parkinson's disease. *Brain: A Journal of Neurology*, *115 Pt 1*, 211–225. https://doi.org/10.1093/brain/115.1.211

Paule, M. G., Meck, W. H., McMillan, D. E., McClure, G. Y., Bateson, M., Popke, E. J., Chelonis, J. J., & Hinton, S. C. (1999). The use of timing behaviors in animals and humans to detect drug and/or toxicant effects. *Neurotoxicology and Teratology*, *21*(5), 491–502. https://doi.org/10.1016/s0892-0362(99)00015-x

Peterburs, J., & Desmond, J. E. (2016). The role of the human cerebellum in performance monitoring. *Current Opinion in Neurobiology*, *40*, 38–44. https://doi.org/10.1016/j.conb.2016.06.011

Petter, E. A., Gershman, S. J., & Meck, W. H. (2018). Integrating Models of Interval Timing and Reinforcement Learning. *Trends in Cognitive Sciences*, *22*(10), 911–922. https://doi.org/10.1016/j.tics.2018.08.004

Piras, F., & Coull, J. T. (2011). Implicit, Predictive Timing Draws upon the Same Scalar Representation of Time as Explicit Timing. *PLoS ONE*, *6*(3), e18203. https://doi.org/10.1371/journal.pone.0018203

Plichta, M. M., Wolf, I., Hohmann, S., Baumeister, S., Boecker, R., Schwarz, A. J., Zangl, M., Mier, D., Diener, C., Meyer, P., Holz, N., Ruf, M., Gerchen, M. F., Bernal-Casas, D., Kolev, V., Yordanova, J., Flor, H., Laucht, M., Banaschewski, T., … Brandeis, D. (2013). Simultaneous EEG and fMRI Reveals a Causally Connected Subcortical-Cortical Network during Reward Anticipation. *The Journal of Neuroscience*, *33*(36), 14526–14533. https://doi.org/10.1523/JNEUROSCI.0631-13.2013

Pouget, A., Drugowitsch, J., & Kepecs, A. (2016). Confidence and certainty: Distinct probabilistic quantities for different goals. *Nature Neuroscience*, *19*(3), 366–374. https://doi.org/10.1038/nn.4240

Pouthas, V., George, N., Poline, J., Pfeuty, M., VandeMoorteele, P., Hugueville, L., Ferrandez, A., Lehéricy, S., LeBihan, D., & Renault, B. (2005). Neural network involved in time perception: An fMRI study comparing long and short interval estimation. *Human Brain Mapping*, *25*(4), 433–441. https://doi.org/10.1002/hbm.20126

Praamstra, P., & Pope, P. (2007). Slow Brain Potential and Oscillatory EEG Manifestations of Impaired Temporal Preparation in Parkinson's Disease. *Journal of Neurophysiology*, *98*(5), 2848–2857. https://doi.org/10.1152/jn.00224.2007

Prochnow, A., Bluschke, A., Novotna, B., Hagen, M. von der, & Beste, C. (2022). Feedback-Based Learning of Timing in Attention-Deficit/Hyperactivity Disorder and Neurofibromatosis Type 1. *Journal of the International Neuropsychological Society*, *28*(1), 12–21. https://doi.org/10.1017/S1355617721000072

Protopapa, F., Hayashi, M. J., Kulashekhar, S., Zwaag, W. van der, Battistella, G., Murray, M. M., Kanai, R., & Bueti, D. (2019). Chronotopic maps in human supplementary motor area. *PLOS Biology*, *17*(3), e3000026. https://doi.org/10.1371/journal.pbio.3000026

Quilodran, R., Rothé, M., & Procyk, E. (2008). Behavioral shifts and action valuation in the anterior cingulate cortex. *Neuron*, *57*(2), 314–325. https://doi.org/10.1016/j.neuron.2007.11.031

Rabbitt, P. (1979). How old and young subjects monitor and control responses for accuracy and speed. *British Journal of Psychology*, *70*(2), 305–311. https://doi.org/10.1111/j.2044-8295.1979.tb01687.x

Raichle, M. E., MacLeod, A. M., Snyder, A. Z., Powers, W. J., Gusnard, D. A., & Shulman, G. L. (2001). A default mode of brain function. *Proceedings of the National Academy of Sciences of the United States of America*, *98*(2), 676–682.

Rammsayer, T. H. (1997). On the relationship between personality and time estimation. *Personality and Individual Differences*, *23*(5), 739–744. https://doi.org/10.1016/S0191-8869(97)00117-7

Rao, S. M., Mayer, A. R., & Harrington, D. L. (2001). The evolution of brain activation during temporal processing. *Nature Neuroscience*, *4*(3), 317–323. https://doi.org/10.1038/85191

Ratcliff, R. (1978). A theory of memory retrieval. *Psychological Review*, *85*(2), 59–108. https://doi.org/10.1037/0033-295X.85.2.59

Ratcliff, R., & McKoon, G. (2008). The Diffusion Decision Model: Theory and Data for Two-Choice Decision Tasks. *Neural Computation*, *20*(4), 873–922. https://doi.org/10.1162/neco.2008.12-06-420

Rattat, A.-C., & Droit-Volet, S. (2012). What is the best and easiest method of preventing counting in different temporal tasks? *Behavior Research Methods*, *44*(1), 67–80. https://doi.org/10.3758/s13428-011-0135-3

Ridderinkhof, K. R., Ullsperger, M., Crone, E. A., & Nieuwenhuis, S. (2004). The role of the medial frontal cortex in cognitive control. *Science (New York, N.Y.)*, *306*(5695), 443–447. https://doi.org/10.1126/science.1100301

Riemer, M., Kubik, V., & Wolbers, T. (2019). The effect of feedback on temporal error monitoring and timing behavior. *Behavioural Brain Research*, *369*, 111929. https://doi.org/10.1016/j.bbr.2019.111929

Rohrbaugh, J. W., & Gaillard, A. W. K. (1983). 13 Sensory and Motor Aspects of the Contingent Negative Variation. In A. W. K. Gaillard & W. Ritter (Eds.), *Advances in Psychology* (Vol. 10, pp. 269–310). North-Holland. https://doi.org/10.1016/S0166-4115(08)62044-0

Rommerskirchen, L., Lange, L., & Osinsky, R. (2021). The reward positivity reflects the integrated value of temporally threefold-layered decision outcomes. *Psychophysiology*, *58*(5), e13789. https://doi.org/10.1111/psyp.13789

Rouault, M., Lebreton, M., & Pessiglione, M. (2021). *A shared brain system forming confidence judgment across cognitive domains* [Preprint]. Neuroscience. https://doi.org/10.1101/2021.09.17.460809

Rutishauser, U., Ye, S., Koroma, M., Tudusciuc, O., Ross, I. B., Chung, J. M., & Mamelak, A. N. (2015). Representation of retrieval confidence by single neurons in the human medial temporal lobe. *Nature Neuroscience*, *18*(7), 1041–1050. https://doi.org/10.1038/nn.4041

Ryan, L. J. (2016). Why doesn't feedback correct Vierordt's law? *Journal of Cognitive Psychology*, *28*(8), 948–964. https://doi.org/10.1080/20445911.2016.1221829

Ryan, L. J., & Robey, T. B. (2002). Learning and performance effects of accurate and erroneous knowledge of results on time perception. *Acta Psychologica*, *111*(1), 83–100. https://doi.org/10.1016/S0001-6918(02)00044-6

Sahai, V., & Tandon, O. P. (2000). Task related changes in contingent negative variation (CNV) response of endogenous evoked potentials. *Indian Journal of Physiology and Pharmacology*, *44*(3), 311–316.

Sailer, U., Fischmeister, F. P. S., & Bauer, H. (2010). Effects of learning on feedback-related brain potentials in a decision-making task. *Brain Research*, *1342*, 85–93. https://doi.org/10.1016/j.brainres.2010.04.051

Salmoni, A. W., Schmidt, R. A., & Walter, C. B. (1984). Knowledge of results and motor learning: A review and critical reappraisal. *Psychological Bulletin*, *95*(3), 355–386.

San Martín, R. (2012). Event-related potential studies of outcome processing and feedback-guided learning. *Frontiers in Human Neuroscience*, *6*. https://www.frontiersin.org/article/10.3389/fnhum.2012.00304

Schlerf, J., Ivry, R. B., & Diedrichsen, J. (2012). Encoding of Sensory Prediction Errors in the Human Cerebellum. *Journal of Neuroscience, 32*(14), 4913–4922. https://doi.org/10.1523/JNEUROSCI.4504-11.2012

Schultz, W. (2016). Dopamine reward prediction error coding. *Dialogues in Clinical Neuroscience*, *18*(1), 23–32.

Schultz, W., Dayan, P., & Montague, P. R. (1997). A Neural Substrate of Prediction and Reward. *Science, 275*(5306), 1593–1599. https://doi.org/10.1126/science.275.5306.1593

Schwartze, M., Rothermich, K., & Kotz, S. A. (2012). Functional dissociation of pre-SMA and SMA-proper in temporal processing. *NeuroImage*, *60*(1), 290–298. https://doi.org/10.1016/j.neuroimage.2011.11.089

Sedaghat-Nejad, E., & Shadmehr, R. (2021). The cost of correcting for error during sensorimotor adaptation. *Proceedings of the National Academy of Sciences*, *118*(40), e2101717118. https://doi.org/10.1073/pnas.2101717118

Seo, H., & Lee, D. (2007). Temporal Filtering of Reward Signals in the Dorsal Anterior Cingulate Cortex during a Mixed-Strategy Game. *Journal of Neuroscience*, *27*(31), 8366–8377. https://doi.org/10.1523/JNEUROSCI.2369-07.2007

Shi, Z., Ganzenmüller, S., & Müller, H. J. (2013). Reducing Bias in Auditory Duration Reproduction by Integrating the Reproduced Signal. *PLOS ONE, 8*(4), e62065. https://doi.org/10.1371/journal.pone.0062065

Shidara, M., & Richmond, B. J. (2002). Anterior Cingulate: Single Neuronal Signals Related to Degree of Reward Expectancy. *Science, 296*(5573), 1709–1711.

Shima, K., & Tanji, J. (1998). Role for cingulate motor area cells in voluntary movement selection based on reward. *Science (New York, N.Y.)*, *282*(5392), 1335–1338. https://doi.org/10.1126/science.282.5392.1335

Simen, P., Balci, F., deSouza, L., Cohen, J. D., & Holmes, P. (2011). A Model of Interval Timing by Neural Integration. *Journal of Neuroscience*, *31*(25), 9238–9253. https://doi.org/10.1523/JNEUROSCI.3121-10.2011

Simen, P., & Matell, M. (2016). Why does time seem to fly when we're having fun? *Science (New York, N.Y.)*, *354*(6317), 1231–1232. https://doi.org/10.1126/science.aal4021

Soares, S., Atallah, B. V., & Paton, J. J. (2016). Midbrain dopamine neurons control judgment of time. *Science*, *354*(6317), 1273–1277. https://doi.org/10.1126/science.aah5234

Steinhauser, M., & Yeung, N. (2010). Decision processes in human performance monitoring. *The Journal of Neuroscience: The Official Journal of the Society for Neuroscience*, *30*(46), 15643–15653. https://doi.org/10.1523/JNEUROSCI.1899-10.2010

Tanaka, M., Kunimatsu, J., Suzuki, T. W., Kameda, M., Ohmae, S., Uematsu, A., & Takeya, R. (2021). Roles of the Cerebellum in Motor Preparation and Prediction of Timing. *Neuroscience*, *462*, 220–234. https://doi.org/10.1016/j.neuroscience.2020.04.039

Tarantino, V., Ehlis, A.-C., Baehne, C., Boreatti-Huemmer, A., Jacob, C., Bisiacchi, P., & Fallgatter, A. J. (2010). The time course of temporal discrimination: An ERP

study. *Clinical Neurophysiology*, *121*(1), 43–52. https://doi.org/10.1016/j.clinph.2009.09.014

Teghil, A., Boccia, M., D'Antonio, F., Di Vita, A., de Lena, C., & Guariglia, C. (2019). Neural substrates of internally-based and externally-cued timing: An activation likelihood estimation (ALE) meta-analysis of fMRI studies. *Neuroscience & Biobehavioral Reviews*, *96*, 197–209. https://doi.org/10.1016/j.neubiorev.2018.10.003

Teghil, A., D'Antonio, F., Di Vita, A., Guariglia, C., & Boccia, M. (2022). Temporal learning in the suprasecond range: Insights from cognitive style. *Psychological Research*. https://doi.org/10.1007/s00426-022-01667-x

Tervo, D. G. R., Kuleshova, E., Manakov, M., Proskurin, M., Karlsson, M., Lustig, A., Behnam, R., & Karpova, A. Y. (2021). The anterior cingulate cortex directs exploration of alternative strategies. *Neuron*, *109*(11), 1876-1887.e6. https://doi.org/10.1016/j.neuron.2021.03.028

Tomassini, A., Ruge, D., Galea, J. M., Penny, W., & Bestmann, S. (2016). The Role of Dopamine in Temporal Uncertainty. *Journal of Cognitive Neuroscience*, *28*(1), 96–110. https://doi.org/10.1162/jocn_a_00880

Toren, I., Aberg, K., & Paz, R. (2020). Prediction errors bidirectionally bias time perception. *Nature Neuroscience*, *23*, 1–5. https://doi.org/10.1038/s41593-020-0698-3

Tregellas, J. R., Davalos, D. B., & Rojas, D. C. (2006). Effect of task difficulty on the functional anatomy of temporal processing. *NeuroImage*, *32*(1), 307–315. https://doi.org/10.1016/j.neuroimage.2006.02.036

Treisman, M. (2013). The Information-Processing Model of Timing (Treisman, 1963): Its Sources and Further Development. *Timing & Time Perception*, *1*(2), 131–158. https://doi.org/10.1163/22134468-00002017

Tse, C.-Y., & Penney, T. B. (2006). Preattentive timing of empty intervals is from marker offset to onset. *Psychophysiology*, *43*(2), 172–179. https://doi.org/10.1111/j.1469-8986.2006.389.x

Tsukamoto, T., Kotani, Y., Ohgami, Y., Omura, K., Inoue, Y., & Aihara, Y. (2006). Activation of insular cortex and subcortical regions related to feedback stimuli in a time estimation task: An fMRI study. *Neuroscience Letters*, *399*(1), 39–44. https://doi.org/10.1016/j.neulet.2006.01.061

Ullsperger, M., & Danielmeier, C. (2016). Reducing Speed and Sight: How Adaptive Is Post-Error Slowing? *Neuron*, *89*(3), 430–432. https://doi.org/10.1016/j.neuron.2016.01.035

Ullsperger, M., Fischer, A. G., Nigbur, R., & Endrass, T. (2014). Neural mechanisms and temporal dynamics of performance monitoring. *Trends in Cognitive Sciences*, *18*(5), 259–267. https://doi.org/10.1016/j.tics.2014.02.009

Umbach, G., Kantak, P., Jacobs, J., Kahana, M., Pfeiffer, B. E., Sperling, M., & Lega, B. (2020). Time cells in the human hippocampus and entorhinal cortex support

episodic memory. *Proceedings of the National Academy of Sciences*, *117*(45), 28463–28474. https://doi.org/10.1073/pnas.2013250117

Umemoto, A., HajiHosseini, A., Yates, M. E., & Holroyd, C. B. (2017). Reward-based contextual learning supported by anterior cingulate cortex. *Cognitive, Affective & Behavioral Neuroscience*, *17*(3), 642–651. https://doi.org/10.3758/s13415-017-0502-3

Üstün, S., Kale, E. H., & Çiçek, M. (2017). Neural Networks for Time Perception and Working Memory. *Frontiers in Human Neuroscience*, *11*, 83. https://doi.org/10.3389/fnhum.2017.00083

Utevsky, A. V., Smith, D. V., & Huettel, S. A. (2014). Precuneus Is a Functional Core of the Default-Mode Network. *Journal of Neuroscience*, *34*(3), 932–940. https://doi.org/10.1523/JNEUROSCI.4227-13.2014

van Noordt, S. J. R., & Segalowitz, S. J. (2012). Performance monitoring and the medial prefrontal cortex: A review of individual differences and context effects as a window on self-regulation. *Frontiers in Human Neuroscience*, *6*, 197. https://doi.org/10.3389/fnhum.2012.00197

van Veen, V., Holroyd, C. B., Cohen, J. D., Stenger, V. A., & Carter, C. S. (2004). Errors without conflict: Implications for performance monitoring theories of anterior cingulate cortex. *Brain and Cognition*, *56*(2), 267–276. https://doi.org/10.1016/j.bandc.2004.06.007

Vicario, C. M., Martino, D., & Koch, G. (2013). Temporal accuracy and variability in the left and right posterior parietal cortex. *Neuroscience*, *245*, 121–128. https://doi.org/10.1016/j.neuroscience.2013.04.041

Walsh, M. M., & Anderson, J. R. (2012). Learning from experience: Event-related potential correlates of reward processing, neural adaptation, and behavioral choice. *Neuroscience and Biobehavioral Reviews*, *36*(8), 1870–1884. https://doi.org/10.1016/j.neubiorev.2012.05.008

Walsh, V. (2003). A theory of magnitude: Common cortical metrics of time, space and quantity. *Trends in Cognitive Sciences*, *7*(11), 483–488. https://doi.org/10.1016/j.tics.2003.09.002

Walter, W. G., Cooper, R., Aldridge, V. J., McCALLUM, W. C., & Winter, A. L. (1964). Contingent Negative Variation: An Electric Sign of Sensori-Motor Association and Expectancy in the Human Brain. *Nature*, *203*(4943), 380–384. https://doi.org/10.1038/203380a0

Wang, J., Hosseini, E., Meirhaeghe, N., Akkad, A., & Jazayeri, M. (2020). Reinforcement regulates timing variability in thalamus. *ELife*, *9*, e55872. https://doi.org/10.7554/eLife.55872

Wearden, J. H. (n.d.). *Decision processes in models of timing*. 15.

Wearden, J. H., Denovan, L., Fakhri, M., & Haworth, R. (1997). Scalar timing in temporal generalization in humans with longer stimulus durations. *Journal of Experimental Psychology. Animal Behavior Processes*, *23*(4), 502–511. https://doi.org/10.1037//0097-7403.23.4.502

Wiener, M. (2014). Transcranial Magnetic Stimulation Studies of Human Time Perception: A Primer. *Timing & Time Perception*, *2*(3), 233–260. https://doi.org/10.1163/22134468-00002022

Wiener, M., Lee, Y.-S., Lohoff, F. W., & Coslett, H. B. (2014). Individual differences in the morphometry and activation of time perception networks are influenced by dopamine genotype. *NeuroImage*, *89*, 10–22. https://doi.org/10.1016/j.neuroimage.2013.11.019

Wiener, M., Lohoff, F. W., & Coslett, H. B. (2011). Double Dissociation of Dopamine Genes and Timing in Humans. *Journal of Cognitive Neuroscience*, *23*(10), 2811–2821. https://doi.org/10.1162/jocn.2011.21626

Wiener, M., Turkeltaub, P., & Coslett, H. B. (2010). The image of time: A voxel-wise meta-analysis. *NeuroImage*, *49*(2), 1728–1740. https://doi.org/10.1016/j.neuroimage.2009.09.064

Wittmann, M., Simmons, A. N., Aron, J. L., & Paulus, M. P. (2010). Accumulation of neural activity in the posterior insula encodes the passage of time. *Neuropsychologia*, *48*(10), 3110–3120. https://doi.org/10.1016/j.neuropsychologia.2010.06.023

Ye, Q., Zou, F., Lau, H., Hu, Y., & Kwok, S. C. (2018). Causal Evidence for Mnemonic Metacognition in Human Precuneus. *Journal of Neuroscience*, *38*(28), 6379–6387. https://doi.org/10.1523/JNEUROSCI.0660-18.2018

Yeung, N., & Summerfield, C. (2012). Metacognition in human decision-making: Confidence and error monitoring. *Philosophical Transactions of the Royal Society*

of London. Series B, Biological Sciences, *367*(1594), 1310–1321. https://doi.org/10.1098/rstb.2011.0416

Zhang, M., Zhang, K., Zhou, X., Zhan, B., He, W., & Luo, W. (2021). Similar CNV Neurodynamic Patterns between Sub- and Supra-Second Time Perception. *Brain Sciences*, *11*(10), 1362. https://doi.org/10.3390/brainsci11101362

Zheng, Y., Wang, L., Gerlofs, D. J., Duan, W., Wang, X., Yin, J., Yan, C., Allé, M. C., Berna, F., Wang, J., Tang, Y., & Kwok, S. C. (2022). Atypical meta-memory evaluation strategy in schizophrenia patients. *Schizophrenia Research: Cognition*, *27*, 100220. https://doi.org/10.1016/j.scog.2021.100220

Zioga, I., Hassan, R., & Luft, C. D. B. (2019). Success, but not failure feedback guides learning during neurofeedback: An ERP study. *NeuroImage*, *200*, 26–37. https://doi.org/10.1016/j.neuroimage.2019.06.002

BIOGRAPHY

Farah Nikhath Bader graduated from Emory University and received her Bachelor of Science in Neuroscience and Behavioral Biology. She obtained her Master's in Public Health from the Bloomberg School of Public Health at Johns Hopkins University. She has previously worked for the US Medical Research Institute of Chemical Defense and National Institute of Neurological Disorders and Stroke/National Institute of Health. More recently, she was employed as a program analyst at Fogarty International Center/National Institute of Health for seven years prior to returning to graduate school.